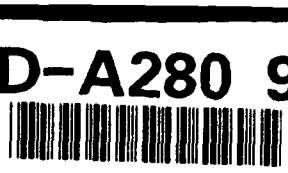

NAVAL POSTGRADUATE SCHOOL
Monterey, California

THESIS

EXPERIMENTAL STUDY OF SPATIALLY INCOMPLETE STRUCTURAL SYSTEM IDENTIFICATION

by

Vincent C. Gomes

March, 1994

Thesis Advisor : Joshua H. Gordis

REPORT DOCUMENTATION PAGE	Form Approved OMB No. 0704-

1. AGENCY USE ONLY *(Leave blank)*	2. REPORT DATE	3. REPORT TYPE AND DATES COVERED
	March 1994	Master's Thesis

4. TITLE AND SUBTITLE	5. FUNDING NUMBERS
Experimental Study of Spatially Incomplete Structural System Identification	
6. AUTHOR(S) Vincent C. Gomes	
7. PERFORMING ORGANIZATION NAME(S) AND ADDRESS(ES) Naval Postgraduate School Monterey CA 93943-5000	8. PERFORMING ORGANIZATION REPORT NUMBER -
9. SPONSORING/MONITORING AGENCY NAME(S) AND ADDRESS(ES)	10. SPONSORING/MONITORING AGENCY REPORT NUMBER -

11. SUPPLEMENTARY NOTES
The views expressed in this thesis are those of the author and do not reflect the official policy or position of the Department of Defense or the U.S. Government.

12a. DISTRIBUTION/AVAILABILITY STATEMENT	12b. DISTRIBUTION CODE
Approved for public release; distribution is unlimited.	

13. ABSTRACT : A frequency domain transformation is the basis for a general approach to the identification of finite element modeling errors. The transformation provides information as to the location of modeling errors and provides the error matrices of stiffness, mass, and damping. The transformation is shown to have the unique property of directly revealing that the process of instrumenting an actual structure with a finite number of response transducers defines a reduced order system, with an attendant set of singular frequencies responsible for the nonlinear distortion imposed on the corrective parameters of stiffness, mass, and damping. Actual test data demonstrating this phenomenon will be presented.

14. SUBJECT TERMS	15. NUMBER OF PAGES 189
	16. PRICE CODE

17. SECURITY CLASSIFICATION OF REPORT	18. SECURITY CLASSIFICATION OF THIS PAGE	19. SECURITY CLASSIFICATION OF ABSTRACT	20. LIMITATION OF ABSTRACT
Unclassified	Unclassified	Unclassified	UL

NSN 7540-01-280-5500 Standard Form 298 (Rev. 2-89)

Approved for public release; distribution is unlimited.

EXPERIMENTAL STUDY OF SPATIALLY INCOMPLETE STRUCTURAL SYSTEM IDENTIFICATION

by

Vincent C. Gomes
Lieutenant Commander, United States Navy
B.S., Oregon State University, 1979

Submitted in partial fulfillment
of the requirements for the degree of

MASTER OF SCIENCE IN MECHANICAL ENGINEERING

from the

NAVAL POSTGRADUATE SCHOOL
March 1994

Author: _____
Vincent C. Gomes

Approved by: _____
Joshua H. Gordis, Thesis Advisor

_____
Matthew D. Kelleher, Chairman
Department of Mechanical Engineering

ABSTRACT

A frequency domain transformation is the basis for a general approach to the identification of finite element modeling errors. The transformation provides information as to the location of modeling errors and provides the error matrices of stiffness, mass, and damping. The transformation is shown to have the unique property of directly revealing that the process of instrumenting an actual structure with a finite number of response transducers defines a reduced order system, with an attendant set of singular frequencies responsible for the nonlinear distortion imposed on the corrective parameters of stiffness, mass, and damping. Actual test data demonstrating this phenomenon will be presented.

TABLE OF CONTENTS

LIST OF TABLES

LIST OF FIGURES

I. INTRODUCTION

A. GENERAL

Structural system identification refers to procedures designed to verify or improve a structural model by using dynamic test data. It requires a comparison between two frequency domain models. The process of structural system identification is composed of two major steps, localization and identification. Localization will determine the portions of the finite element (FE) model which are in error. Identification results in the solution for the correction to the model. The identification process is influenced by two main structural variables, stiffness and mass.

It is not physically possible to perform a complete structural system identification on a real structure since an infinite number of measurements would be required. Thus, structural system identification must be done with spatially incomplete data. Spatially incomplete data imposes a frequency dependency on identifying model errors that are otherwise frequency independent. The fundamental characteristic is inherent in all structural identification procedures, and is the focus of this thesis.

This thesis will use the theoretical development discussed in reference [1] to perform structural system identification on a simple beam.

The first study will use a computer simulation to identify the error in a flawed (purposely installed error) beam model compared with an ideal beam model. The second study will use the same flawed model and perform an error identification using data obtained from an experiment instead of simulated data from an ideal beam model. The two main variables, stiffness and mass, will be examined separately in both of the studies. Case I will perform an error identification with a large stiffness error installed in the flawed model. Case II will repeat the procedure with a small mass error installed in the flawed model.

B. NOMENCLATURE

GENERAL TERMS

C: *Damping Matrix*
K: *Stiffness Matrix*
M: *Mass Matrix*
H: *Frequency Response Function*
Z: *Impedance Matrix*
x: *Generalized Harmonic Response*
f: *Generalized Harmonic Excitation*
λ: *eigenvalue* sec^{-2}
Ω: *circular frequency* sec^{-1}
‖ ‖ *matrix*
| | *vector*

SUPERSCRIPTS:

a: *Analytical Finite Element Model*
x: *Measured (Experimental) Model*

SUBSCRIPTS:

a: *Retained Coordinates*
o: *Omitted Coordinates*
i: *Non-error Coordinates*
c: *Error Coordinates*

II. THEORETICAL DEVELOPMENT

A. *FINITE ELEMENT DESCRIPTION*

The finite element model of a given structure can be defined by the relationship of structure displacement with respect to an applied force.

$$\begin{Bmatrix} f_i \\ f_c \end{Bmatrix} = \begin{bmatrix} Z^a_{ii} & Z^a_{ic} \\ Z^a_{ic} & Z^a_{cc} \end{bmatrix} \begin{Bmatrix} x_i \\ x_c \end{Bmatrix} \tag{2.1}$$

The force and response vectors are denoted by "f" and "x" respectively. These vectors and the impedance matrix (Z) are complex-valued and frequency dependent. The subscripts "i" and "c" denote non error and error coordinates respectively. The superscript "a" says that the quantity is calculated from a finite element (analytical) model. If the values were obtained from experimental test data, the superscript would be "x". Thus for the experimental model the impedance relation would be in a format shown in equation (2.2).

$$\begin{Bmatrix} f_i \\ f_c \end{Bmatrix} = \begin{bmatrix} Z^x_{ii} & Z^x_{ic} \\ Z^x_{ci} & Z^x_{cc} \end{bmatrix} \begin{Bmatrix} x_i \\ x_c \end{Bmatrix} \tag{2.2}$$

The error impedance matrix quantifies the difference between the analytical and experimental models, as a function of frequency.

It is determined from the analytical and test models by obtaining the difference between the analytical and experimental impedance matrices. Equation (2.3) describes the error impedance matrix relation.

$$\begin{Vmatrix} 0 & 0 \\ 0 & \Delta Z \end{Vmatrix} = \begin{Vmatrix} Z^a_{ii} & Z^a_{ic} \\ Z^a_{ci} & Z^a_{cc} \end{Vmatrix} - \begin{Vmatrix} Z^x_{ii} & Z^x_{ic} \\ Z^x_{ci} & Z^x_{cc} \end{Vmatrix} \tag{2.3}$$

The result is that the errors in the finite element model are associated with the error coordinates.

B. STRUCTURAL SYNTHESIS TRANSFORMATION

The impedance matrix associated with the experimental test data is not available. The difficulty is to identify the impedance error using frequency response function data. The analytical tool involved in the identification between two dynamic systems can be derived using the structural synthesis transformation (SST)[Ref. 2]. The SST is constructed from the as yet unknown impedance error in the finite element model. The SST is applied to the finite element frequency response function model producing the test frequency response function model. The frequency response function describes the structure response to applied excitation. The frequency response function is the inverse of the impedance matrix.

$$\begin{vmatrix} x_i \\ x_c \end{vmatrix} = \begin{Vmatrix} H^c_{ii} & H^a_{ic} \\ H^a_{ci} & H^a_{cc} \end{Vmatrix} \begin{vmatrix} f_i \\ f_c \end{vmatrix} \tag{2.4}$$

Equation (2.4) has partitioned the finite element model into error and non-error coordinates. The response coordinate "c" can be subject to applied forces due to the error impedances and from applied excitation (external forces). The response coordinate "i" will only experience externally applied forces. Thus the force vector in equation (2.4) can be written in the following format.

$$f_c = f_c^{ext} + f_c^{\Delta z} \qquad (2.5a)$$

$$f_i = f_i^{ext} \qquad (2.5b)$$

Expanding equation (2.4) into two equations and substituting equation (2.5) into the appropriate elements results in equation (2.6).

$$x_i = H_{ii}^a f_i^{ext} + H_{ic}^a f_c^{ext} + H_{ic}^a f_c^{\Delta z} \qquad (2.6a)$$

$$x_c = H_{ci}^a f_i^{ext} + H_{cc}^a f_c^{ext} + H_{cc}^a f_c^{\Delta z} \qquad (2.6b)$$

Equation (2.6) can be reduced into a matrix format as shown in equation (2.7). Although there are only two expressions associated with equation (2.6), there are three harmonic excitation terms. The matrix associated with equation (2.7) will have three rows to account for the harmonic excitation terms.

$$\begin{Vmatrix} x_i \\ x_c \\ x_c \end{Vmatrix} = \begin{Vmatrix} H_{ii}^a & H_{ic}^a & H_{ic}^a \\ H_{ci}^a & H_{cc}^a & H_{cc}^a \\ H_{ci}^a & H_{cc}^a & H_{cc}^a \end{Vmatrix} \begin{Vmatrix} f_i^{ext} \\ f_c^{ext} \\ f_c^{\Delta z} \end{Vmatrix} \qquad (2.7)$$

The coordinates "c" and "i" can be condensed into a coordinate "e" (e = c U i).

$$\{ f_e \} = [\ [f_i^{ext}]\ [f_c^{ext}]\ ]^T \tag{2.8a}$$

$$\{ f_c \} = \{ f_c^{\Delta z} \} \tag{2.8b}$$

Equation (2.7) can be further condensed by utilizing the set union and equations (2.8a,b).

$$\begin{Vmatrix} x_e \\ x_c \end{Vmatrix} = \begin{Vmatrix} H_{ee}^a & H_{ec}^a \\ H_{ce}^a & H_{cc}^a \end{Vmatrix} \begin{Vmatrix} f_e \\ f_c \end{Vmatrix} \tag{2.9}$$

The error impedance is the difference between the analytical finite element and test models. A transformation needs to be constructed that will use equation (2.9) and produce a similar result for the test system. It is expected that the transformation will be constructed from the as yet unknown impedance error. The impedance error is generally described by equation (2.10).

$$\{ f_c \} = -[\ [\Delta K] - \Omega^2[\Delta M] + j\Omega[\Delta C]\ ] \{ x_c \} \tag{2.10a}$$

$$\{ f_c \} = -[\Delta Z(\Omega)] \{ x_c \} \tag{2.10b}$$

The minus sign in equation (2.10) indicates the reaction forces imposed by the impedance errors on the finite element model are being considered. A transformation matrix can be developed by using the results of equation (2.10b).

$$\begin{vmatrix} f_e \\ f_c \end{vmatrix} = \begin{Vmatrix} I & 0 \\ 0 & -\Delta Z \end{Vmatrix} \begin{vmatrix} f_e \\ x_c \end{vmatrix} \qquad (2.11)$$

The results of equation (2.11) are substituted into equation (2.9).

$$\begin{vmatrix} x_e \\ x_c \end{vmatrix}^* = \begin{Vmatrix} H_{ee}^a & H_{ec}^a \\ H_{ce}^a & H_{cc}^a \end{Vmatrix} \begin{Vmatrix} I & 0 \\ 0 & -\Delta Z \end{Vmatrix} \begin{vmatrix} f_e \\ x_c \end{vmatrix}^* \qquad (2.12)$$

Equation (2.12) can be reduced into the format described in equation (2.13).

$$\begin{vmatrix} x_e \\ x_c \end{vmatrix}^* = \begin{Vmatrix} H_{ee}^a & -H_{ec}^a \Delta Z \\ H_{ce}^a & -H_{cc}^a \Delta Z \end{Vmatrix} \begin{vmatrix} f_e \\ x_c \end{vmatrix}^* \qquad (2.13)$$

Expanding equation (2.13) into two equations and using the superscript "*" to denote a synthesized coupled response, will result in the expression given in equation (2.14).

$$x_c^* = H_{ce}^a f_e - H_{cc}^a \Delta Z x_c^* \qquad (2.14a)$$

$$x_e^* = H_{ee}^a f_e - H_{ec}^a \Delta Z x_c^* \qquad (2.14b)$$

Thus to solve for the synthesized response, equation (2.14a) must be further analyzed.

$$[I + H^{a}_{cc}\Delta Z]x^{*}_{c} = H^{a}_{ce}f_{e} \qquad (2.15a)$$

$$\text{but,} \qquad x_{c} = H^{a}_{ce}f_{e} \qquad (2.15b)$$

$$\text{thus,} \quad [I + H^{a}_{cc}\Delta Z]x^{*}_{c} = x_{c} \qquad (2.15c)$$

$$\text{solving for } x^{*}_{c}$$

$$x^{*}_{c} = [I + H^{a}_{cc}\Delta Z]^{-1}x_{c} \qquad (2.15d)$$

Substituting equation (2.15d) into equation (2.14b) will result in the expression provided in equation (2.16).

$$x^{*}_{e} = H^{a}_{ee}f_{e} - H^{a}_{ec}\Delta Z[I + H^{a}_{cc}\Delta Z]^{-1}x_{c} \qquad (2.16a)$$

$$\text{since } x_{c} = H^{a}_{ce}f_{e} \qquad (2.16b)$$

$$\text{thus,} \quad x^{*}_{e} = H^{a}_{ee}f_{e} - H^{a}_{ec}\Delta Z[I + H^{a}_{cc}\Delta Z]^{-1}\, H^{a}_{ce}f_{e} \qquad (2.16c)$$

Equation (2.4) describes a general identity involving the frequency response function. Using the synthesized uncoupled response designation, the following relation can be written.

$$x^{*}_{e} = [H^{*}_{ee}]\{ f_{e} \} \qquad (2.17)$$

Substituting equation (2.17) into equation (2.16c) will provide the expression given in equation (2.18).

$$[H^{*}_{ee}]\{f_e\} = [H^{a}_{ee}]\{f_e\} - [H^{a}_{ec}][\Delta Z][I + H^{a}_{cc}\Delta Z]^{-1}\,[H^{a}_{ce}]\{f_e\} \quad (2.18a)$$

multiply by $\{f_e\}^{-1}$

$$[H^{*}_{ee}] = [H^{a}_{ee}] - [H^{a}_{ec}][\Delta Z][I + H^{a}_{cc}\Delta Z]^{-1}\,[H^{a}_{ce}] \quad (2.18b)$$

Equation (2.18b) can be further analyzed.

$$[I + H^{a}_{cc}\Delta Z]^{-1} = [(\Delta Z^{-1} + H^{a}_{cc})\Delta Z]^{-1} \quad (2.19a)$$

given $([a][b])^{-1} = [b]^{-1}\,[a]^{-1}$ (2.19b)

results $[I + H^{a}_{cc}\Delta Z]^{-1} = [\Delta Z]^{-1}\,[\Delta Z^{-1} + H^{a}_{cc}]^{-1}$ (2.19c)

Equation (2.18b) can be updated by using the substituting equation (2.19c) into the appropriate terms. The "*" superscript that denotes the synthesized coupled response, is replaced with an "x" superscript indicating the test system.

$$H^{x}_{ee} = H^{a}_{ee} - H^{a}_{ec}[\Delta Z^{-1} + H^{a}_{cc}]^{-1}H^{a}_{ce} \quad (2.20)$$

Equation (2.20) can be further expanded into a full matrix.

$$\begin{vmatrix} H^{x}_{ii} & H^{x}_{ic} \\ H^{x}_{ci} & H^{x}_{cc} \end{vmatrix} = \begin{vmatrix} H^{a}_{ii} & H^{a}_{ic} \\ H^{a}_{ci} & H^{a}_{cc} \end{vmatrix} - \begin{vmatrix} H^{a}_{ic} \\ H^{a}_{cc} \end{vmatrix} [\Delta Z^{-1} + H^{a}_{cc}]^{-1}[H^{a}_{ic} \;\; H^{a}_{cc}] \quad (2.21)$$

Equation (2.20) (or equation (2.21)) is used for identification via structural synthesis transformation.

Equation (2.20) is dependent on both the test and analytical frequency response functions. Since information concerning both frequency response functions is known, the impedance error can therefore be determined. The impedance error can be further dissected into mass, stiffness, and damping errors via equation (2.10).

C. FREQUENCY DOMAIN LOCALIZATION

As previously discussed, the error impedance can be determined from the analytical and test frequency response functions. The frequency response function is dependent upon frequency, therefore, the error impedance is also dependent upon frequency. The next step is to define a localization matrix that will provide spatial diagnostic information. The localization matrix will also provide information that will ensure a unique identification. The following terms are identified in equations (2.22a) and (2.22b).

$$\Delta H_{ee} = H^{a}_{ee} - H^{x}_{ee} \qquad (2.22a)$$

$$D = [\Delta Z^{-1} + H^{a}_{cc}] \qquad (2.22b)$$

Equation (2.20) can be reduced by substituting equations (2.22a) and (2.22b) into the appropriate terms.

$$\Delta H_{ee} = H^{a}_{ec} D^{-1} H^{a}_{ce} \qquad (2.23)$$

The localization matrix is defined by equation (2.24).

$$L = Z^{a}_{ee} \, \Delta H_{ee} \, Z^{a}_{ee} \qquad (2.24)$$

The localization matrix can be further defined by substituting equation (2.23) into equation (2.24).

$$L = Z_{ee}^{a} H_{ec}^{a} D^{-1} H_{ce}^{a} Z_{ee}^{a} \qquad (2.25a)$$

The coordinate "e" can also be expanded into error and non error coordinates.

$$L = \begin{Vmatrix} Z_{ii}^{a} & Z_{ic}^{a} \\ Z_{ci}^{a} & Z_{cc}^{a} \end{Vmatrix} \begin{Vmatrix} H_{ic}^{a} \\ H_{cc}^{a} \end{Vmatrix} [D^{-1}] \begin{vmatrix} H_{ic}^{a} & H_{cc}^{a} \end{vmatrix} \begin{Vmatrix} Z_{ii}^{a} & Z_{ic}^{a} \\ Z_{ci}^{a} & Z_{cc}^{a} \end{Vmatrix} \qquad (2.25b)$$

The frequency response matrix is the inverse of the impedance matrix. Multiplying these two matrices will result in the identity matrix. Partitioning the FRF and impedance matrices into error and non error coordinates results in the relationship provided in equation (2.26).

$$\begin{Vmatrix} Z_{ii} & Z_{ic} \\ Z_{ci} & Z_{cc} \end{Vmatrix} \begin{Vmatrix} H_{ii} & H_{ic} \\ H_{ci} & H_{cc} \end{Vmatrix} = \begin{Vmatrix} I & 0 \\ 0 & I \end{Vmatrix} \qquad (2.26)$$

Equation (2.26) implies that all elements with mixed "i" and "c" coordinates will be zero. The results from equation (2.26), equation (2.25b) can be rewritten in the format of equations (2.27a) and (2.27b).

$$L = \begin{Vmatrix} 0 \\ I \end{Vmatrix} \| D^{-1} \| \| 0 \quad I \| \qquad (2.27a)$$

$$L = \begin{Vmatrix} 0 & 0 \\ 0 & D^{-1} \end{Vmatrix} \qquad (2.27b)$$

Equation (2.27b) indicates that the localization matrix will produce a non zero value in the partition corresponding to the response error coordinate set "c".

D. IMPEDANCE ERROR

The impedance error can be determined from equation (2.21). The conclusion from equation (2.27b) is that terms associated with non error coordinates will be zero. Applying this conclusion to equation (2.21), the non error coordinate elements will assumed to be zero, and equation (2.21) can be simplified.

$$H_{cc}^{x} = H_{cc}^{a} - H_{cc}^{a}[\Delta Z^{-1} + H_{cc}^{a}]^{-1}H_{cc}^{a} \qquad (2.28)$$

Equation (2.28) can be solved such that the impedance error is dependent upon the analytical and test frequency response functions at error coordinates determined from the localization matrix.

$$[\Delta Z] = (\overline{[H_{cc}^{x}]} - [H_{cc}^{a}])^{-1} \qquad (2.29a)$$

$$\text{where } \overline{[H_{cc}^{x}]} = ([H_{cc}^{a}]^{-1}[\Delta H][H_{cc}^{a}]^{-1})^{-1} \qquad (2.29b)$$

Equations (2.29a) and (2.29b) are used to solve for the error impedance at a single frequency. A system of several equations over a range of frequencies can be used to solve for the impedance.

$$\begin{Bmatrix} \Delta Z_c(\Omega_1) \\ \vdots \\ \Delta Z_c(\Omega_2) \\ \vdots \\ \Delta Z_c(\Omega_n) \end{Bmatrix} = \begin{bmatrix} I & -\Omega^{2_1} I & j\Omega_1 I \\ \vdots & \vdots & \vdots \\ I & -\Omega^{2_2} I & j\Omega_2 I \\ \vdots & \vdots & \vdots \\ I & -\Omega^{2_n} I & j\Omega_n I \end{bmatrix} \begin{Bmatrix} \Delta K_c \\ \Delta M_c \\ \Delta C_c \end{Bmatrix} \qquad (2.30)$$

E. SYSTEM REDUCTION

It is physically not possible to perform a complete structural system identification over a frequency domain. This would require the number of response coordinate locations and measuring devices to be equal to the number of elements of the finite element model. The result for a real world structure is a measured frequency response function matrix that is spatially incomplete. To perform the structural system identification using the equations developed in this section, the analytical frequency response function matrix must be reduced in size such that it is equivalent in size to the test frequency response function matrix. Two reduction methods will be investigated; Extraction Reduction [Refs. 2,3], and Improved Reduction System (IRS) [Ref. 4].

1. Extraction Reduction

Extraction Reduction is a process which extracts selected elements from a frequency response function matrix. The extracted elements pertain to those coordinates for which measured data is available. The procedure requires determining the impedance matrix from the complete stiffness and mass matrices associated with the finite element model.

The frequency response function (FRF) matrix is then obtained by inverting the impedance matrix. The reduced FRF matrix is obtained by extracting the elements associated with the desired coordinates. The retained coordinates are known as "ASET" coordinates, are associated with the measured points on the structure. The reduced FRF matrix consists of ASET coordinates. The omitted coordinates are known as "OSET" coordinates. The reduced impedance matrix is then calculated by inverting the reduced FRF matrix.

2. Improved Reduction System (IRS)

The Extraction Reduction method introduces the "ASET" and "OSET" coordinates. The general impedance relation of equation (2.1) can be adjusted to reflect this coordinate system.

$$\begin{Vmatrix} f_a \\ f_o \end{Vmatrix} = \begin{Vmatrix} Z_{aa} & Z_{ao} \\ Z_{oa} & Z_{oo} \end{Vmatrix} \begin{Vmatrix} x_a \\ x_o \end{Vmatrix} \qquad (2.31)$$

$$f_a = Z_{aa}x_a + Z_{ao}x_o \qquad (2.32a)$$

$$f_o = Z_{oa}x_a + Z_{oo}x_o \qquad (2.32b)$$

Equation (2.31) can be expanded into two equations.

Since the OSET coordinates are not associated with measurement locations on the structure, they are coordinates of non interest. Therefore the forcing function at the OSET coordinates can be set equal to zero.

Adjusting equation (2.32b) will result in the solution for the generalized structural response.

$$x_o = -Z_{oo}^{-1} Z_{oa} x_a \tag{2.33a}$$

$$\begin{Vmatrix} x_a \\ x_o \end{Vmatrix} = \begin{Vmatrix} I \\ -Z_{oo}^{-1} Z_{oa} \end{Vmatrix} [x_a] \tag{2.33b}$$

Equation (2.34) is obtained by substituting the results of equation (2.33b) into equation (2.31).

$$\begin{Vmatrix} f_a \\ 0 \end{Vmatrix} = \begin{Vmatrix} Z_{aa} & Z_{ao} \\ Z_{oa} & Z_{oo} \end{Vmatrix} \begin{Vmatrix} I \\ -Z_{oo}^{-1} Z_{oa} \end{Vmatrix} \{x_a\} \tag{2.34a}$$

$$\{f_a\} = [Z_{aa} - Z_{ao} Z_{oo}^{-1} Z_{oa}] \{x_a\} \tag{2.34b}$$

In the static case (frequency is zero), the general impedance relationship of equation (2.10a), demonstrates that only the structural stiffness will influence the correlation between the retained and omitted coordinate response.

$$\{x_o\} = [-K_{oo}^{-1} K_{oa}] \{x_a\} \tag{2.35}$$

$$\{x_o\} = [-K_{oo}^{-1} K_{oa} + T M_{stat}^{-1} K_{stat}] \{x_a\} \tag{2.36a}$$

$$T = K_{oo}^{-1} M_{oa} - K_{oo}^{-1} M_{oo} K_{oo}^{-1} K_{oa} \tag{2.36b}$$

The IRS relationship [ref. 5] is presented in equations (2.36a) and (2.36b).

The IRS procedure starts with obtaining the complete stiffness and mass matrices from the finite element program. The next step is to partition the matrices into retained and omitted set coordinates.

$$K = \begin{Vmatrix} K_{aa} & K_{ao} \\ K_{oa} & K_{oo} \end{Vmatrix} \qquad (2.37a)$$

$$M = \begin{Vmatrix} M_{aa} & M_{ao} \\ M_{oa} & M_{oo} \end{Vmatrix} \qquad (2.37b)$$

Transforming the retained coordinates (ASET partition) with the transformation matrix will produce the reduced mass and stiffness matrices.

$$\overline{K^a} = t^T K_a t \qquad (2.38a)$$

$$\overline{M^a} = t^T M_a t \qquad (2.38b)$$

Determining the transformation matrix "t" requires two steps. The first step is to solve for "T" with equation (2.36b). Solving equation (2.36b) only solves the lower partition of equation (2.33b). To complete the transformation, the upper partition of equation (2.33b) must be included. To complete the transformation, an identity matrix the size of the number of retained coordinates is added to the "T" matrix.

$$t = \begin{Vmatrix} I \\ T \end{Vmatrix} \qquad (2.39)$$

Utilizing the results from equations (2.38a) and (2.38b), the reduced impedance and FRF matrices can be calculated in a manner similar to that of extraction reduction.

$$\overline{Z^a} = \overline{K^a} - \Omega^2 \overline{M^a} \qquad (2.40a)$$

$$\overline{H^a} = \overline{Z^a}^{-1} \qquad (2.40b)$$

III. COMPUTER SIMULATION

A. BEAM MODEL

1. General Description

Presented in this section are the results of two computer simulations that will elaborate on the theory presented in the previous section.

The structure that will be modeled for the simulation will be a simple beam.

TABLE 3-1: IDEAL BEAM SPECIFICATIONS

PARAMETERS	VALUE	SOURCE
Length	60.625 in	Measured
Width	1.5656 in	Measured
Thickness	0.5339 in	Measured
Density	0.284 lb/cu.in	Calculated
Modulus	28*e+06 psi	Appendix B

The ideal beam model is defined as the finite element model of the beam described in Table 3.1 (Appendix B) and will simulate the test data of the actual structure. The flawed (or error) model is defined similarly to the ideal beam model with the exception of a purposely installed error within the finite element model. The flawed model represents the best attempt at modeling, which results in an imperfect model. Two distinctly flawed models will be investigated. Case I will have a large stiffness error.

Case II will have a small mass error. Table 3.2 furnishes a summary of the details involved in the case studies.

TABLE 3-2: CASE STUDY SUMMARY

CASE	ERROR TYPE	VALUE	LOCATION
I	Modulus	9.0*e+06 psi	Element #2
II	Density	0.25 lbm/in^3	Element #3

The installed errors are graphically represented in Figures 3-1 thru 3-3. The true stiffness and mass errors for each case are displayed. The true error for the case I mass matrix and the case II stiffness matrix are zero.

2. Natural Frequencies

The natural frequencies of the ideal model and both flawed models were calculated by determining the stiffness and mass matrices and then solving for the eigenvalues.

TABLE 3-3: NATURAL FREQUENCIES (HZ)

MODE	IDEAL	CASE I	CASE II
First	29.07	20.27	29.56
Second	79.96	64.33	81.32
Third	157.14	124.47	159.94
Fourth	259.39	222.18	263.26
Fifth	387.85	324.06	396.23

The natural frequency values of case II are much closer to the ideal model than that of case I. This is due to case II having a smaller installed model error.

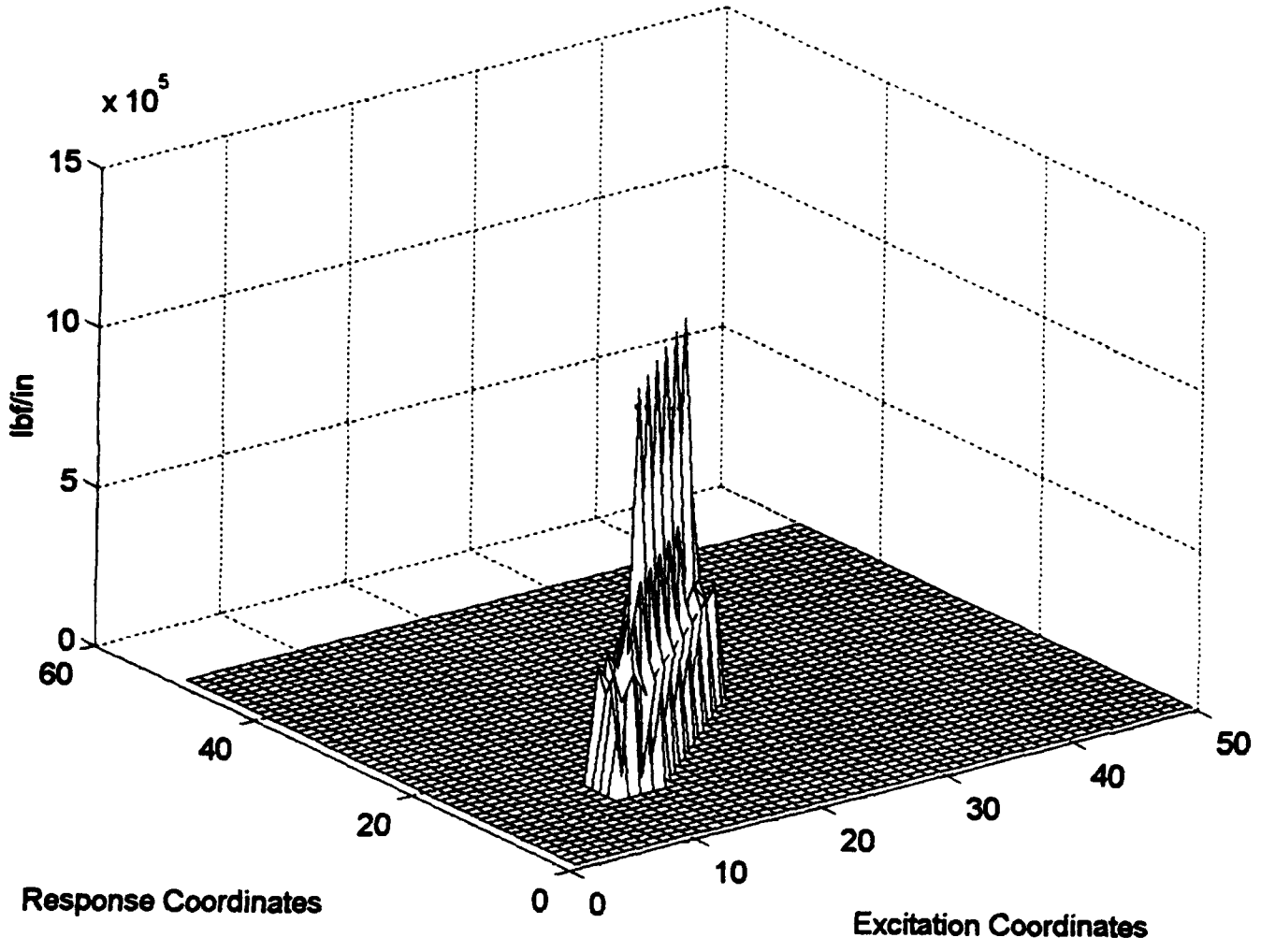

FIGURE 3-1: *True Stiffness Matrix Error - Case I*

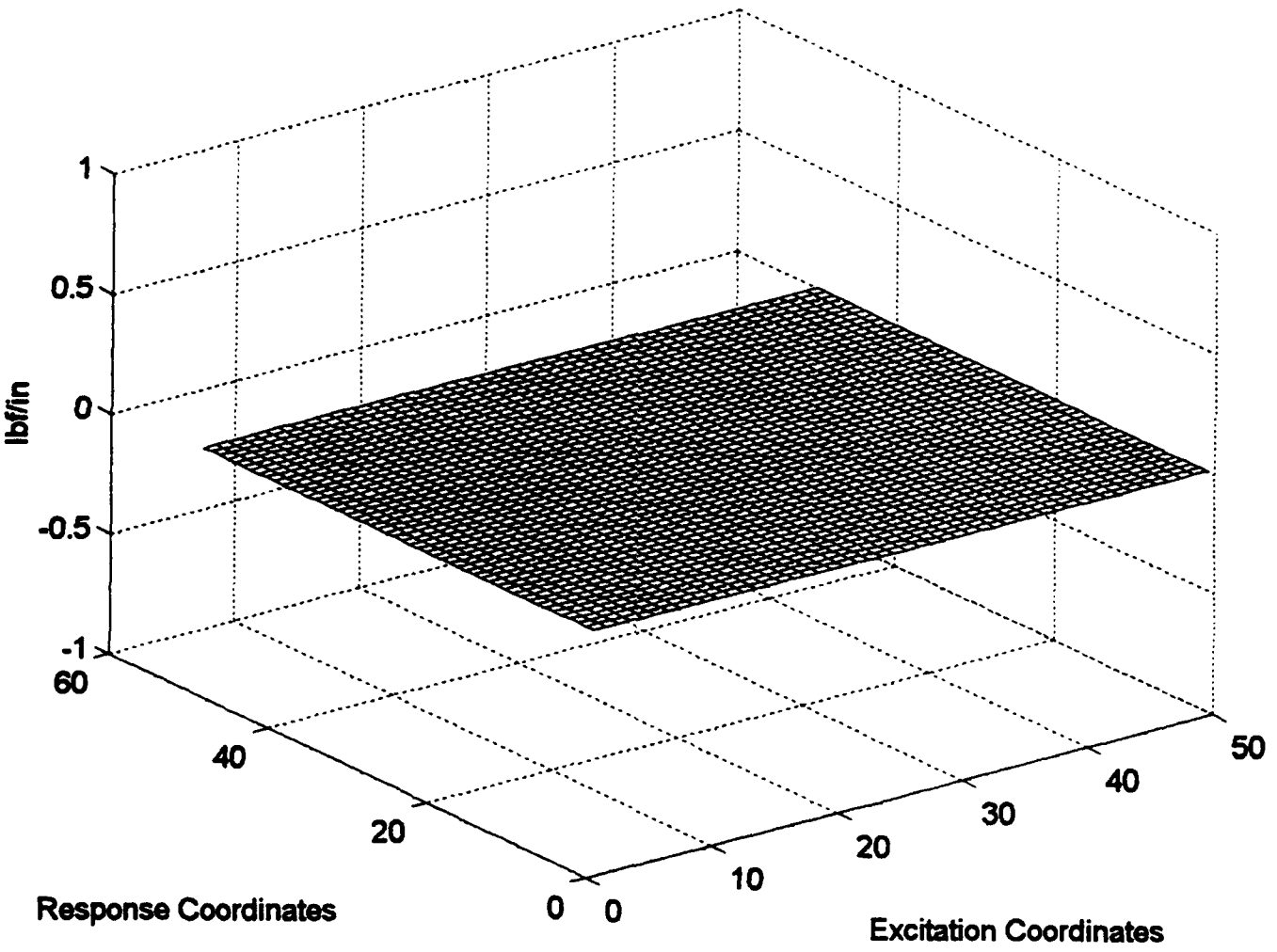

FIGURE 3-2: *True Mass Matrix Error - Case I*

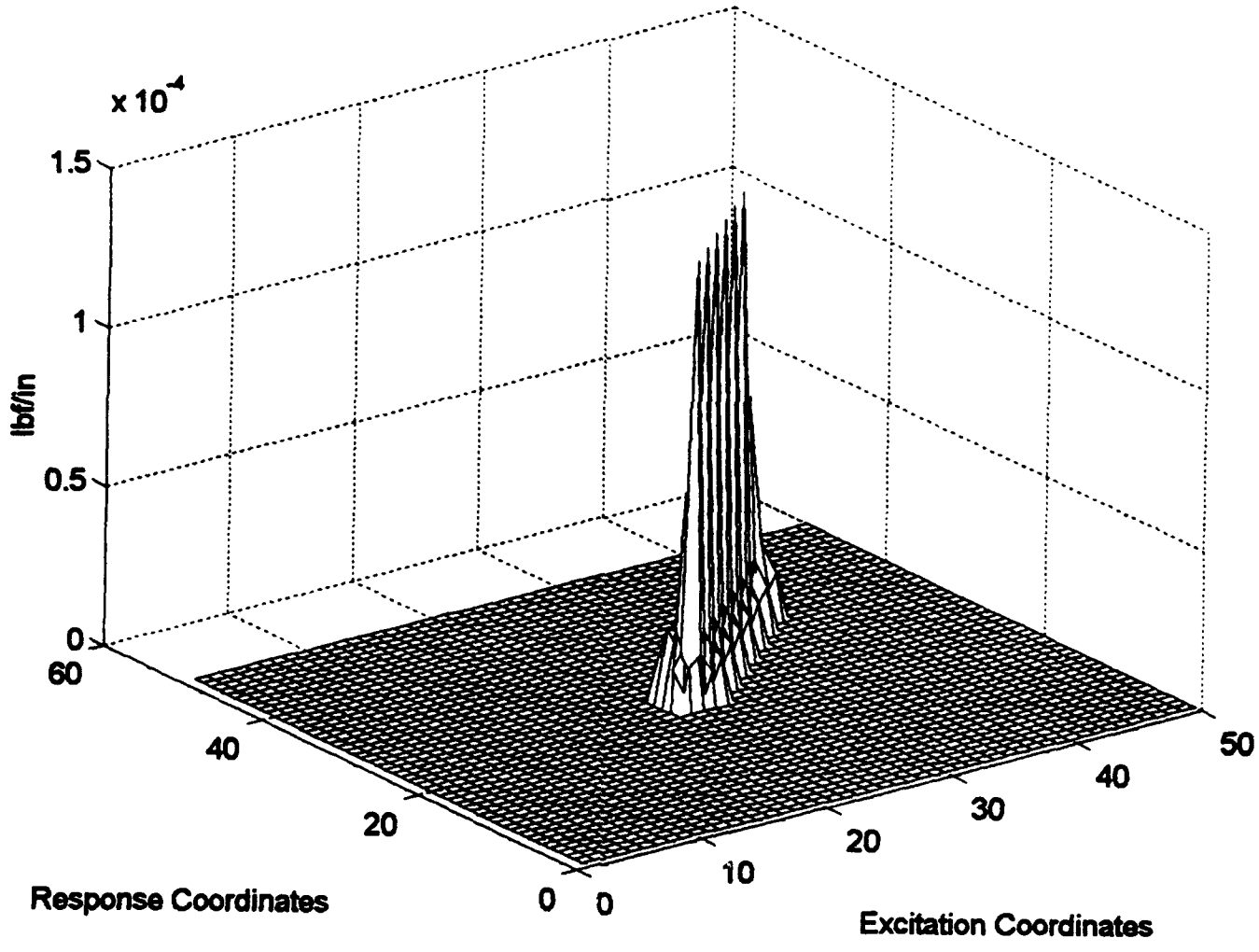

FIGURE 3-3: *True Mass Matrix Error - Case II*

3. Frequency Response

A comparison of the frequency response functions (FRF) of the ideal beam model with each of the flawed beam models was performed. The associated mass and stiffness matrices were determined for each model and used to calculate the FRF matrix (H) at a given frequency. A comparison was done by plotting the "1,1" element of the FRF matrix over a frequency range from 20 to 420 hz. Figures 3-4 and 3-5 display the results of the calculations. The FRF matrices of the flawed and ideal models compare much closer in case II (Figure 3-5) than case I. This is a result of the modeling error being much smaller in case II. A comparison between frequency response functions is important when determining the accuracy of a finite element model. When comparing a finite element model with an actual FRF, the closer the curves approximate each other, the better the model approximates the actual structure.

B. LOCALIZATION MATRIX

The localization matrix provides spatial diagnostic information pertaining to the errors in the finite element model of the structure. The localization matrix reveals the error coordinate subset from the ASET. This is required to ensure a full rank solution for the impedance matrix. The computer simulation will define the flawed finite element model as the analytical model, and the ideal beam finite element model as the test model.

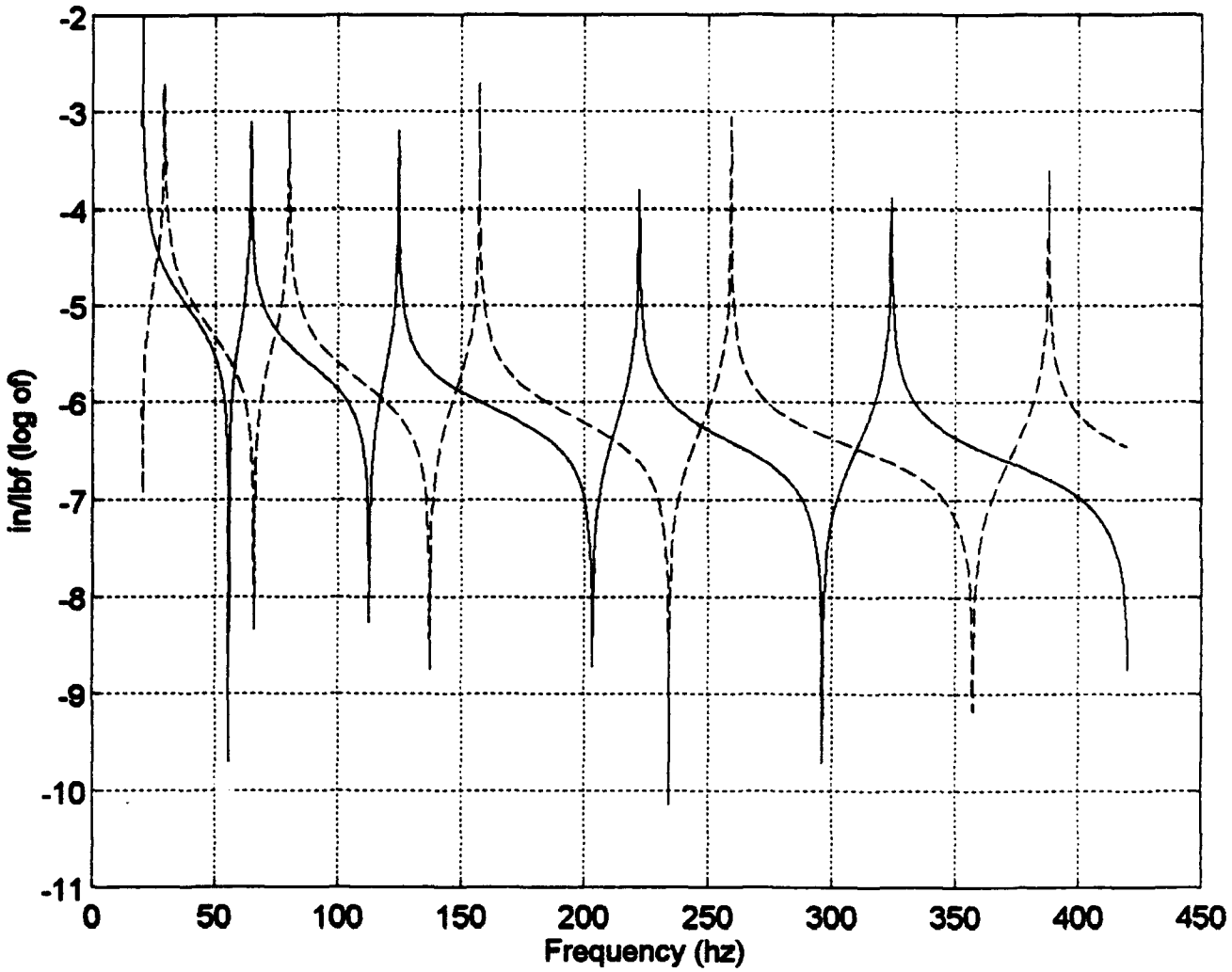

FIGURE 3-4: $H_{11}(\Omega)$
Ideal (—) versus Flawed (- -)
Model - Case I

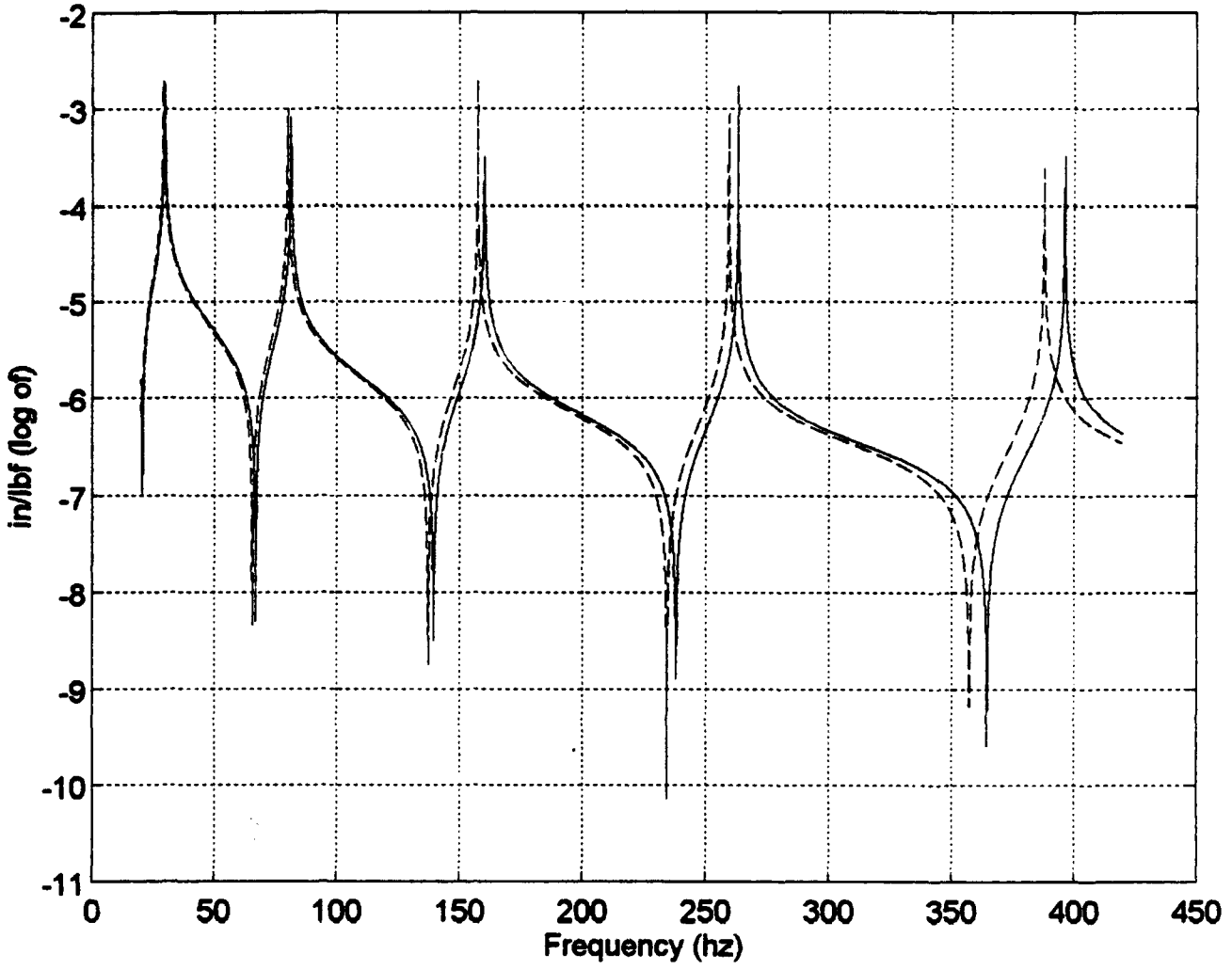

FIGURE 3-5: *$H_{11}(\Omega)$ Ideal (——) versus Flawed (- -) Model - Case II*

A spatially complete localization matrix is calculated and displayed in Figures 3-6 and 3-7. The location of the error described in Figure 3-6 will be a summation of the mass and stiffness errors (Figures 3-1 and 3-2). Since the mass error (Figure 3-2) is zero, the error location in Figure 3-6 matches the error location of Figure 3-1. The results of the spatially complete localization for case II parallels those of case I (Figures 3-7 and 3-3). It is also important to note, that these figures were calculated at a frequency of 50 hz. The figures did not change shape with frequency.

1. Extraction Reduction

Extraction Reduction is the process of extracting selected matrix elements from a given FRF matrix. The selected elements will be associated with those coordinates that have available data. In the computer simulation, the beam is divided into 24 elements, two degrees of freedom per element plus a coordinate at each end. This will result in both the stiffness and mass matrices to be 50x50 elements in size. The FRF matrix, which is calculated from the mass and stiffness matrices, will also be 50x50 elements in size. The goal of the matrix extraction will be to reduce the size of the FRF matrix to 5x5 elements. This will correspond to the translational excitation and response coordinates. Each case will have the localization matrix plotted for three separate frequencies (35,150,350 hz) and an element of the localization matrix plotted over the entire frequency range.

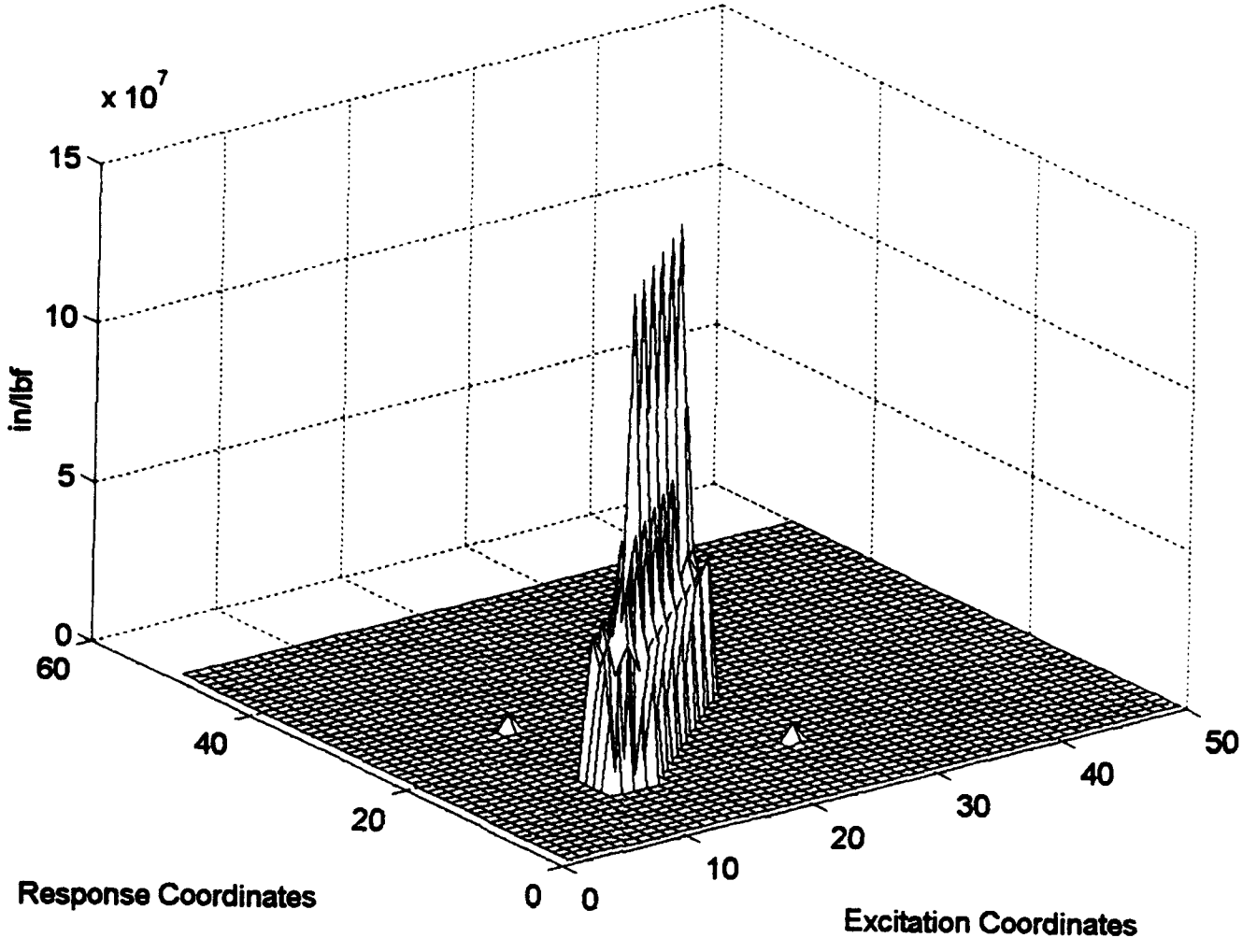

FIGURE **3-6:** *Localization Matrix Spatially Complete Case I*

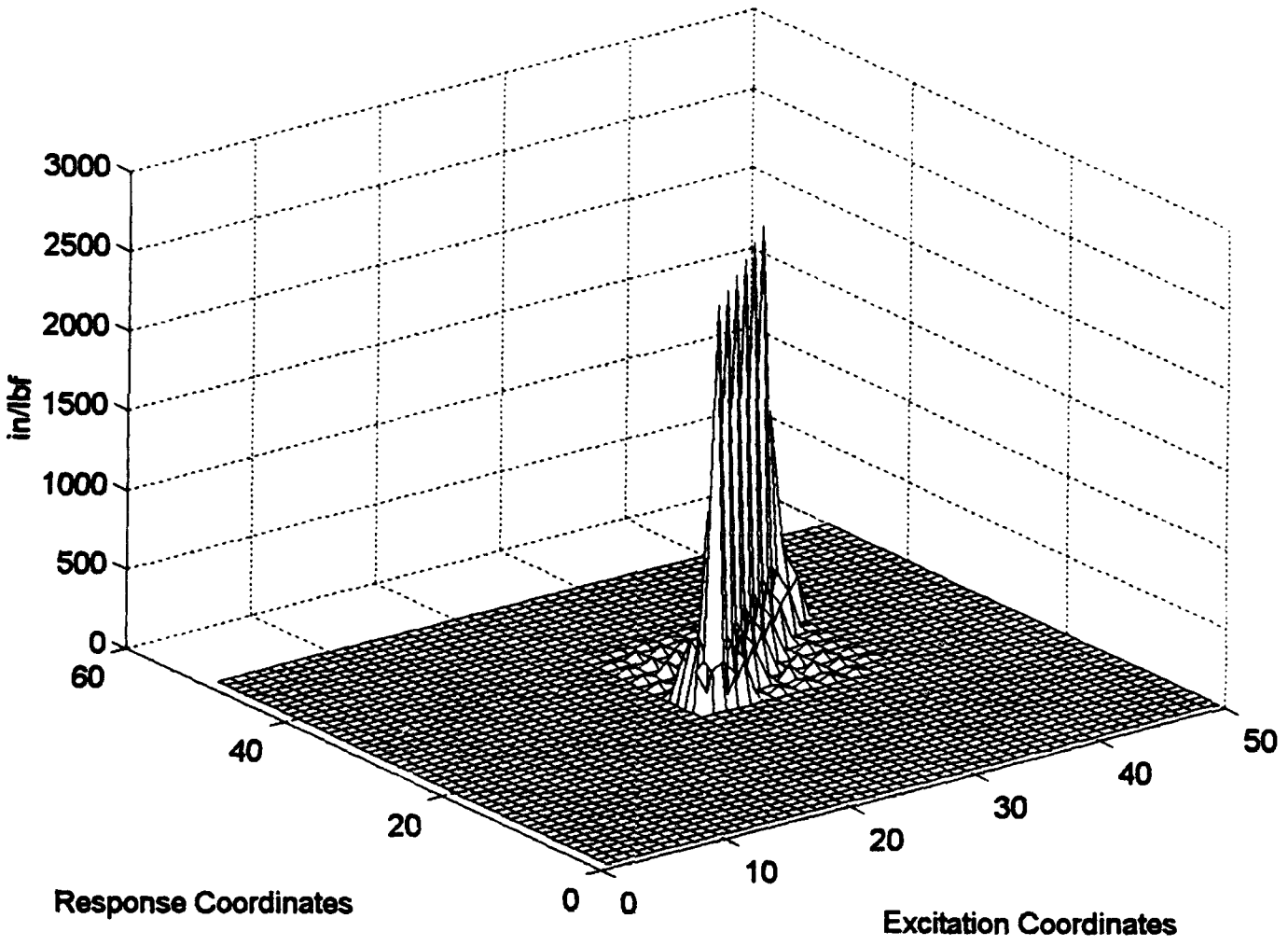

FIGURE 3-7: *Localization Matrix Spatially Complete Case II*

a. Case I (Large Stiffness Error)

Case I involved a large stiffness error between beam elements number two and three. The localization matrix was calculated at three arbitrarily selected frequencies (35,150,350 hz) to ensure spacing throughout the range of 20-420 hz. Figures 3-8 thru 3-10 displays the plots of the localization matrix for the frequencies selected. The actual value of the localization matrix is not the important result, it is the location of that maximum value that is the most meaningful. The location of the maximum value designates the error coordinates and indicates where the significant error exists in the finite element model of the structure. Figures 3-8 and 3-10 indicate an error between the second and third coordinates. Figure 3-9 also shows an error at the third coordinate, with possible errors at the second and fourth coordinates. Figure 3-9 does not conclusively reveal the error location. The overall important result is that these figures correlate with the true error that was installed between the second and third beam elements. These figures also reveal that the localization matrix varies with frequency.

The second calculation involves computing the localization matrix over a frequency range. Figures 3-11 and 3-12 display the plots of the "2,2" and "3,3" elements of the localization matrix over a frequency range of 20 to 420 hz.

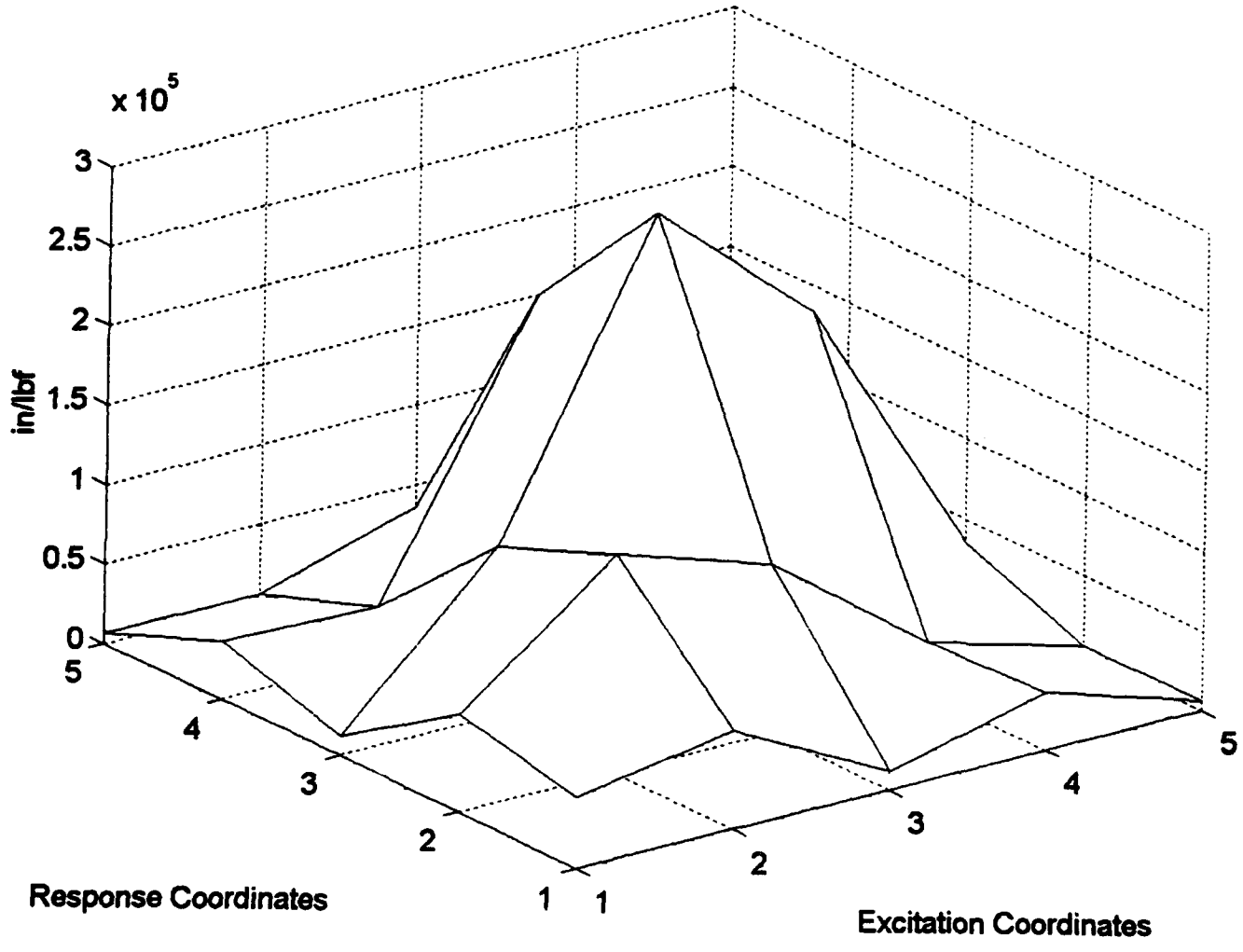

FIGURE 3-8: *Localization Matrix - 35 hz Case I*

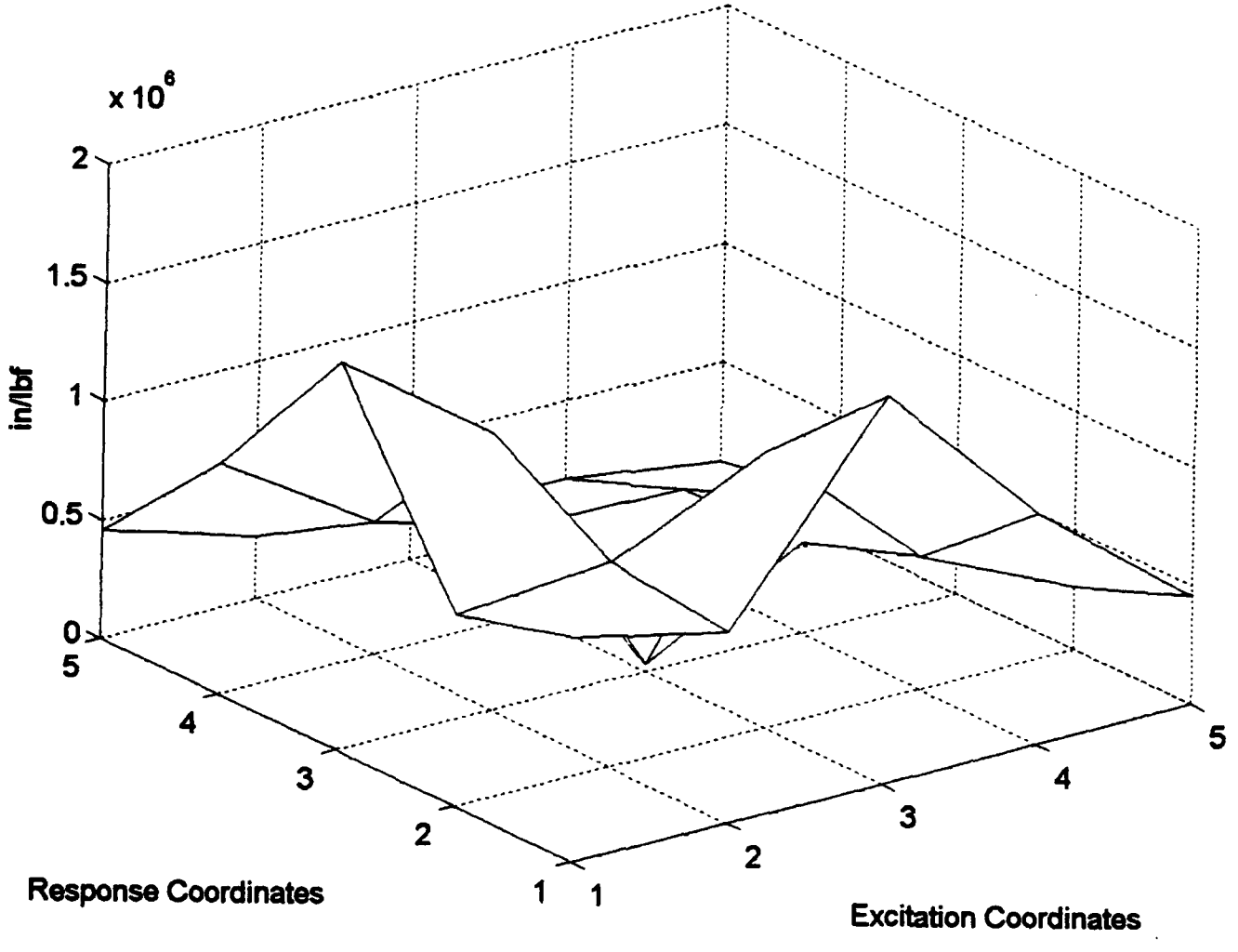

FIGURE 3-9: *Localization Matrix - 150 hz Case I*

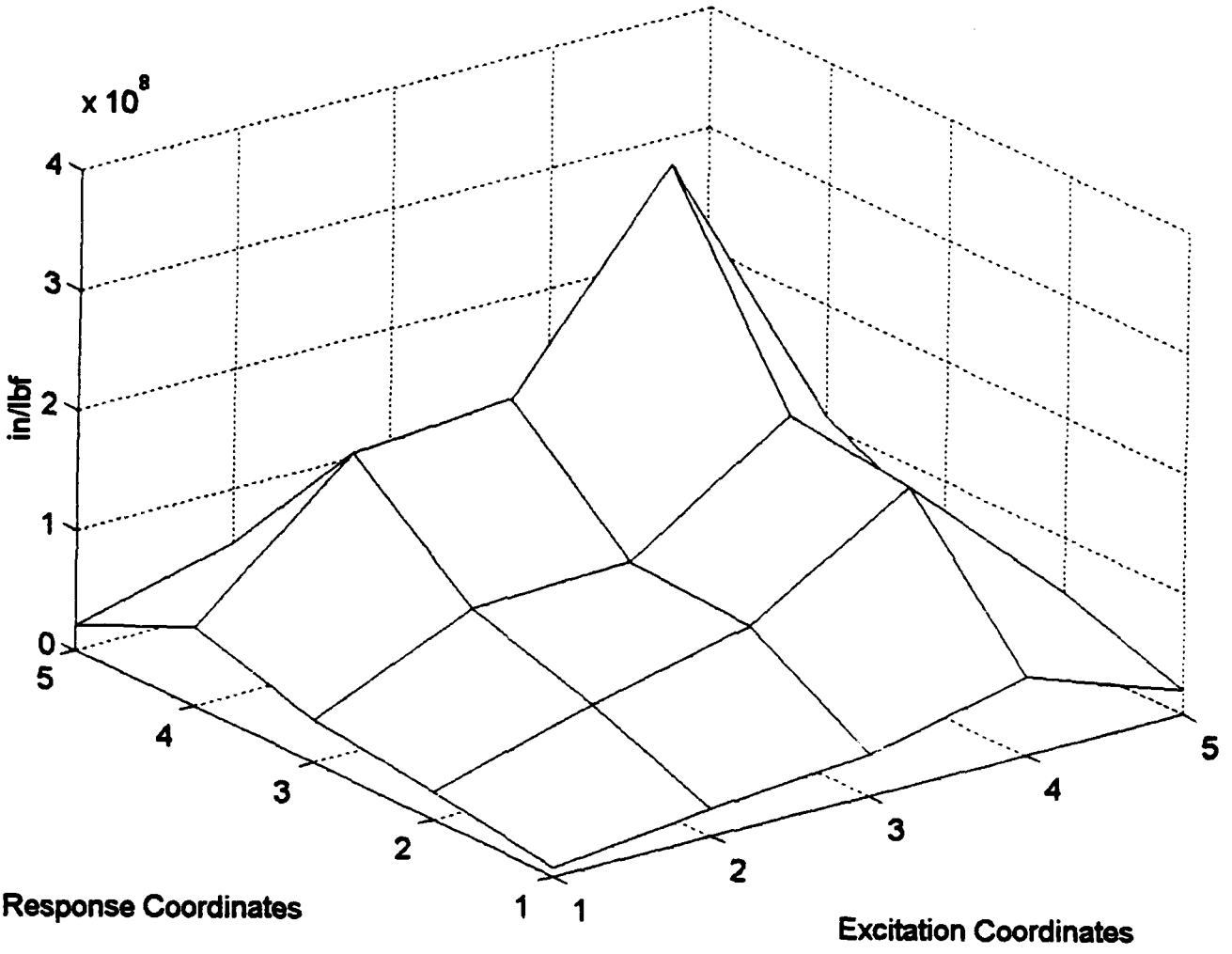

FIGURE **3-10:** *Localization Matrix - 350 hz Case I*

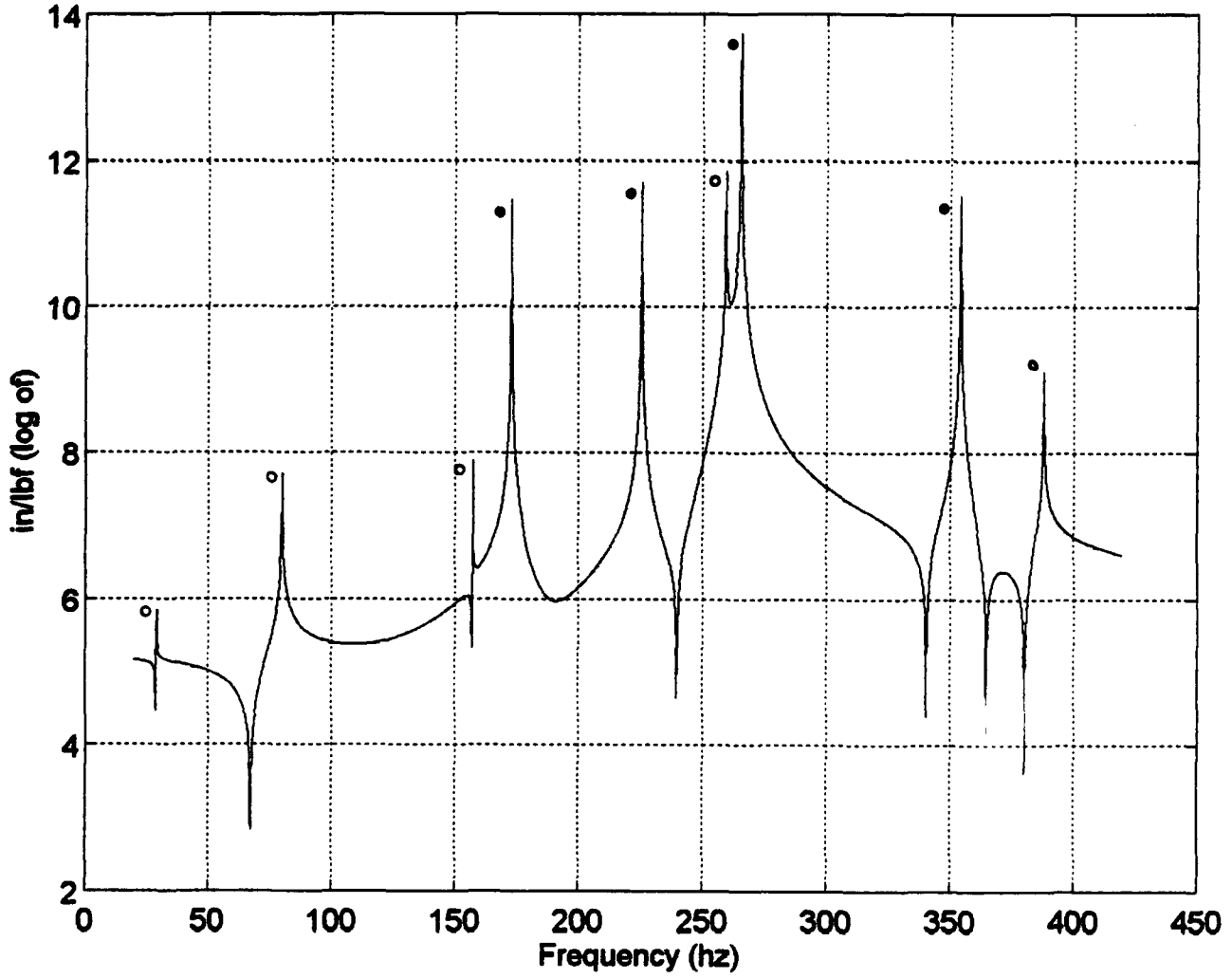

FIGURE 3-11: $L_{22}(\Omega)$

(∘) λ^{x}_{nat} (•) λ^{a}_{oset}

Case I

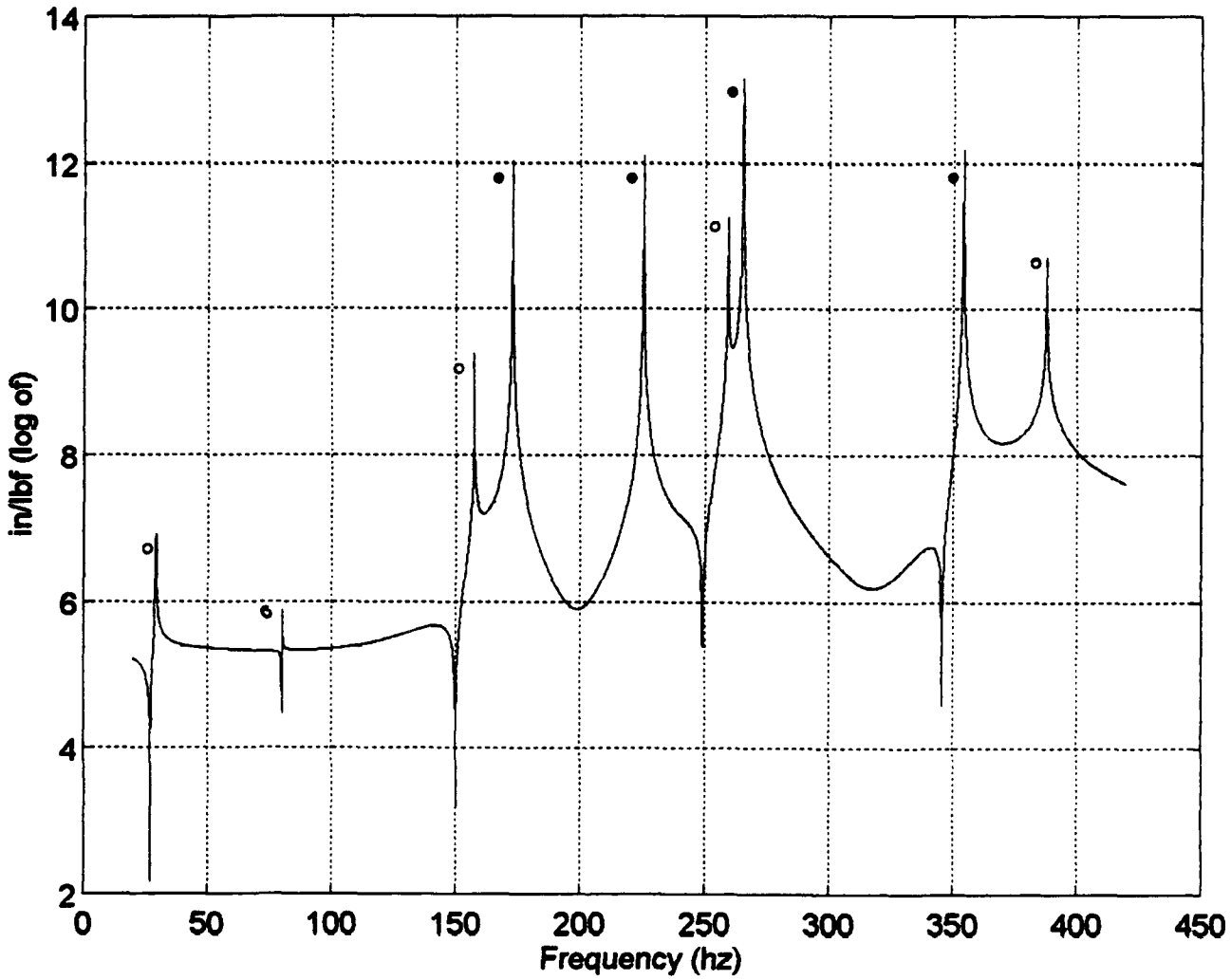

FIGURE 3-12: $L_{33}(\Omega)$
(∘) λ^{x}_{nat} (•) λ^{a}_{oset}
Case I

In comparing Figures 3-11 and 3-12, although the actual value of the elements vary, the peak values occur at the same frequencies. When considering equations (2.24) and (2.22a), large values of the localization matrix element are expected at the test system eigenvalues. Equation (2.34b) indicates that the omitted set impedance will not exist over the entire frequency domain.

$$[Z_{oo}]^{-1} = (\det [Z_{oo}])^{-1} \, adj \, [Z_{oo}] \qquad (3.1a)$$

$$\det [Z_{oo}] = \det [K_{oo} - \omega^2 M_{oo}] \qquad (3.1b)$$

Equation (3.1a) and (3.1b) reveal that for the OSET eigenvalues, the FRF matrix is large (unbounded for undamped systems). The nine peak values in Figures 3-11 and 3-12 correspond to the test model natural frequencies and the eigenvalues of the analytical model omitted coordinates. Table 3-4 provides a summary of the peak frequencies.

TABLE 3-4: PEAK FREQUENCIES - Case I

PEAK FREQUENCY (HZ)	MODEL: TYPE
29.07	Test: Natural Frequency
79.96	Test: Natural Frequency
157.14	Test: Natural Frequency
172.60	Analytical: OSET Frequency
225.34	Analytical: OSET Frequency
259.39	Test: Natural Frequency
265.46	Analytical: OSET Frequency
354.07	Analytical: OSET Frequency
387.05	Test: Natural Frequency

b. Case II (Small Mass Error)

Case II involves a small mass error located between elements number three and four. The localization matrix was calculated at the same frequencies as case I (35, 150, 350 hz), and displayed in Figures 3-13 thru 3-15. It is evident from the figures that a model error is located at the third coordinate. Figures 3-13 and 3-14 show a peak value (although slightly hidden) corresponding to the fourth coordinate. Figure 3-15 shows an error at the second coordinate with a minor error at the fourth coordinate. Figure 3-15 by itself does not conclusively reveal the error location, but the combined evaluation of all three of the mesh plots do provide an approximation to the location of the installed model error. When comparing the results of case II with those of case I (Figures 3-8 thru 3-10), the localization matrix values of case II are smaller in magnitude, but spatial identification of the error locations are more apparent in case II. The localization matrix was also calculated on a frequency domain with a similar procedure used in case I. Figures 3-16 and 3-17 display the plots of the "3,3" and "4,4" elements of the localization matrix. As in case I, the plots associated with case II display peak values at the test system natural frequencies and the analytical model OSET eigenvalues. Table 3-5 provides a summary of these results.

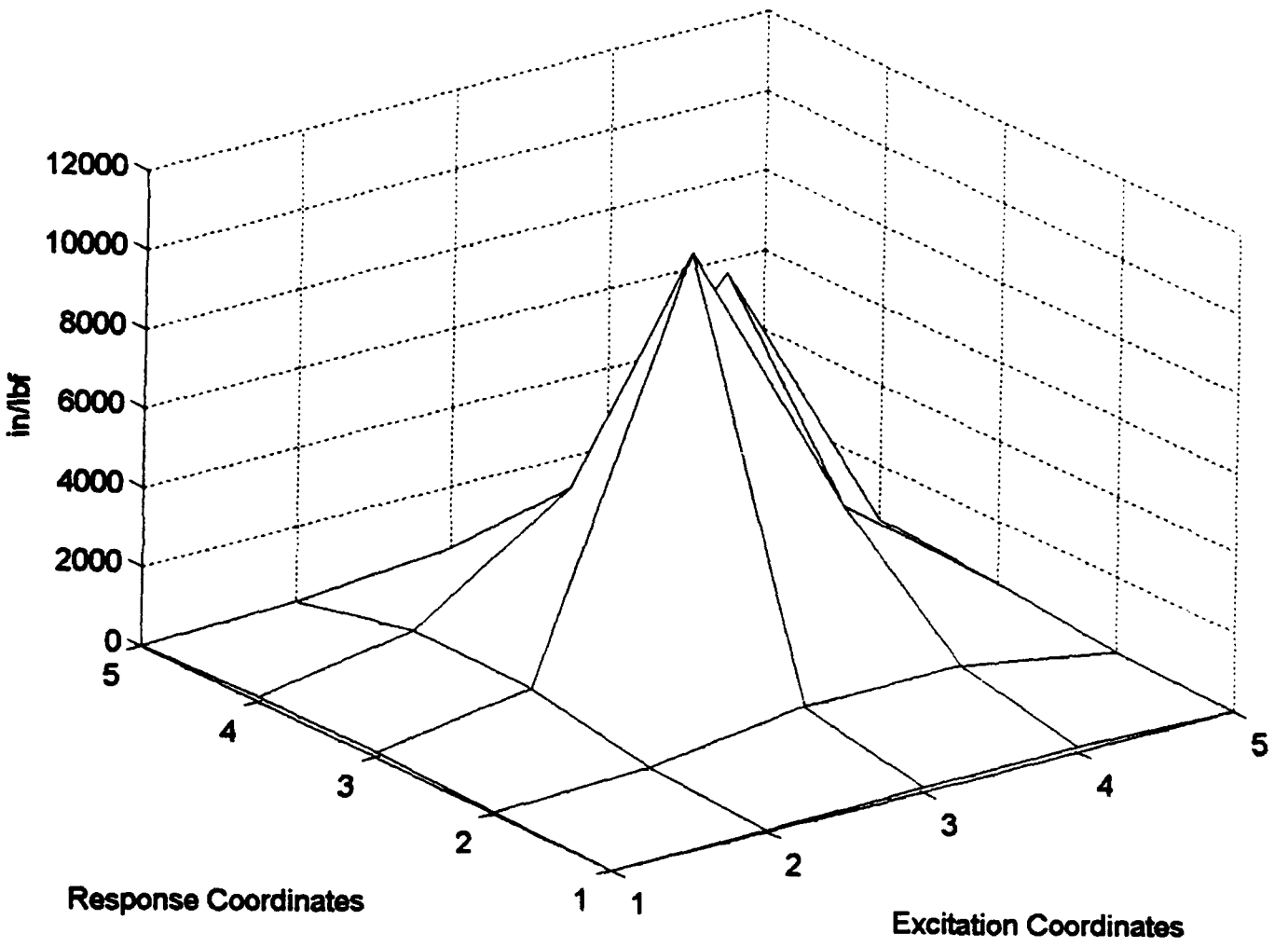

FIGURE *3-13: Localization Matrix - 35 hz Case II*

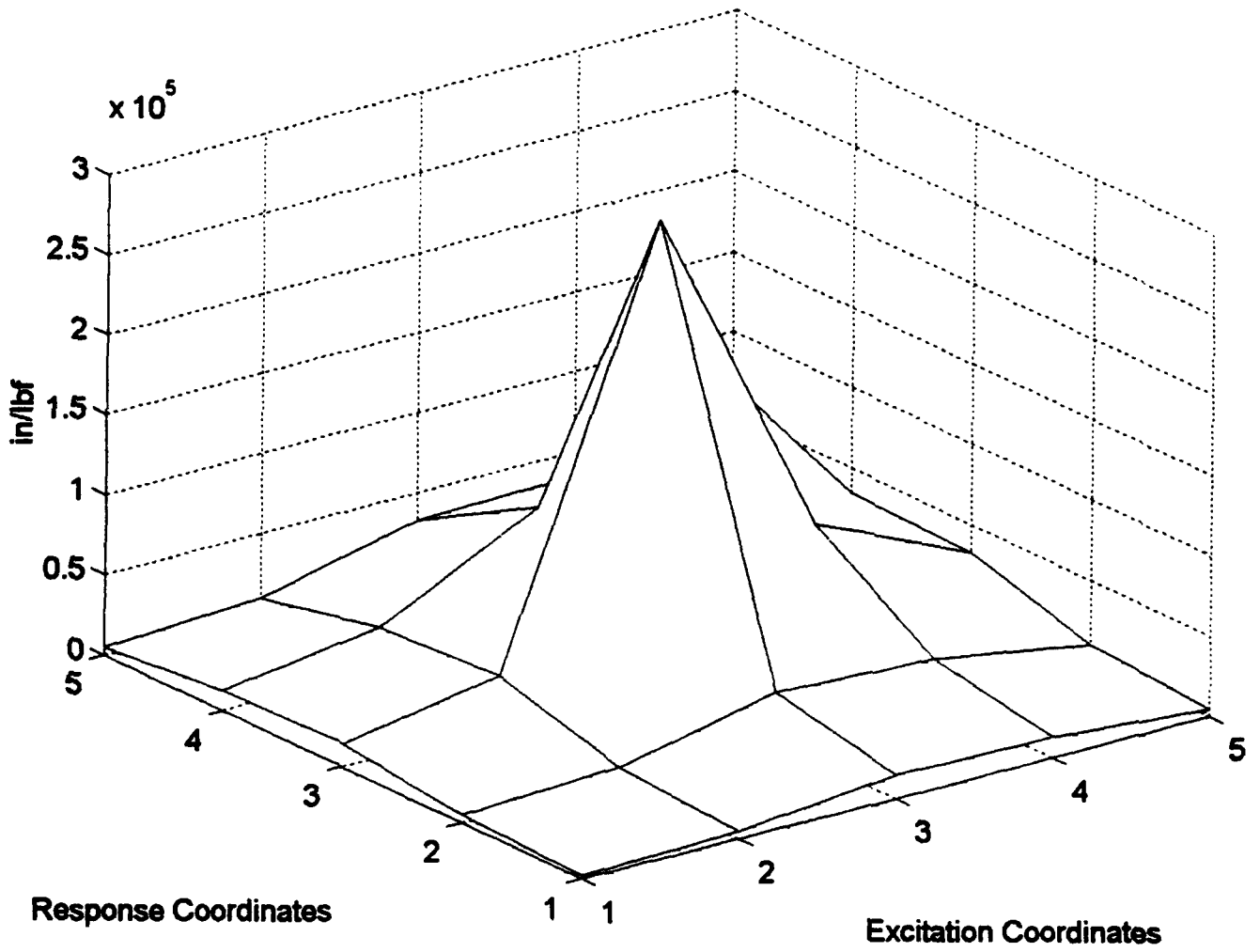

FIGURE 3-14: *Localization Matrix - 150 hz Case II*

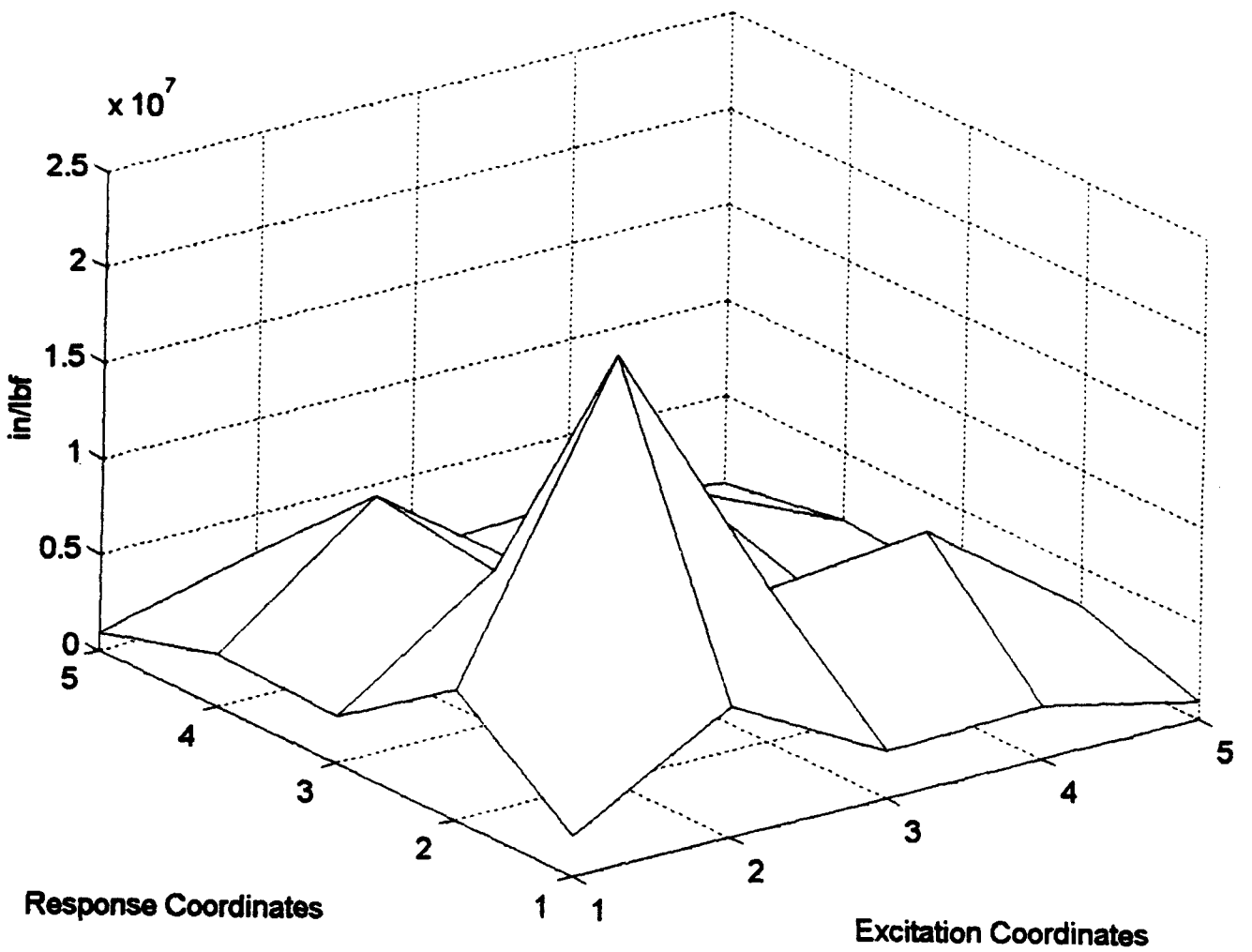

FIGURE 3-15: *Localization Matrix - 350 hz Case II*

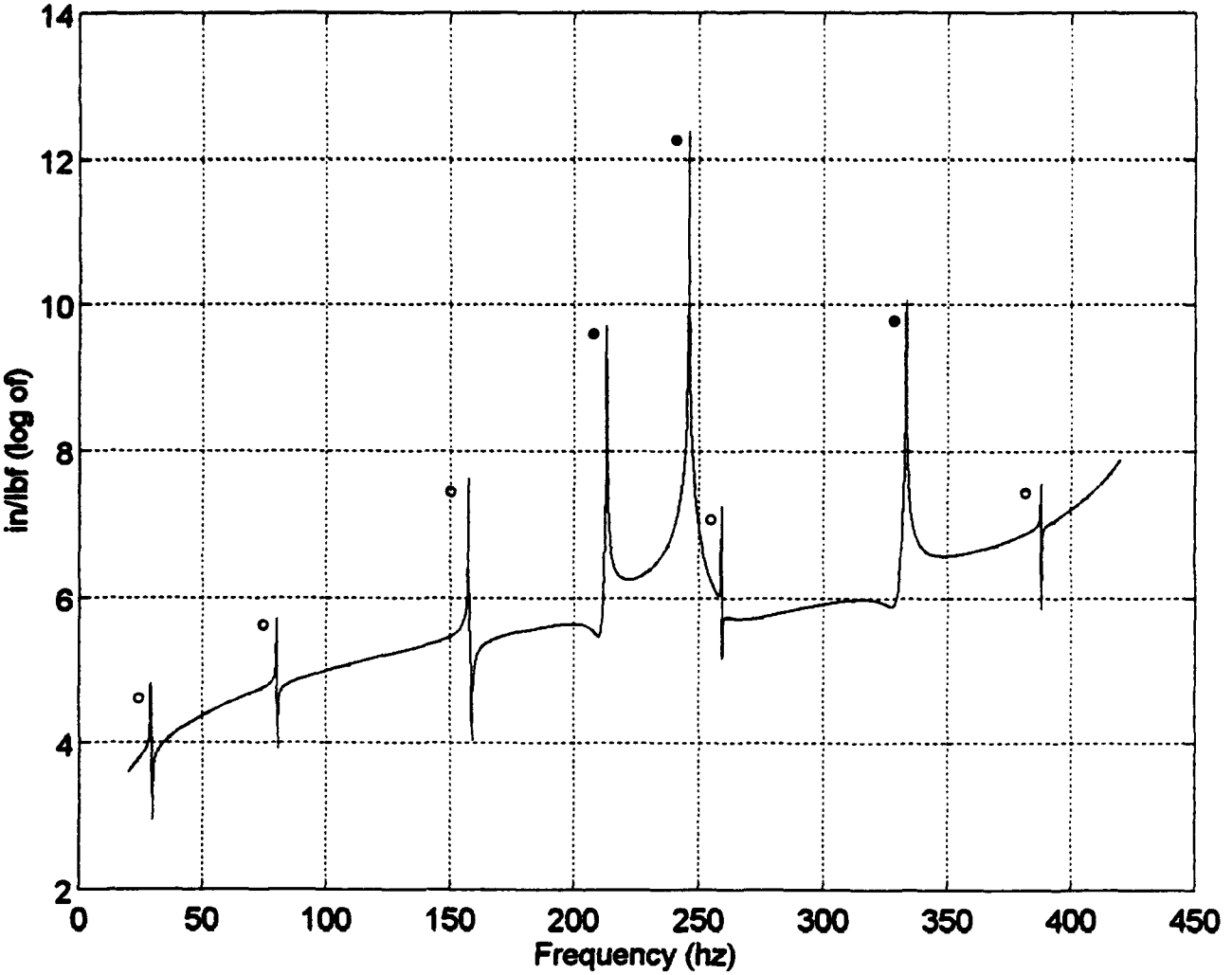

FIGURE 3-16: $L_{33}(\Omega)$
(∘) λ^{x}_{nat} (•) λ^{a}_{oset}
Case II

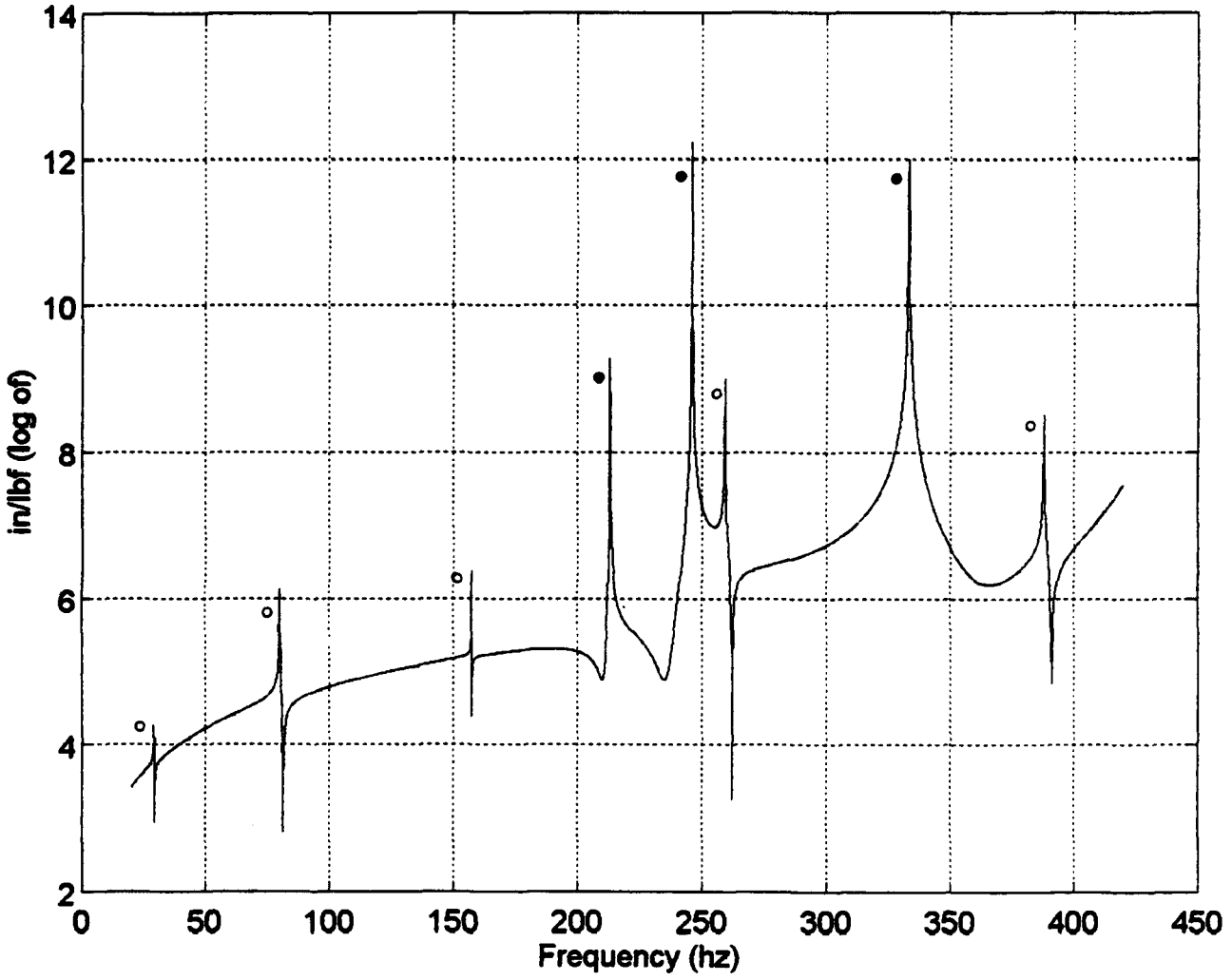

FIGURE 3-17: $L_{44}(\Omega)$
(∘) λ^{x}_{nat} (•) λ^{a}_{oset}
Case II

TABLE 3-5: PEAK FREQUENCIES - CASE II

PEAK FREQUENCY (HZ)	MODEL: TYPE
29.07	Test: Natural Frequency
79.96	Test: Natural Frequency
157.14	Test: Natural Frequency
213.03	Analytical: OSET Frequency
246.12	Analytical: OSET Frequency
259.39	Test: Natural Frequency
333.20	Analytical: OSET Frequency
387.85	Test: Natural Frequency

2. Improved Reduction System (IRS)

Matrix reduction uses the IRS reduction as described in Section II.E.2. The computer simulation will reduce the flawed and ideal model frequency response functions from a 50x50 element matrix to a 5x5 element matrix. The five elements in the reduced matrix will pertain to the translational excitation and response coordinates. In analyzing real structures, the test FRF matrix will already be in the reduced format. It is important to note that the purpose of the matrix reduction is to reduce the analytical model FRF matrix to a size equivalent to that of the test FRF matrix. For the purpose of the computer simulation, the ideal beam model (defined as the test model) will be reduced via extraction reduction in order to reproduce the reduction process inherent in spatially incomplete measurements. The flawed finite element model (defined as the analytical model) will be reduced via IRS.

a. Case I (Large Stiffness Error)

The same calculations that were performed using the extraction reduction method were repeated using the IRS reduction method. The first calculation for determining the localization matrix at a specific frequency was performed at three frequencies (35, 150, 350 hz) and the results are displayed in Figures 3-18 thru 3-20. The first result is that the estimation of the model error location is not identifiable in any of the three figures. The actual value of the localization matrix are seven orders of magnitude higher than the corresponding values for the extraction reduction method. The reason that the error location is not identifiable is that the stiffness and mass matrices are transformed into new coordinates. This effectively hides the location of the model error. The second calculation was to determine the localization matrix over a frequency domain. Figures 3-21 and 3-22 display the plot of the "2,2" and "3,3" elements of the Localization Matrix over a frequency domain of 20 to 420 hz. Since the reduced FRF matrix does not involve the OSET impedance, the singularities expected with the eigenvalues of the analytical model OSET coordinates disappear. The test model natural frequencies continue to appear in both figures 3-21 and 3-22.

b. Case II (Small Mass Error)

Case II results are the same as those of case I. No plots of Case II are provided.

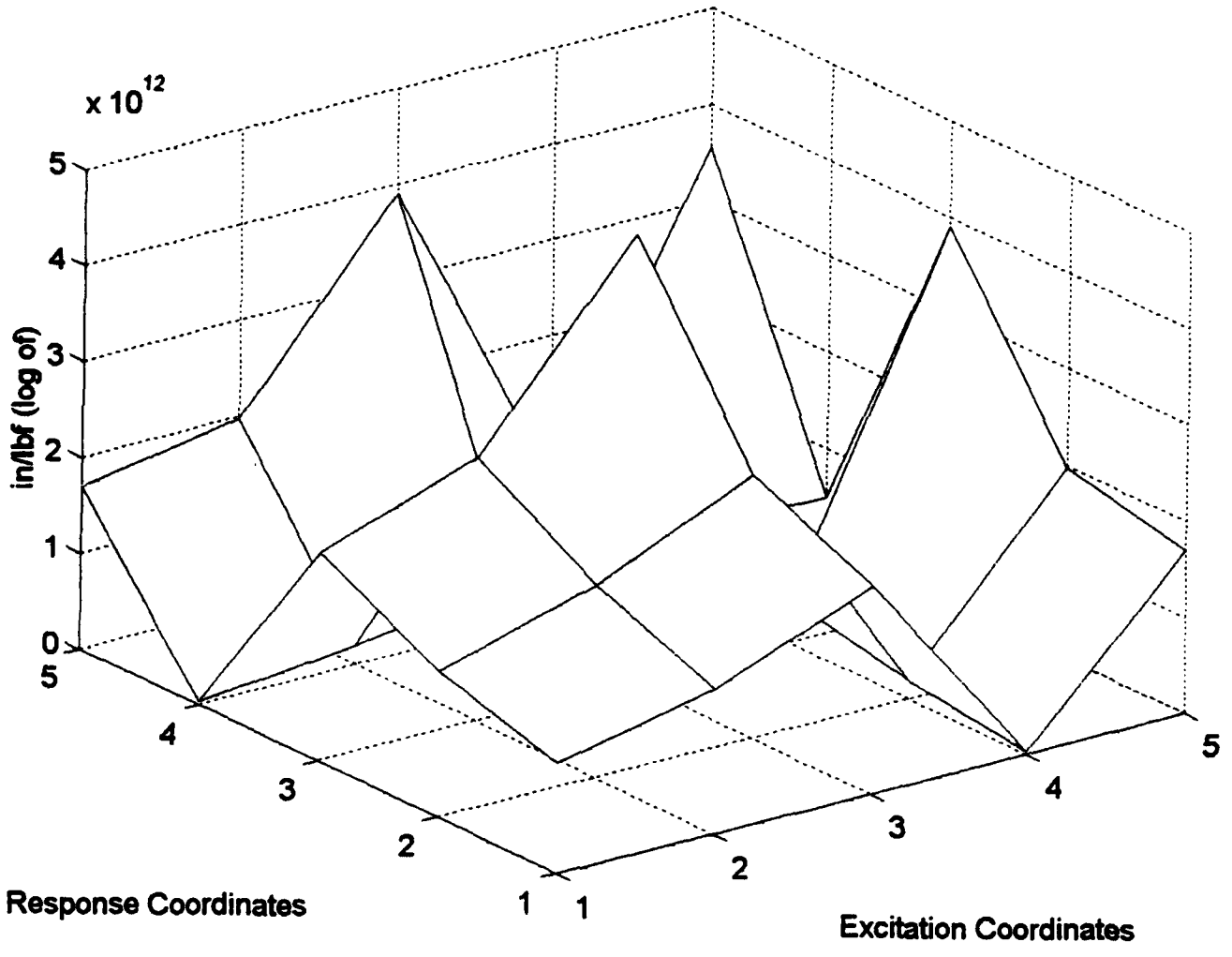

FIGURE 3-18: *Localization Matrix - 35 hz Case I (IRS)*

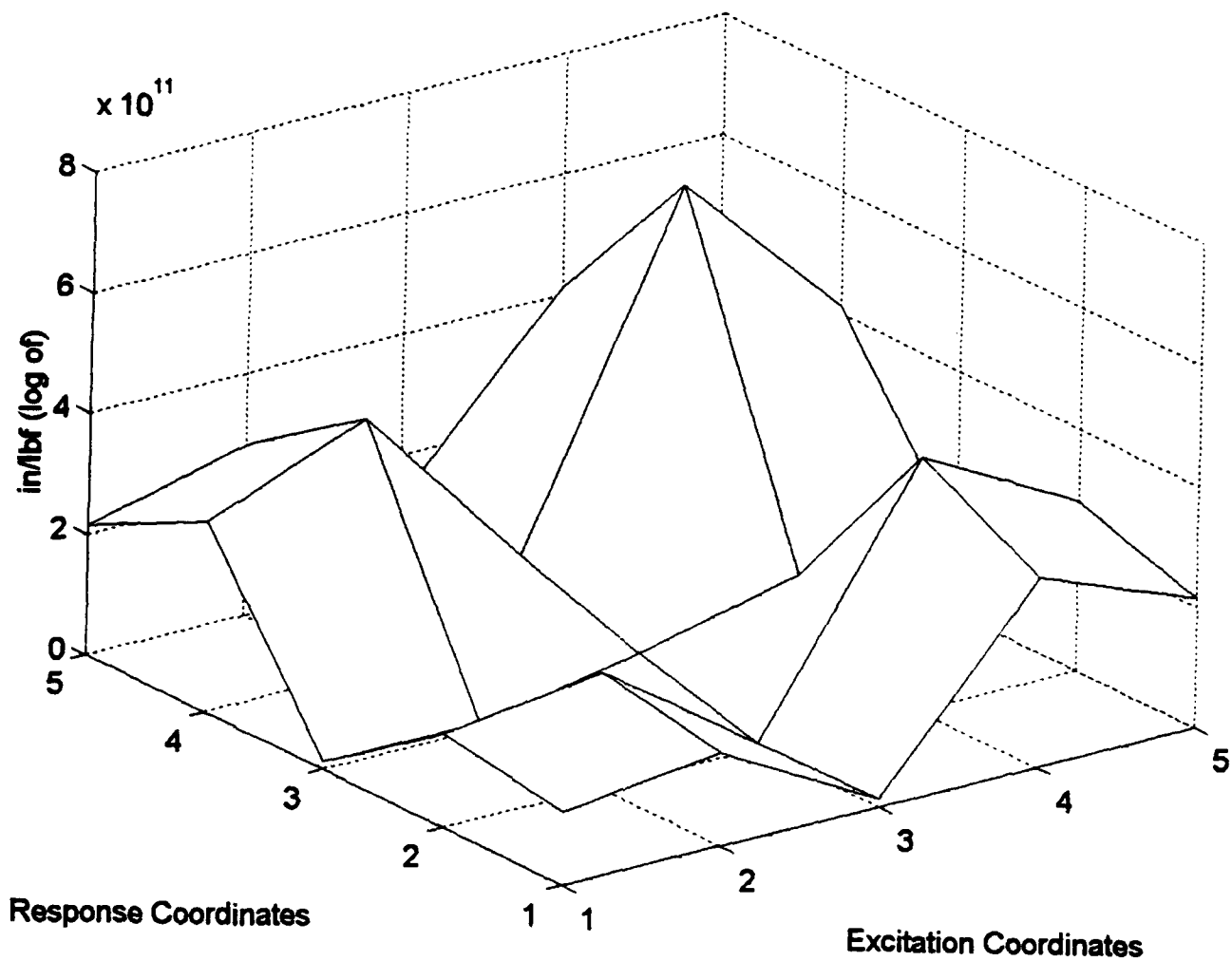

FIGURE 3-19: *Localization Matrix* - 150 *hz Case I* (*IRS*)

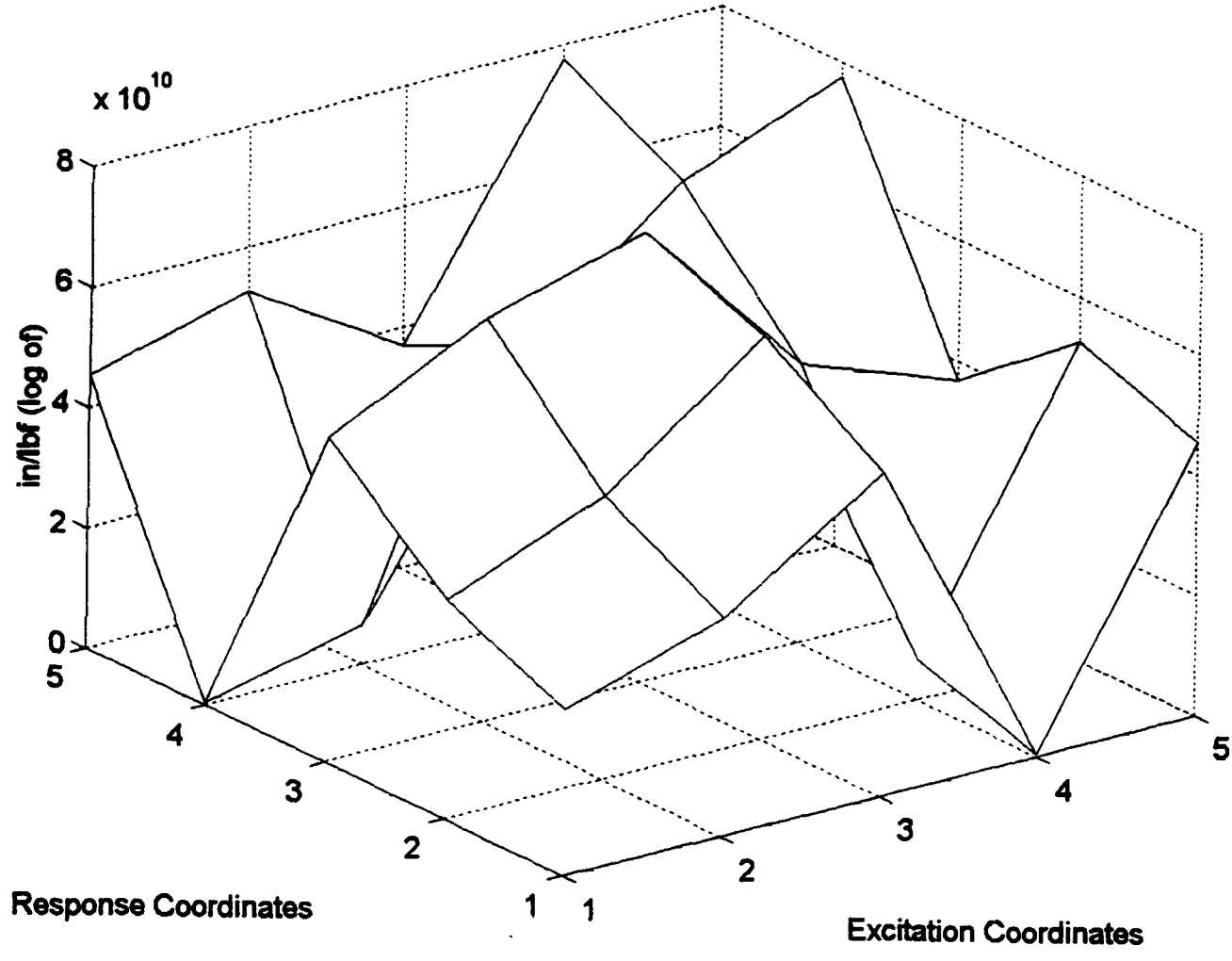

FIGURE 3-20: *Localization Matrix - 350 hz Case I (IRS)*

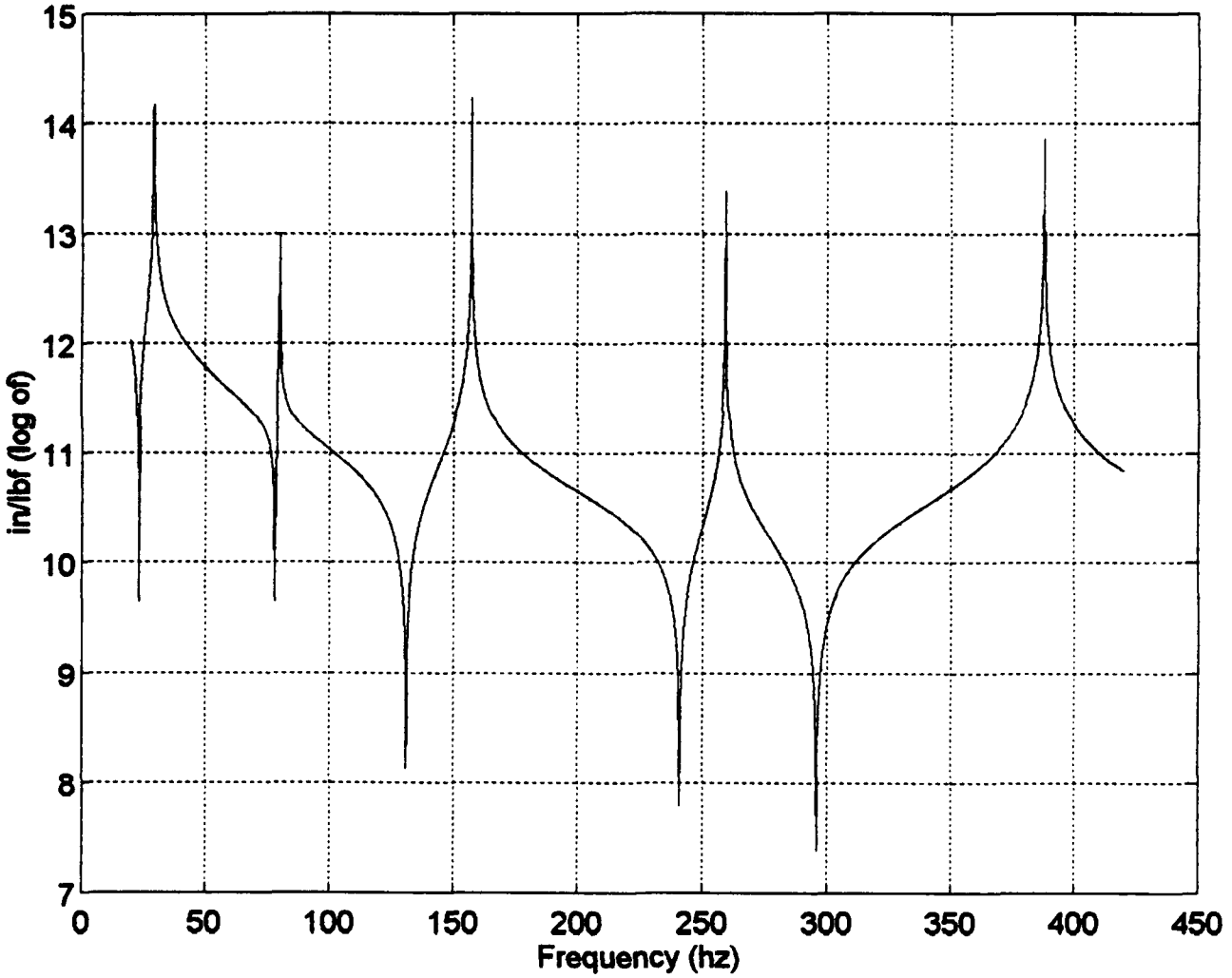

FIGURE 3-21: L_{22} (Ω)
CASE I (IRS)

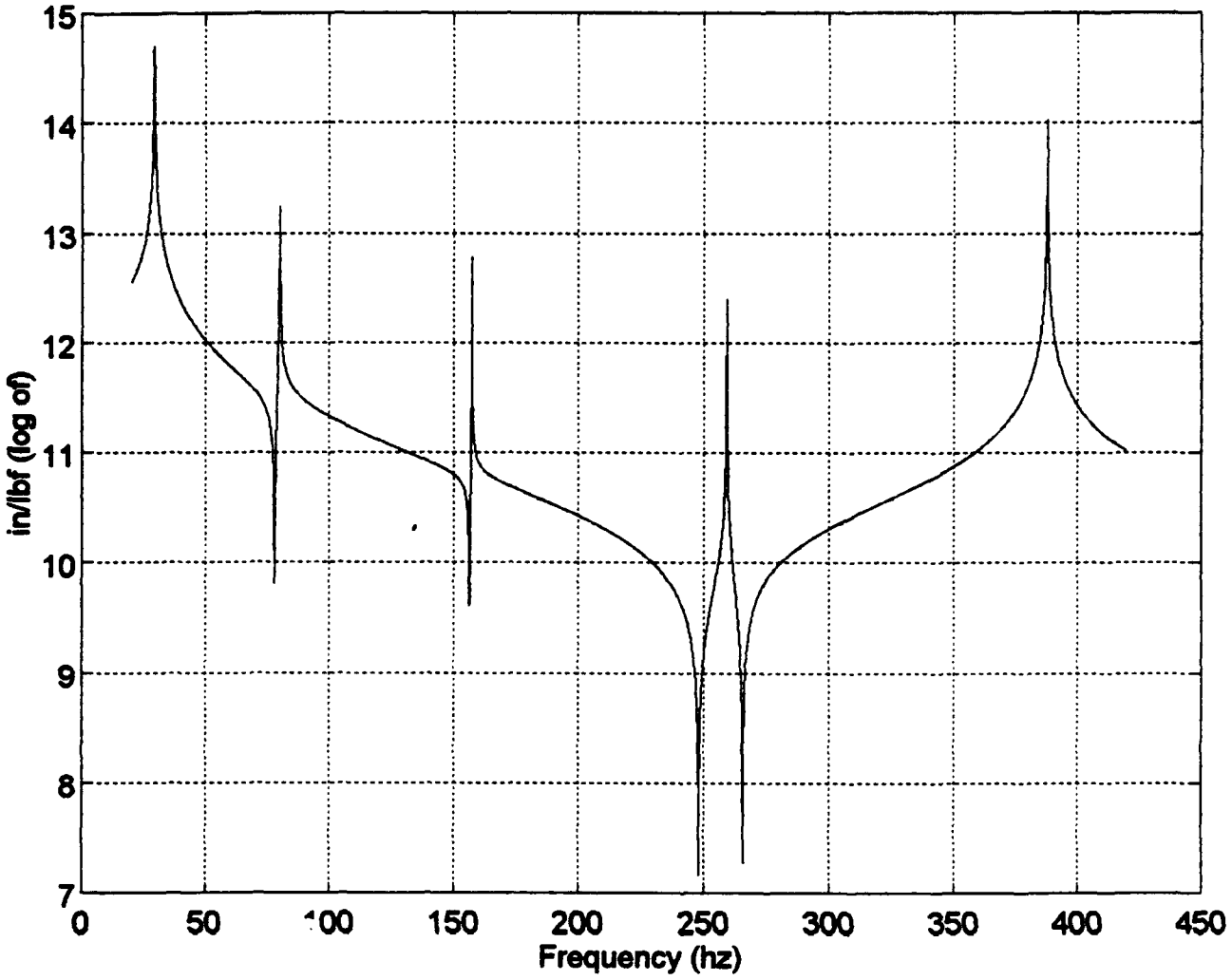

FIGURE 3-22: L_{33} (Ω)
CASE I (IRS)

C. IMPEDANCE ERROR SPECTRA

Equation (2.3) describes the impedance error between the analytical and test models. Equations (2.29a) and (2.29b) provide a method for calculating the impedance error using the analytical and test frequency response functions. The computer simulation will be performed in the same manner as Section III.B to calculate the impedance error for spatially incomplete data.

1. Extraction Reduction

In trying to predict the behavior of the impedance error spectra, equation (2.3) can be considered in the equivalent form (equation (3.2)) in conjunction with equation (2.34b).

$$\Delta Z = Z_{cc}^{x}(\Omega_i) - Z_{cc}^{a}(\Omega_i) \qquad (3.2)$$

The result of this analysis is that for extraction reduction, the impedance error spectra will be large (unbounded for undamped systems) at the OSET eigenvalues of both the analytical and test models.

a. Case I (Large Stiffness Error)

Figure 3-23 is a plot of the "1,1" element of the impedance error over a frequency domain of 20 to 420 hz. All five coordinates from the reduced FRF matrix were used in the calculations. The OSET eigenvalues for both the analytical and test models appear as peak values in the figure. Table 3-6 provides a summary of the peak values.

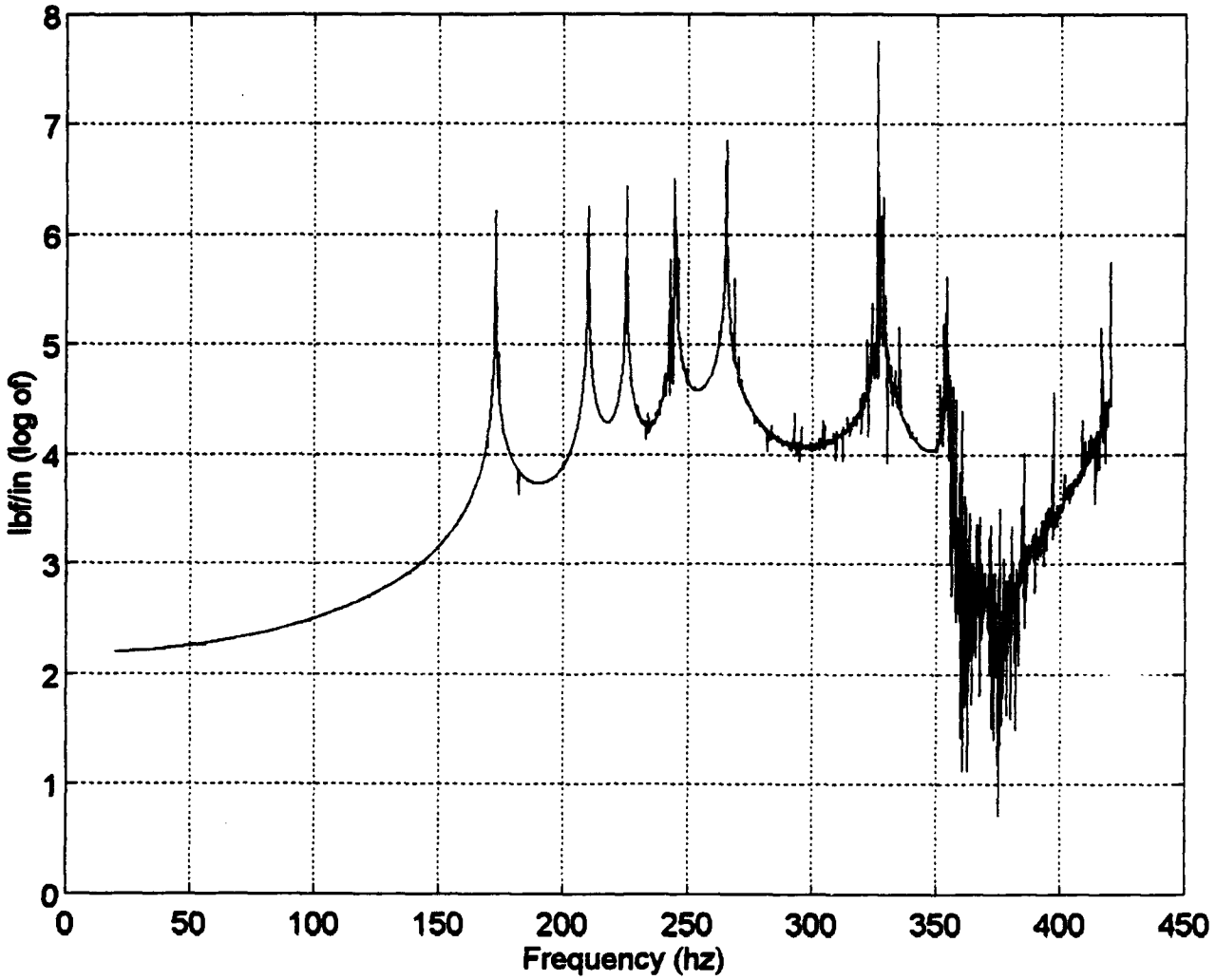

FIGURE 3-23: *$\Delta Z_{11}(\Omega)$ - Case I Extraction Reduction*

TABLE 3-6: OSET EIGENVALUES - CASE I

Analytical Model (hz)	Test Model (hz)
172.60	209.92
225.34	244.90
265.46	327.96
354.07	423.79

Equations (2.34a) and (2.34b) reveal that given the location of the error coordinates from the localization matrix (Figures 3-8 thru 3-10), the calculations of the impedance matrix must be performed by using only the error coordinates instead of the entire reduced matrix. Figure 3-24 is a plot of the impedance error over a frequency domain, using the error coordinates identified from the localization matrix (coordinates two thru four) in the impedance error calculations. The results are not consistent with those of Figure 3-23. A closer investigation of Figures 3-8 thru 3-10 indicates that neglecting coordinates one and five as insignificant was not a good assumption. Values of the localization matrix at these coordinates, although small, are not insignificant. The poor assumption induces an error in the impedance error calculation and causes the plot to be inaccurate. Figure 3-23 also displays a significant amount of "noise" in the plot. This noise is a result of the large difference between the FRF models creating a situation of inverting poorly conditioned matrices during the impedance error calculations.

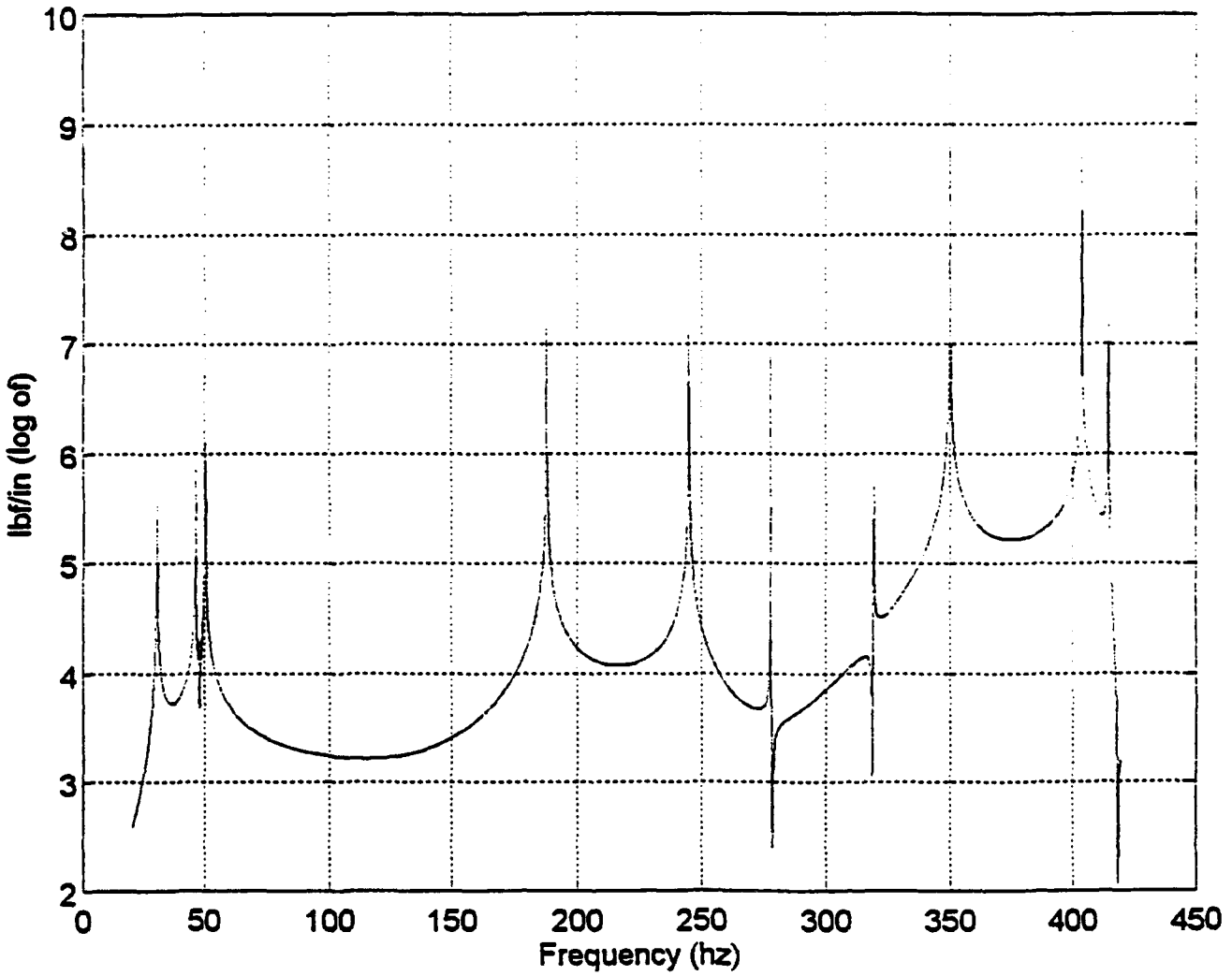

FIGURE 3-24: $\Delta Z_{11}(\Omega)$
Error Coordinates #2 thru #4
Extraction - Case I

b. Case II (Small Mass Error)

Figure 3-25 is the same plot as figure 3-23 with the exception that it applies to case II. The OSET eigenvalues for both the analytical and test models also appear in this figure. Table 3-7 provides the case II summary of the peak values in Figure 3-25.

TABLE 3-7: OSET EIGENVALUES - CASE II

Analytical Model (hz)	Test Model (hz)
213.03	209.92
246.12	244.90
333.20	327.96

2. IRS Reduction

The reduced FRF matrices are not dependent upon the OSET coordinates. The eigenvalues from the OSET coordinates associated with the analytical model do not appear in the impedance error plot. Figures 3-26 and 3-27 display the impedance error calculations using IRS reduction, utilizing all the error coordinates, of case I and case II respectively. The test system OSET coordinate eigenvalues listed in Tables 3-6 and 3-7 appear as peak values in both figures. Since case I and case II have identical OSET eigenvalues for the test system, Figures 3-26 and 3-27 are identical.

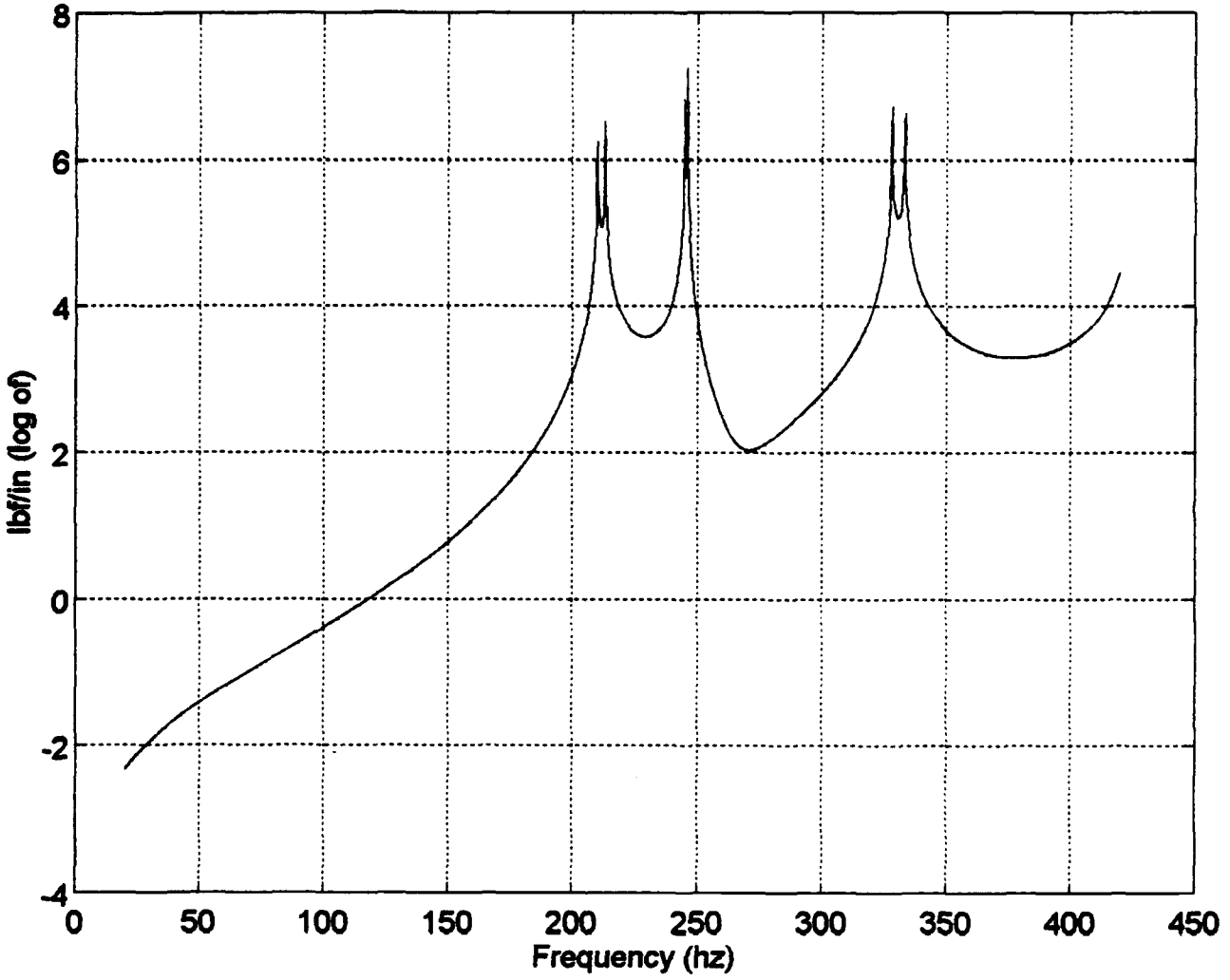

FIGURE 3-25: ΔZ_{11} (Ω) - *Case II Extraction Reduction*

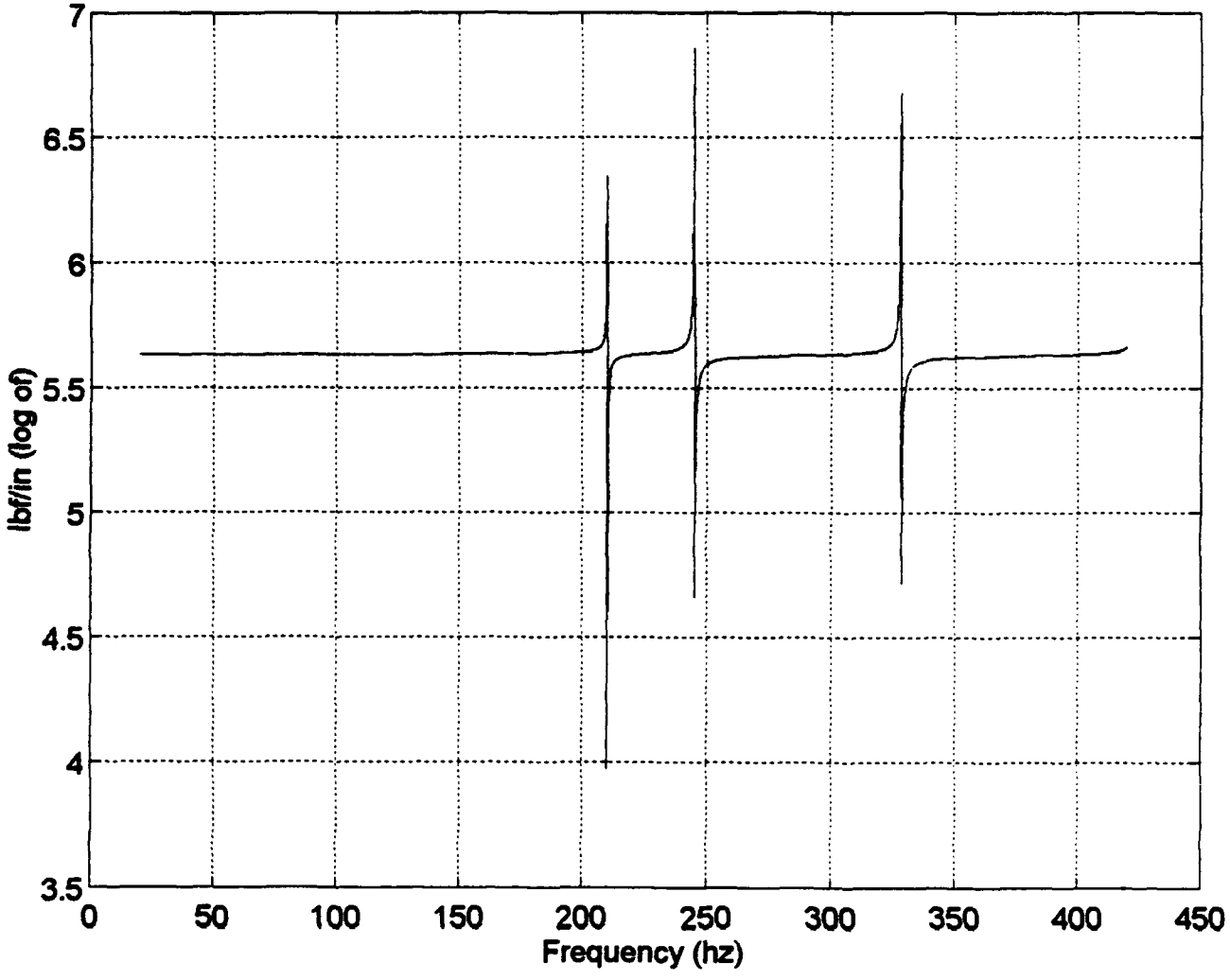

FIGURE 3-26: *ΔZ_{11} (Ω) - CASE I IRS Reduction*

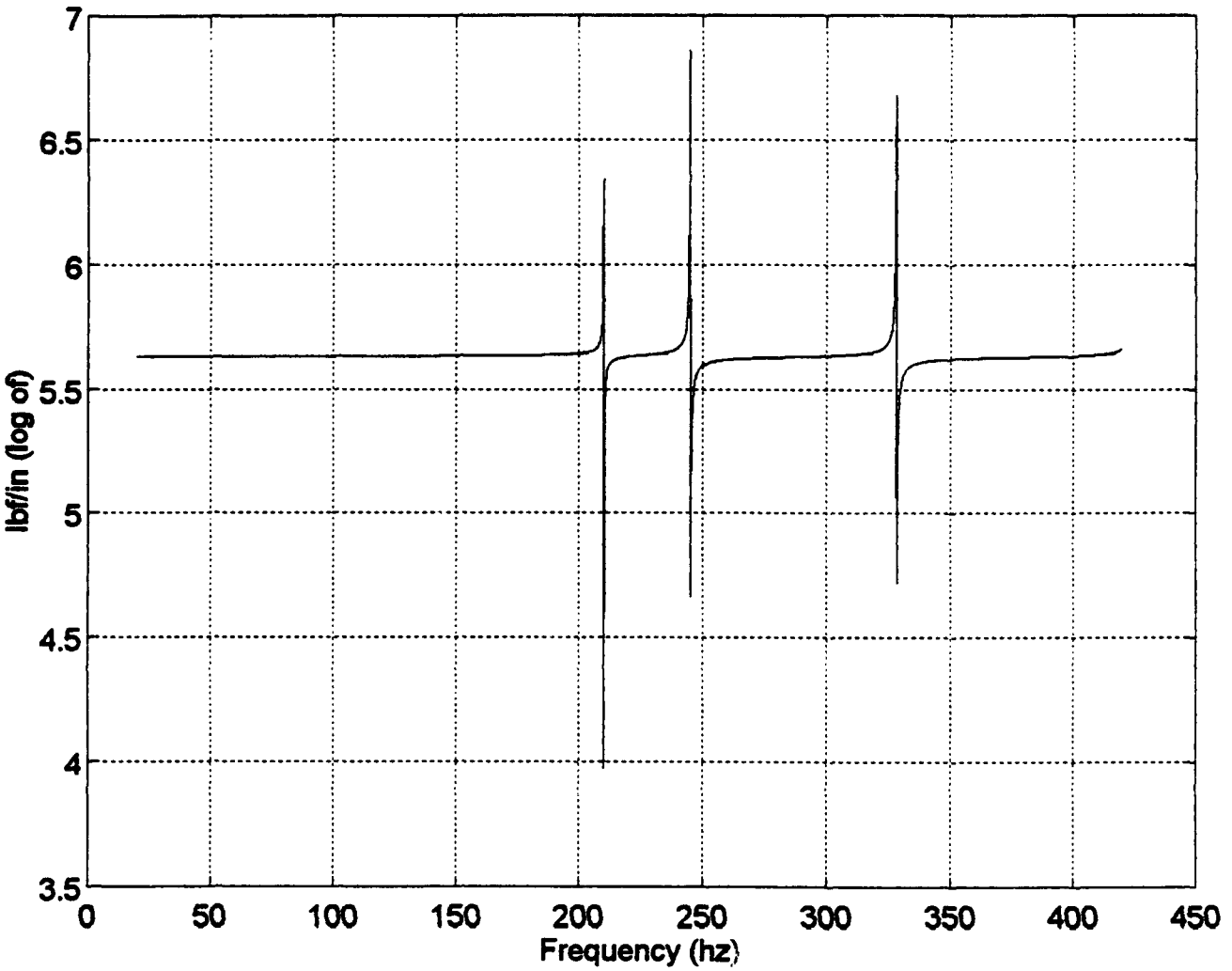

FIGURE 3-27: *ΔZ_{11} (Ω) - CASE II IRS Reduction*

IV. EXPERIMENTAL RESULTS

A. GENERAL

In section III, an analysis of two case studies was performed involving structural system identification of a flawed beam finite element model with an ideal beam finite element model. In this section, the same two case studies will be analyzed, using the same flawed beam finite element models of Section III with experimental FRF data. Details about the procedures used in obtaining and arranging the experimental FRF data is described in Appendix A.

The experimental FRF matrix is obtained in a spatially incomplete form. The experimental FRF matrix elements are made up of coordinates that correspond to the locations in which the structure response and excitation can be measured. The process of structural system identification requires that the sizes of the experimental and analytical model FRF matrix to be equivalent. Thus, the analytical model FRF matrix must be reduced to the same size as the experimental FRF matrix.

B. LOCALIZATION MATRIX

1. Extraction Reduction

The flawed beam finite element model is defined as the analytical model. The analytical model FRF matrix will be reduced by extraction. The translational excitation and response locations will be the retained coordinates.

a. Case I (Large Stiffness Error)

The first calculation performed was determining the localization matrix at a specific frequency. The same frequencies used in Section III (35, 150, 350 hz) are used in this section.

Figures 4-1 thru 4-3 display the results of the localization matrix at the selected frequencies. The initial observation is that larger values of model errors are associated with the second, third, and fourth coordinates. Figure 4-3 emphasizes larger model errors associated with the third and fourth coordinates. Comparing Figures 4-1 thru 4-3 with the appropriate figures from the computer simulation (Figures 3-8 thru 3-10), two of the three figures exhibit similar shapes (location of large model errors). The localization matrix determination with the experimental system does not explicitly identify the actual installed error located between the second and third elements as well as the computer simulation. It must be remembered that although known as an ideal beam model, modeling errors do exist within the ideal beam model when compared with the experimental system. The flawed beam finite element model is based upon the ideal beam finite element model. Therefore, Figures 4-1 thru 4-3 will display errors associated with both the flawed beam and ideal beam finite element models, while Figures 3-8 thru 3-10 only display errors associated with the flawed beam finite element model.

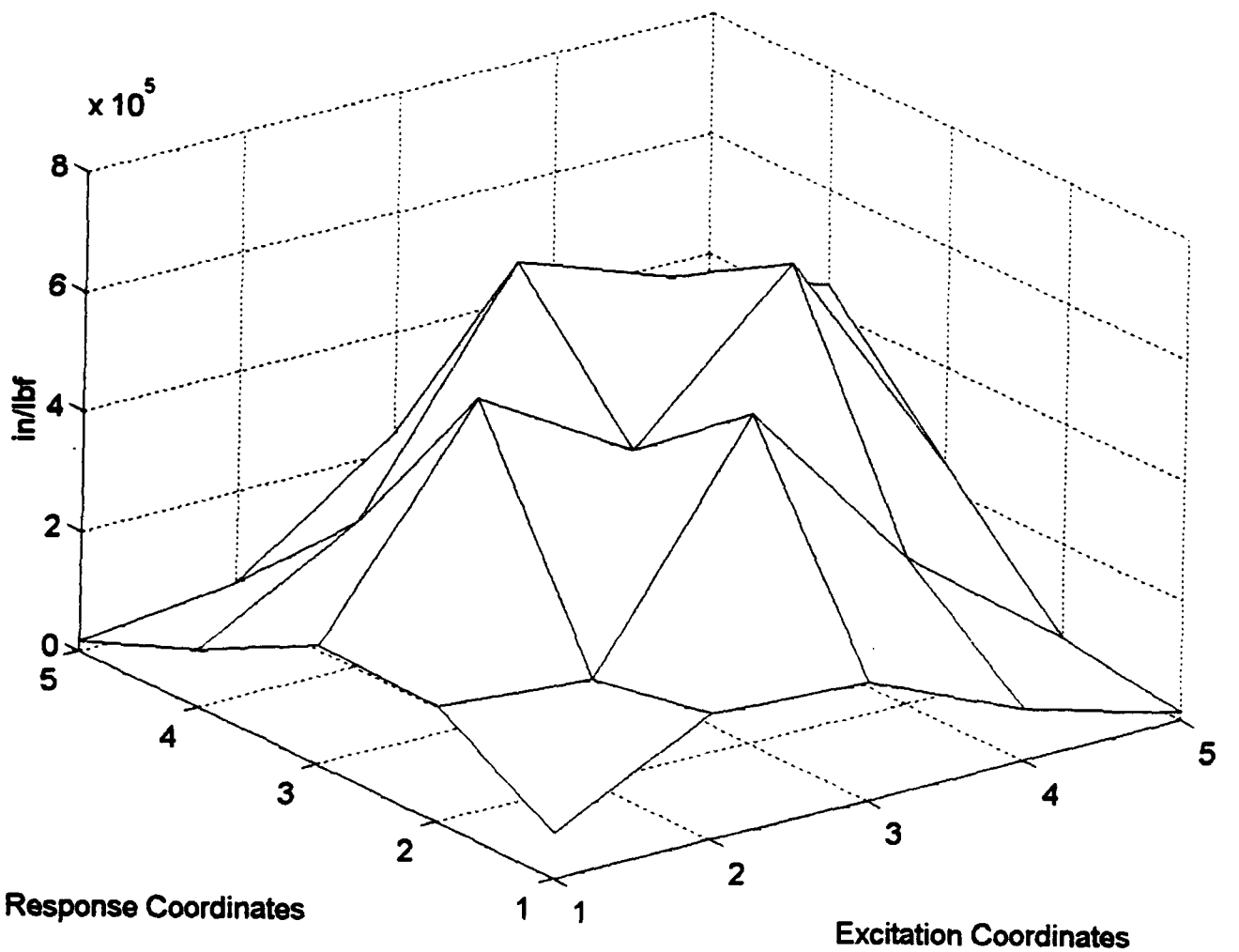

FIGURE *4-1: Localization Matrix - 35 hz Case I*

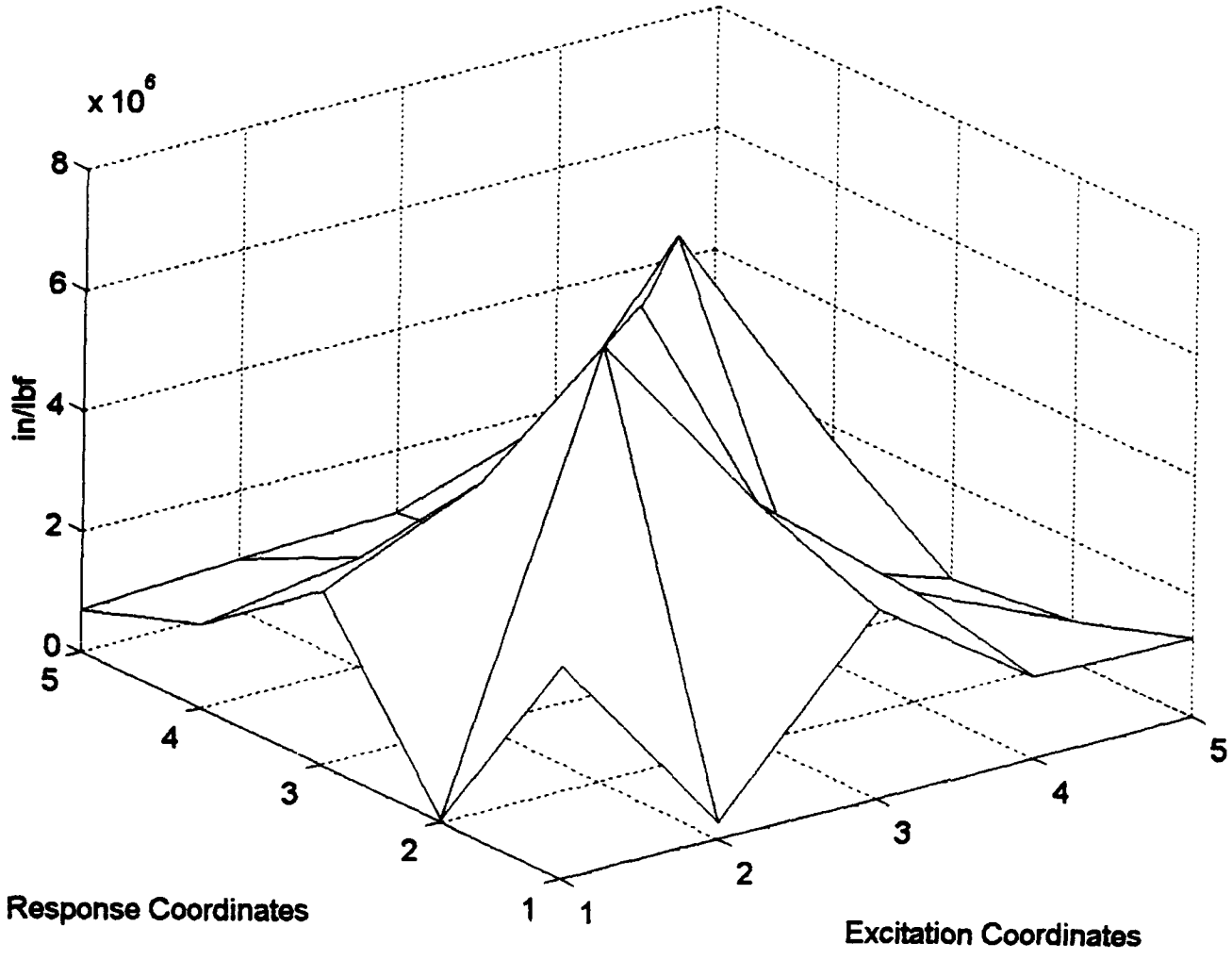

FIGURE 4-2: *Localization Matrix - 150 hz Case I*

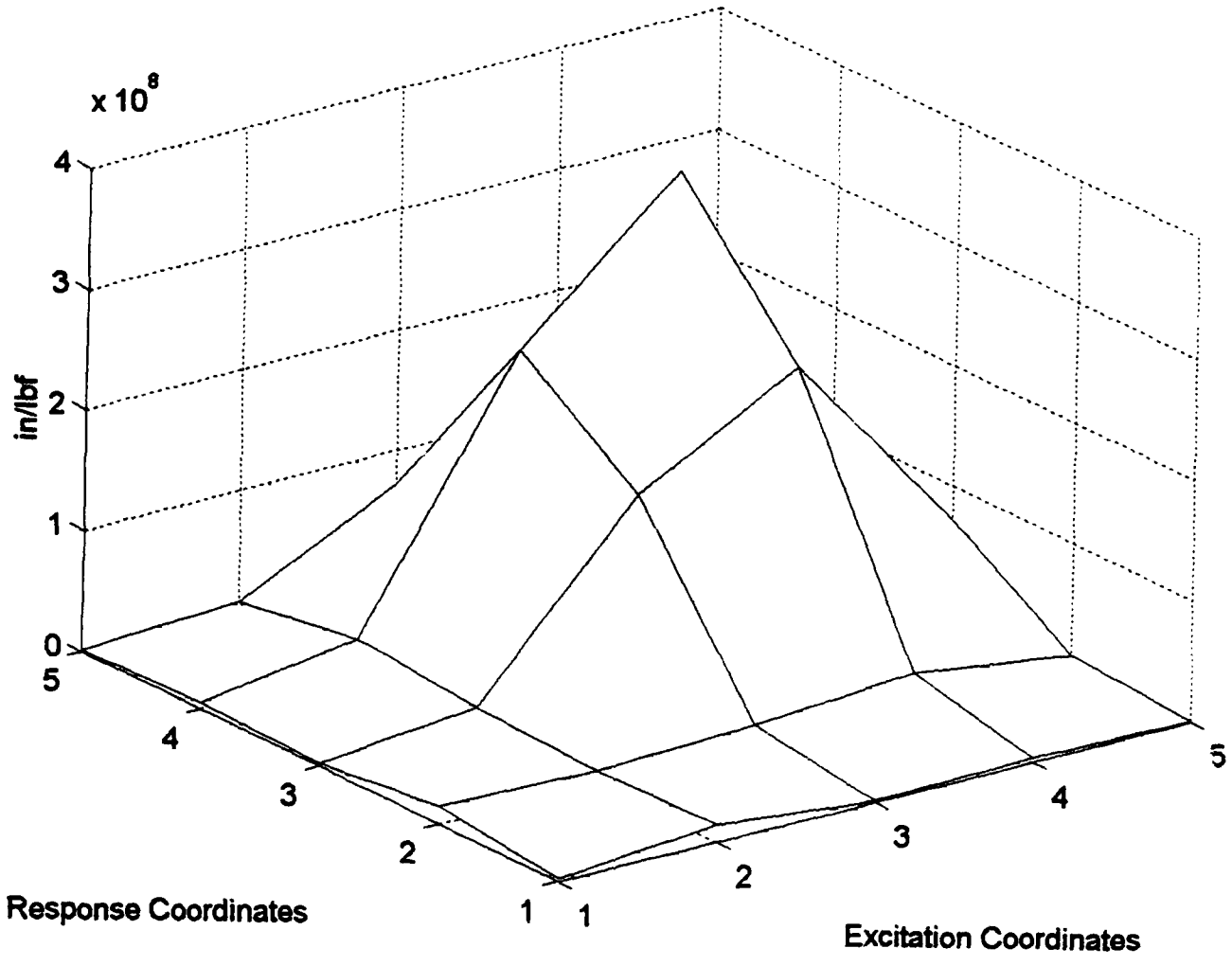

FIGURE 4-3: *Localization Matrix - 350 hz Case I*

The second calculation was to determine the localization matrix over a frequency domain. Figures 4-4 and 4-5 are plots of the "2,2" and "3,3" components of the localization matrix over a frequency range of 20 to 420 hz. All five coordinates of the reduced matrices were used as error coordinates. Figures 4-4 and 4-5 display nine peak values which are associated with the experimental system natural frequencies and the analytical model omitted set (OSET) eigenvalues. These results are consistent with the computer simulation results of Section III.B.1. Table 4-1 provides a summary of the peak values associated with Figures 4-4 and 4-5.

TABLE 4-1: PEAK FREQUENCIES - CASE I

Peak Frequency (hz)	Source:
29.90	Experiment:Natural Frequency
81.20	Experiment:Natural Frequency
155.90	Experiment:Natural Frequency
172.60	Analytical: OSET Frequency
225.34	Analytical: OSET Frequency
258.30	Experiment:Natural Frequency
265.46	Analytical: OSET Frequency
354.07	Analytical: OSET Frequency
387.80	Experiment:Natural Frequency

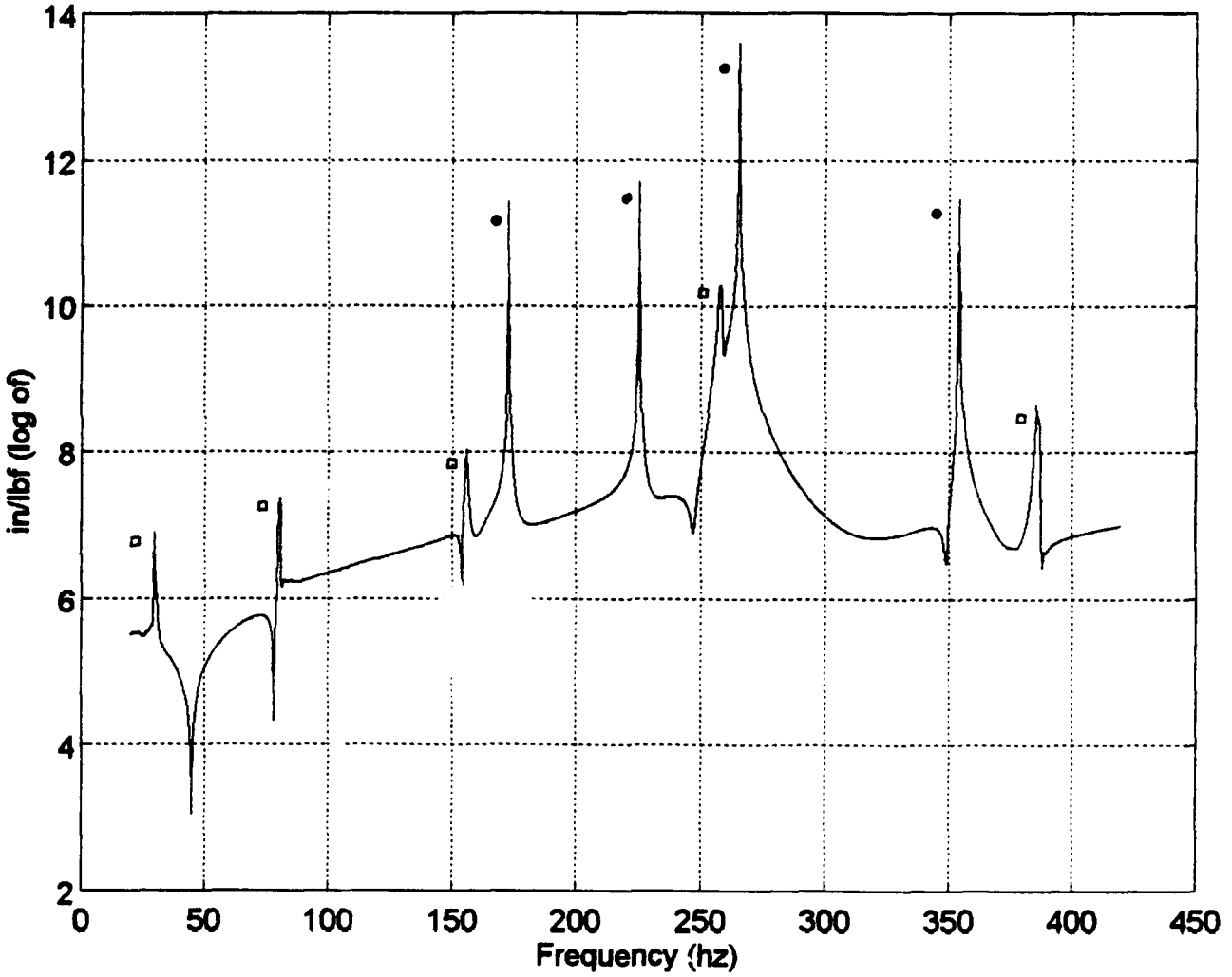

FIGURE 4-4: $L_{22}(\Omega)$

(•) Ω^{a}_{oset} (▫) Ω^{x}_{nat}

Case I

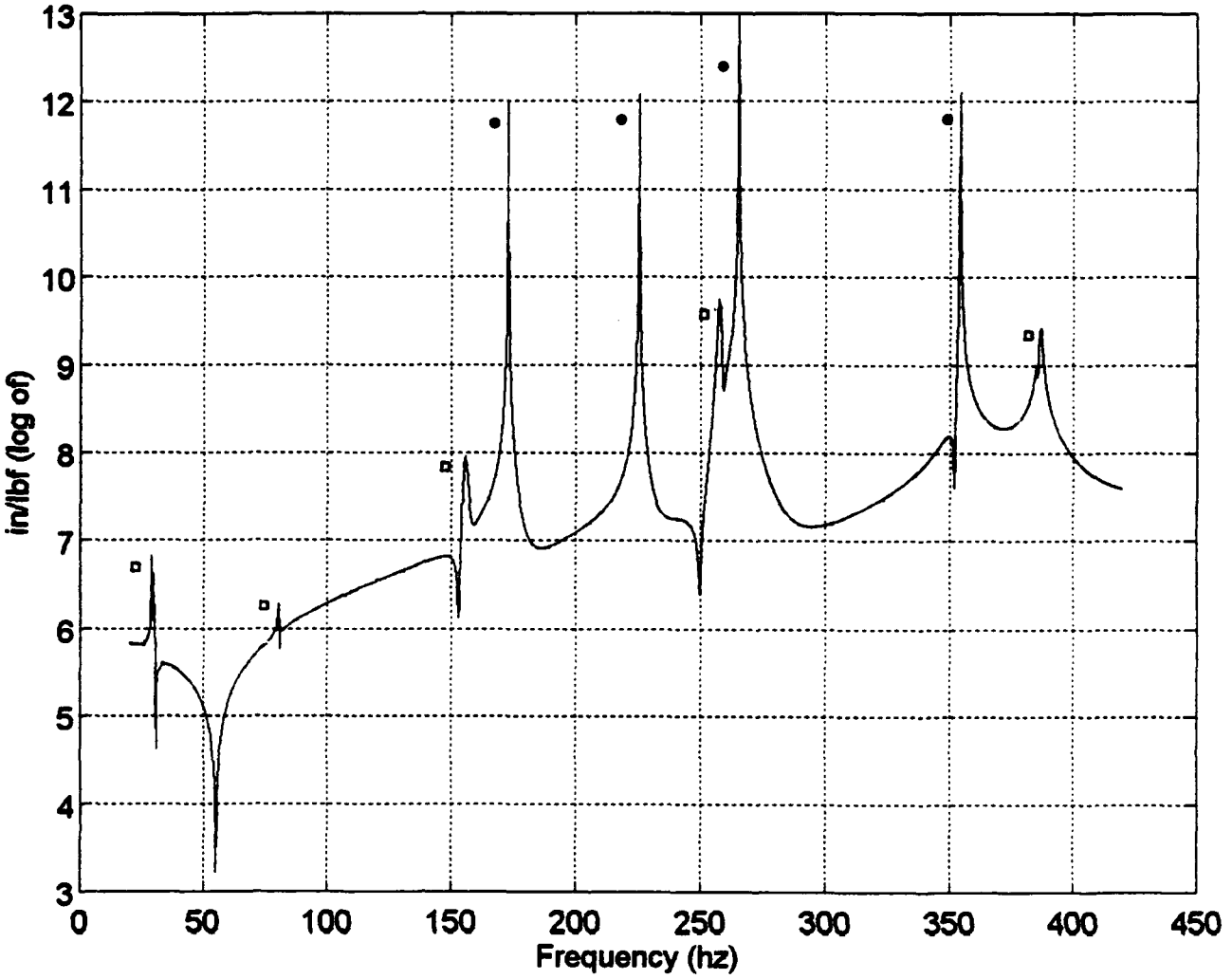

FIGURE 4-5: $L_{33}(\Omega)$

(•) Ω^{a}_{oset} (▫) Ω^{x}_{nat}

Case I

b. Case II (Small Mass Error)

The same calculations were performed for case II. Figures 4-6 thru 4-8 display the localization matrix at a specific frequency (35, 150, 350 hz). All three figures suggest significant model errors existing at elements two, three, and four. When these figures are compared with the computer simulation results (Figures 3-13 thru 3-15), the differences between the plots are much more apparent than was observed in case I. As discussed in case I, there are modeling errors associated with the ideal beam model that are not included in Figures 3-13 thru 3-15. In case I, the ideal beam modeling errors are insignificant compared with the installed errors associated with the flawed beam model. In case II, the flawed beam model installed error is small, thus the ideal beam modeling errors now become significant. The results is a larger apparent difference between Figures 4-6 thru 4-8 and Figures 3-13 thru 3-15.

Figures 4-9 and 4-10 display a plot of the "3,3" and "4,4" elements of the localization matrix over a frequency range from 20 to 420 hz. The peak values displayed in both plots represent the experimental system natural frequencies and the analytical model OSET coordinates. These results remain consistent with those observed in case I and the computer simulation. Table 4-2 is a summary of the peak values observed in Figures 4-9 and 4-10.

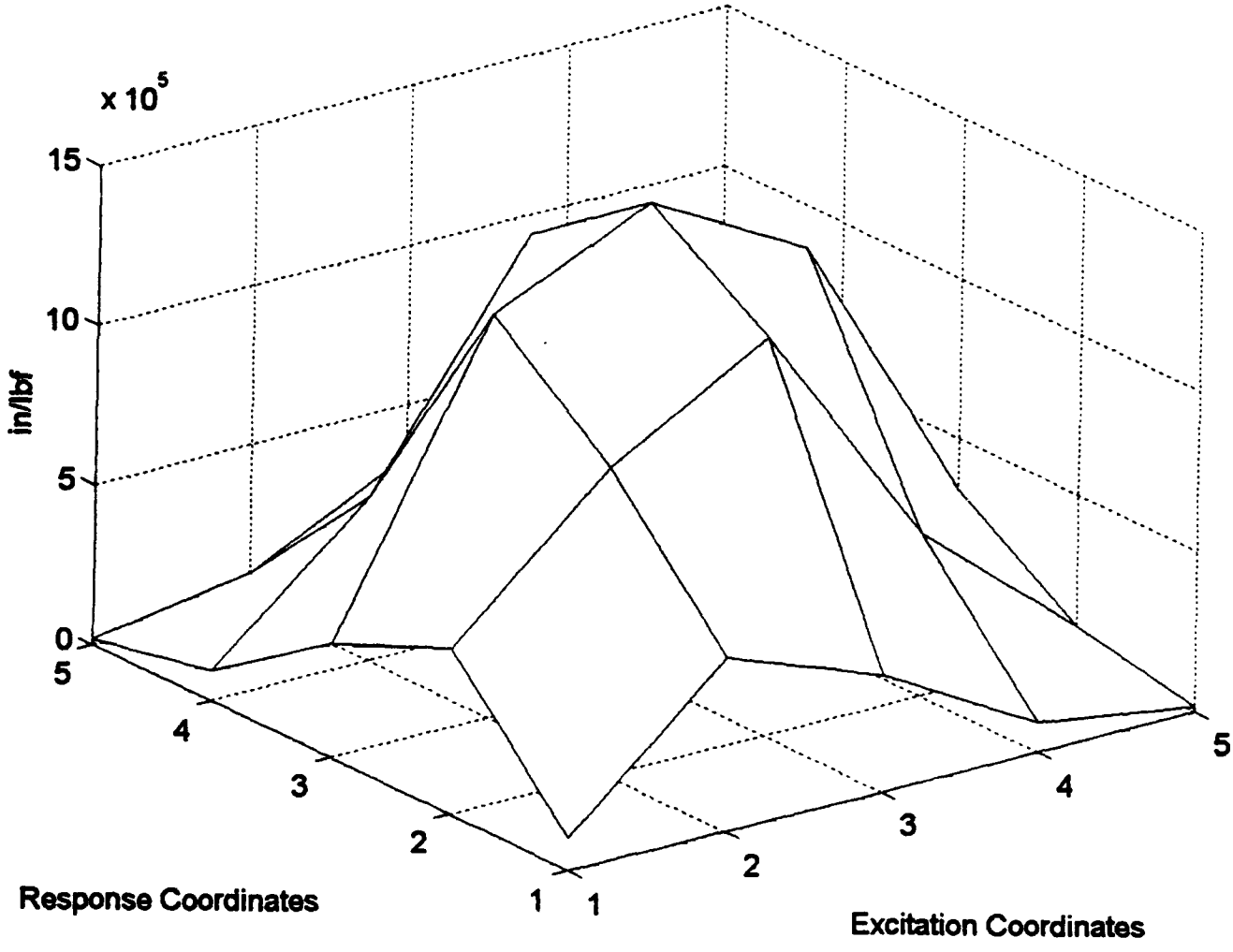

FIGURE 4-6: *Localization Matrix - 35 hz Case II*

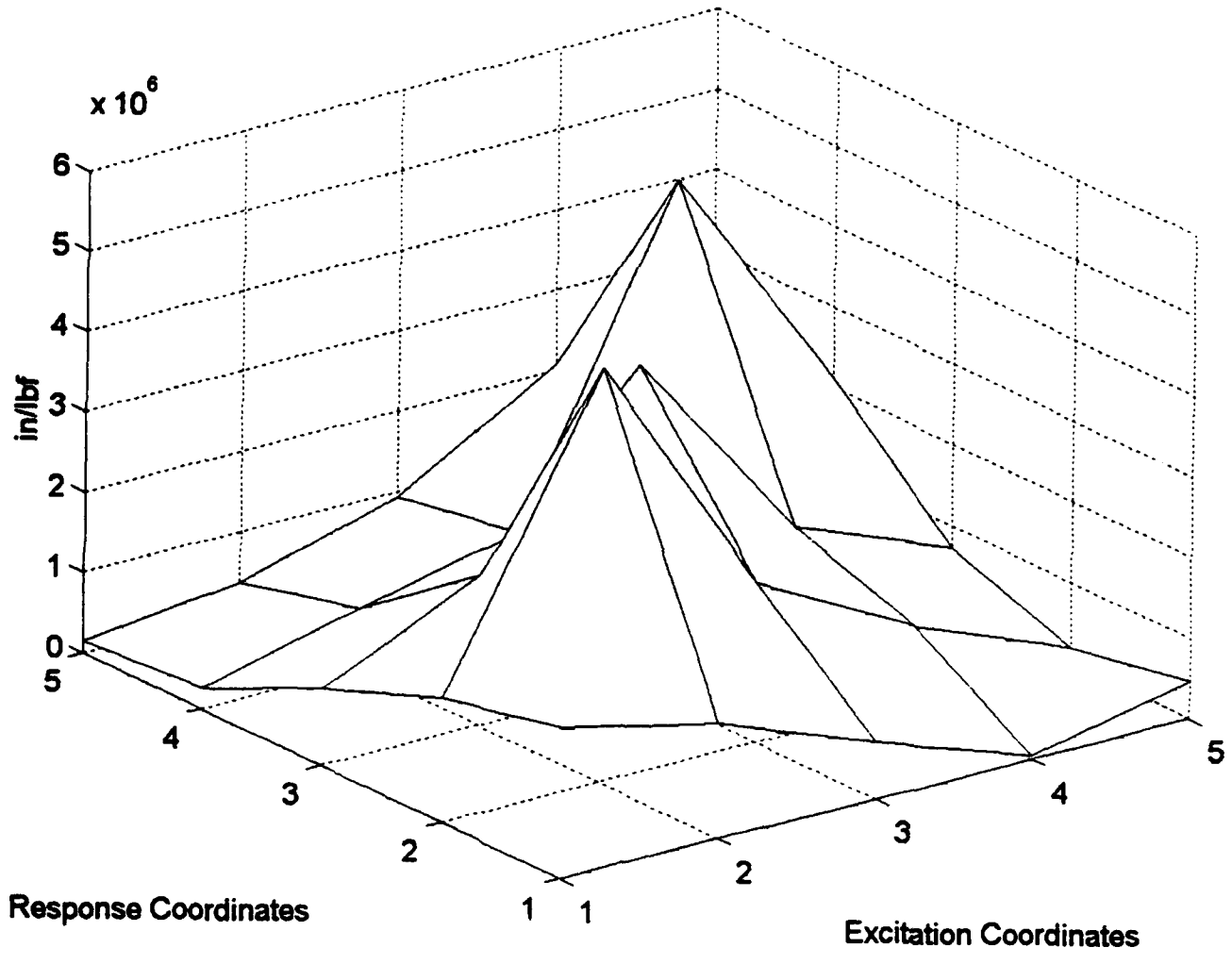

FIGURE 4-7: *Localization Matrix - 150 hz Case II*

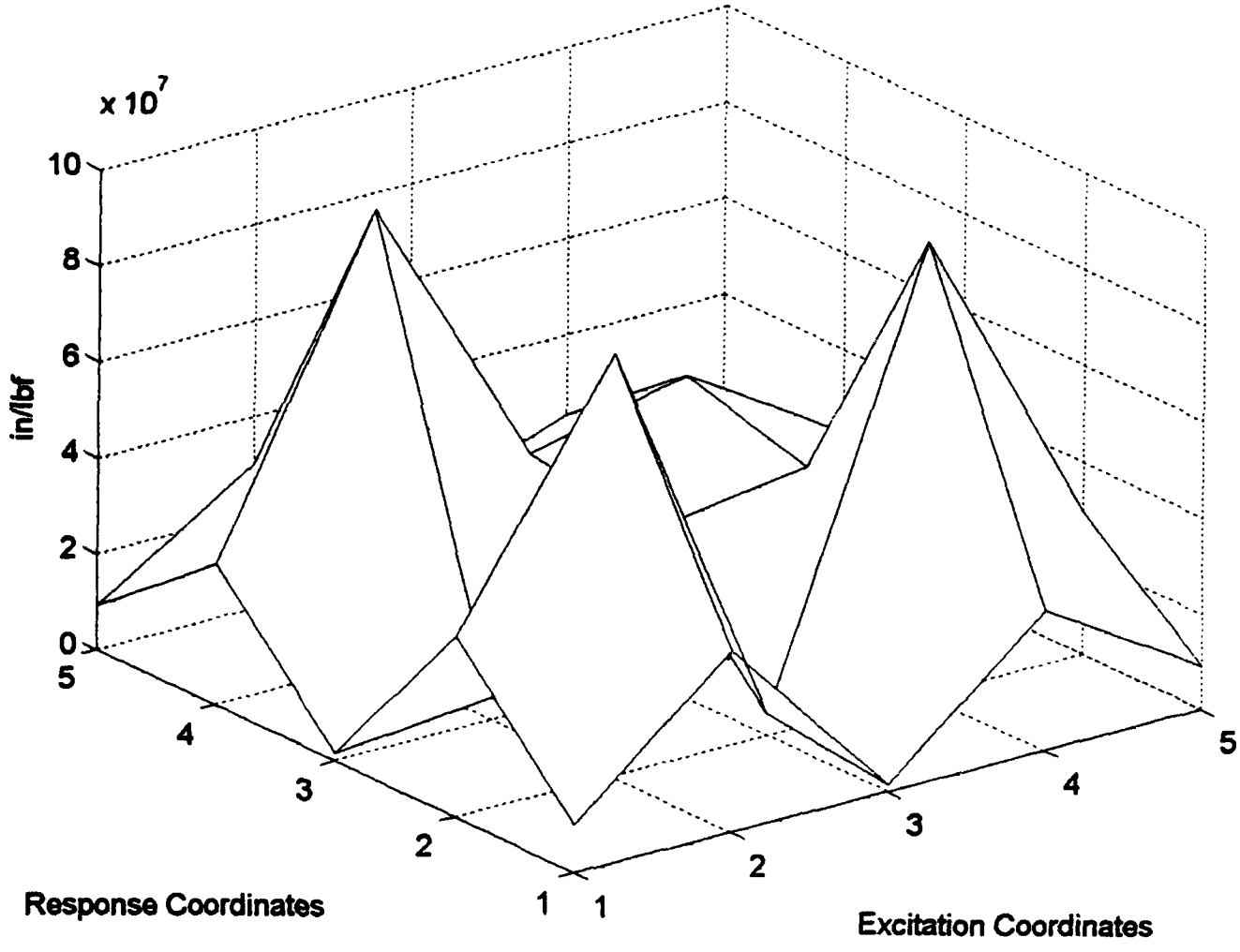

FIGURE 4-8: *Localization Matrix - 350 hz Case II*

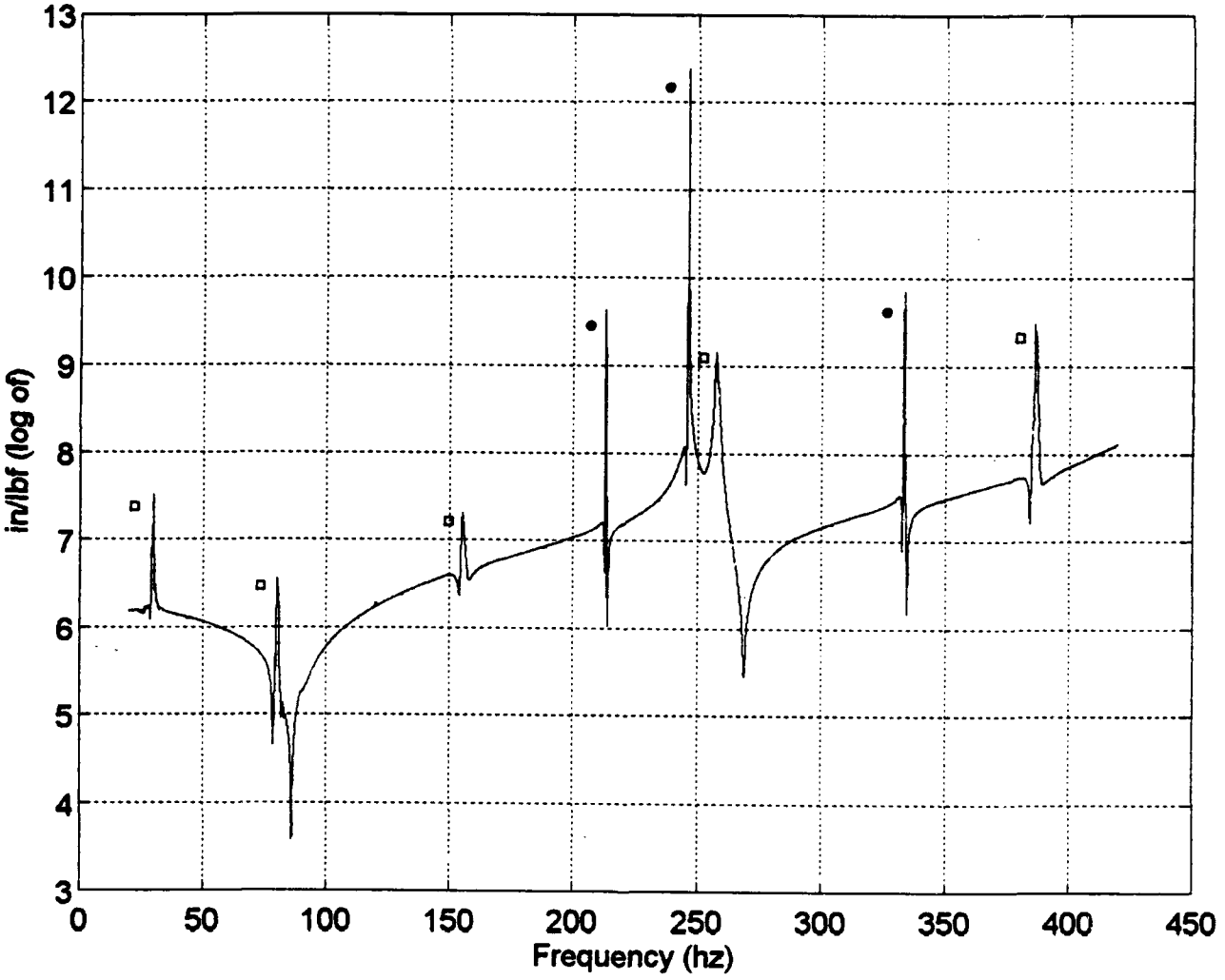

FIGURE 4-9: $L_{33}(\Omega)$
(•) Ω^{a}_{oset} (▫) Ω^{x}_{nat}
Case II

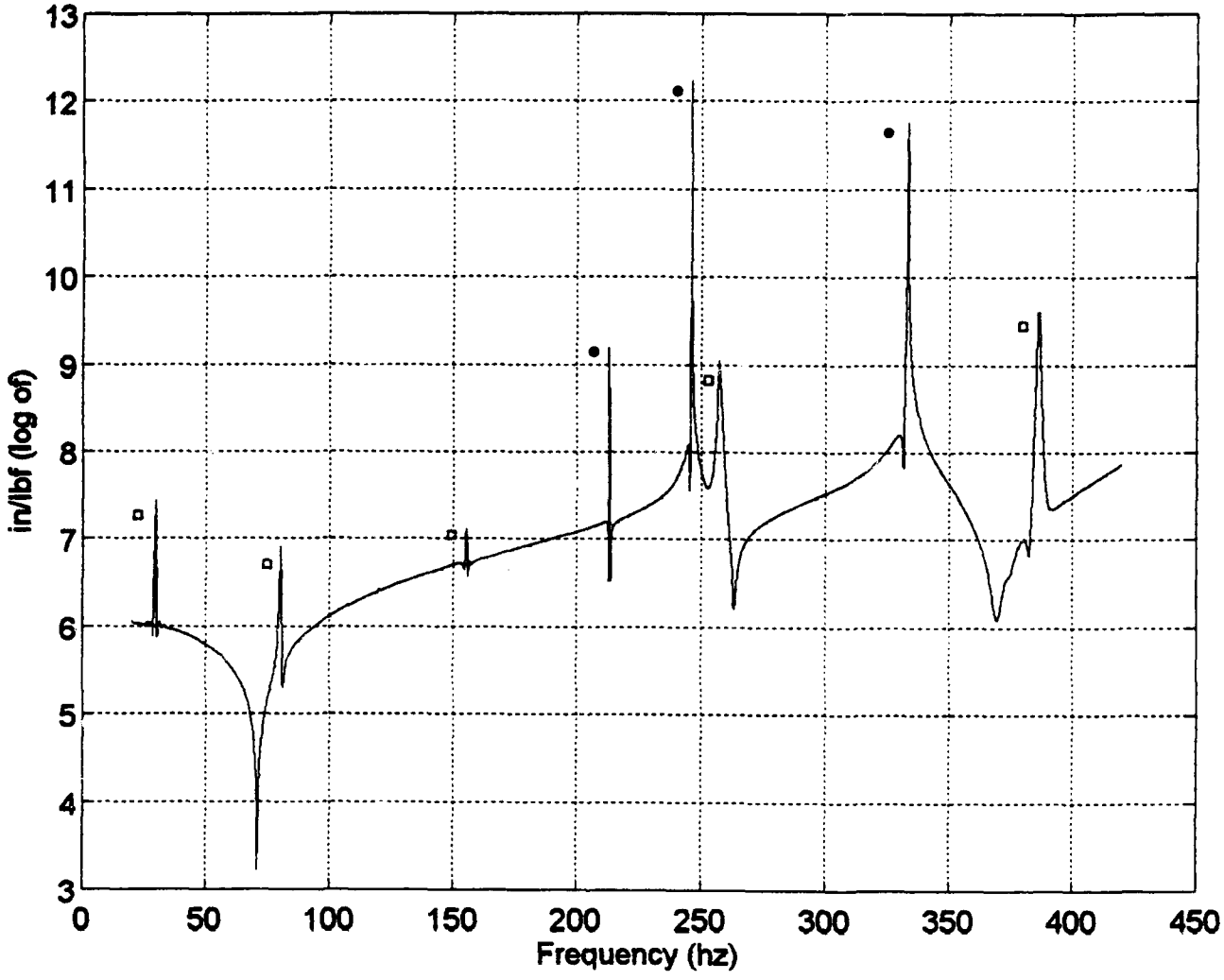

FIGURE 4-10: $L_{44}(\Omega)$
(•) Ω^{a}_{oset} (▫) Ω^{x}_{nat}
Case II

Table 4-2: PEAK FREQUENCIES - CASE II

Peak Frequency (hz)	Source:
29.90	Experiment:Natural Frequency
81.20	Experiment:Natural Frequency
155.90	Experiment:Natural Frequency
213.03	Analytical: OSET Frequency
246.12	Analytical: OSET Frequency
258.30	Experiment:Natural Frequency
333.20	Analytical: OSET Frequency
387.80	Experiment:Natural Frequency

2. Improved Reduction System (IRS)

The procedure used in Section IV.B.1 is repeated in this section with the exception that the analytical model will be reduced via the IRS method.

As discussed in Section III.B.2.a, determining the localization matrix at a specific frequency provides little useful information, thus that calculation will not be performed in this section.

a. Case I (Large Stiffness Error)

Figure 4-11 displays the "2,2" element of the localization matrix plotted over a frequency range of 20 to 420 hz. The five peak values that appear in the figure, are all associated with the experimental system natural frequencies.

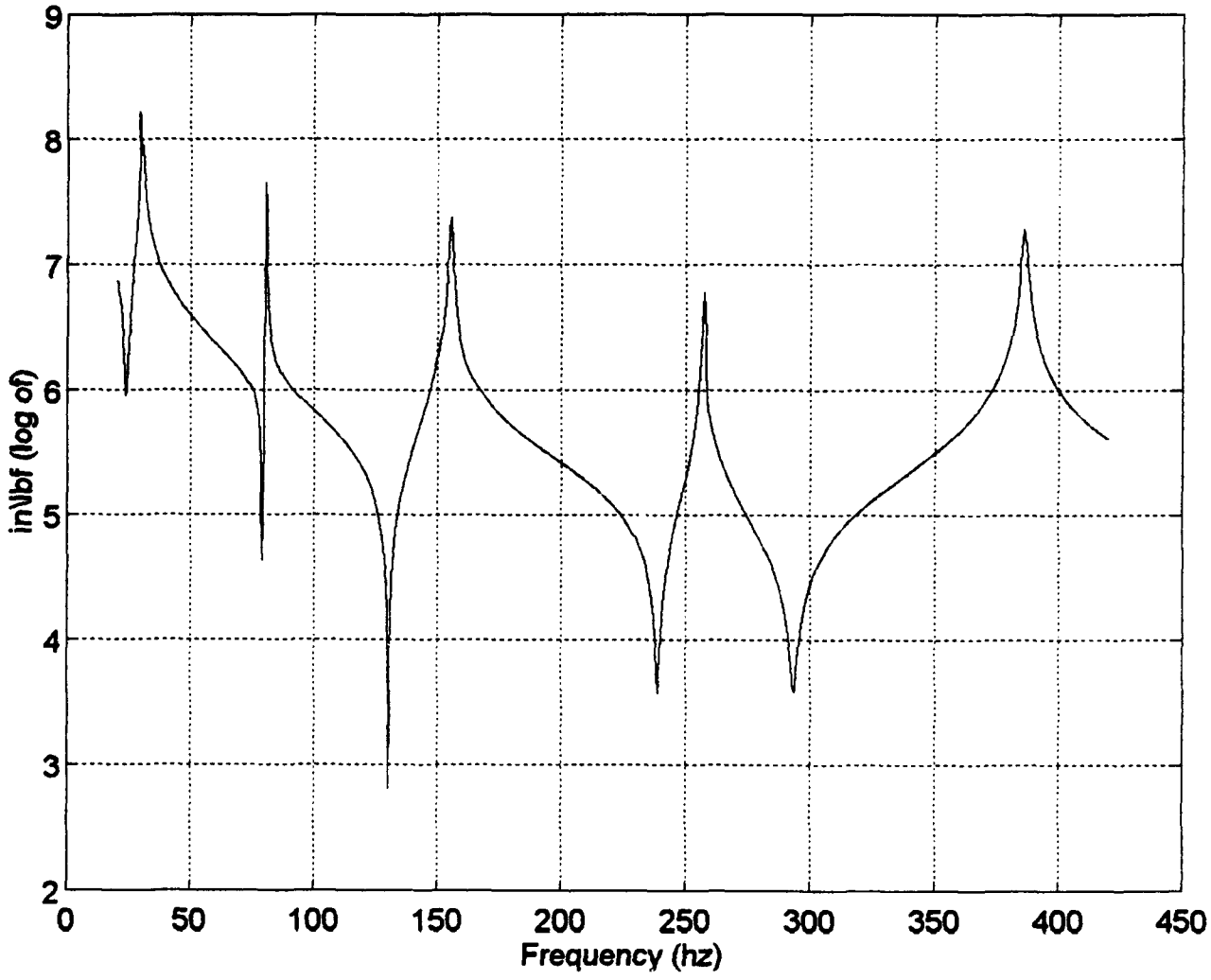

FIGURE 4-11: $L_{22}(\Omega)$

(IRS) Case I

b. Case II (Small Mass Error)

Figure 4-12 displays the "3,3" element of the localization matrix plotted over a frequency range of 20 to 420 hz. The experimental system natural frequencies appear as peak values. This remains consistent with the results from case I and the computer simulation. Table 4-3 is a summary of the peak values displayed in Figures 4-11 and 4-12.

Table 4-3: PEAK VALUES CASE I AND II

Frequency (hz)
29.90
81.20
155.90
258.30
387.80

C. IMPEDANCE ERROR

The impedance error calculations performed in Section III.C. is repeated in this section. The experimental FRF matrix will be used instead of the reduced FRF matrix from the ideal beam finite element.

1. Extraction Reduction

a. Case I (Large Stiffness Error)

Figure 4-13 is a plot of the "1,1" element of the impedance error matrix over a frequency range from 20 to 420 hz.

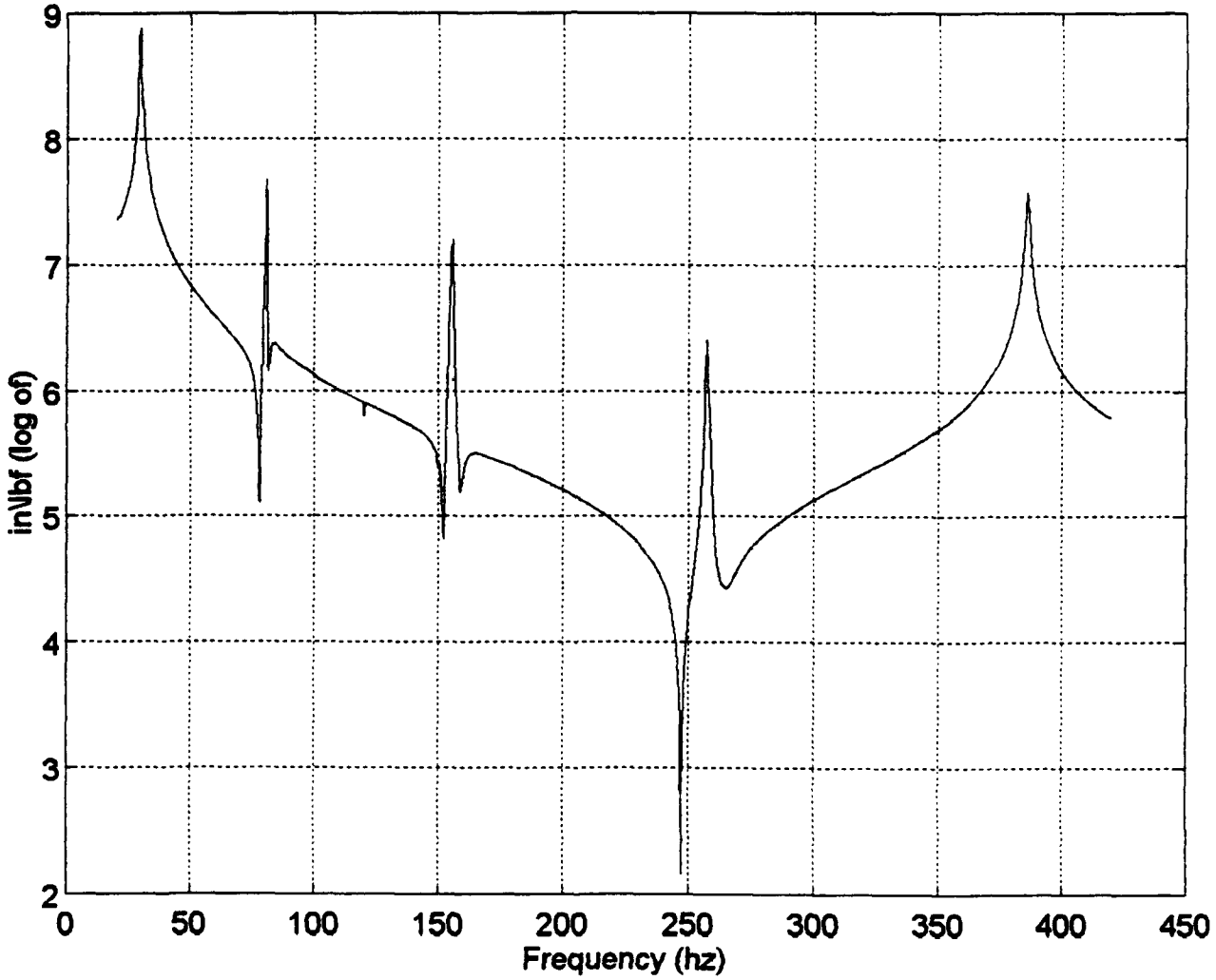

FIGURE 4-12: $L_{33}(\Omega)$

(IRS) Case II

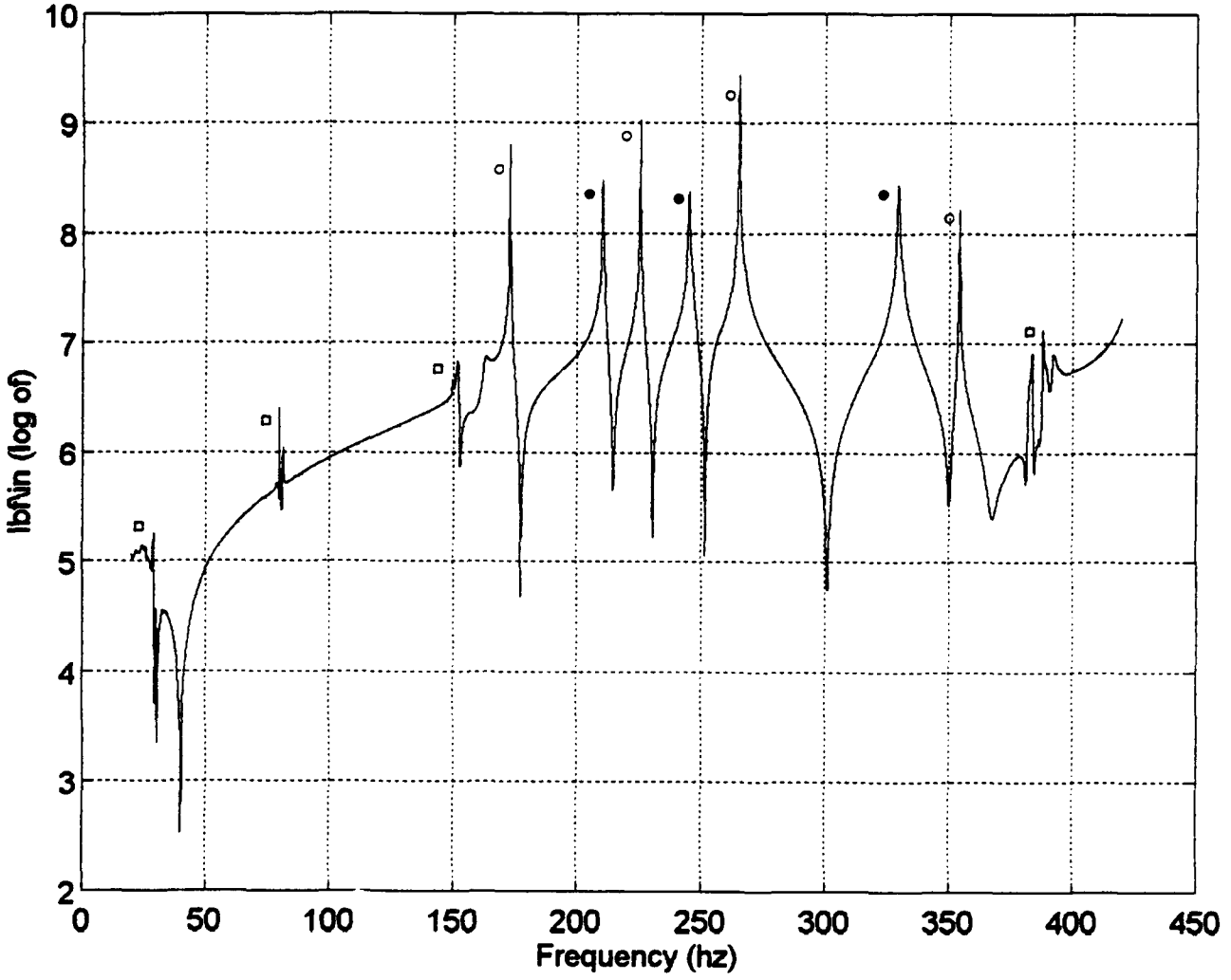

***FIGURE* 4-13:** $\Delta Z_{11}(\Omega)$
(•) Ω^{a}_{oset} (○) Ω^{x}_{oset}
(□) Ω^{x}_{nat} - *Case I*

The results of the impedance error calculations performed in computer simulation (Section III.C.1) reveal that the peak values of the impedance error versus frequency plots were associated with the OSET coordinate eigenvalues from both the analytical and test models. Figure 4-13 does display the expected peak values associated with the OSET coordinate eigenvalues, but four of the five experimental system natural frequencies also appear as peak values within the figure (a peak at 258.30 hz is not visible). The appearance of these natural frequencies is not fully understood. In trying to determine why these natural frequencies appear, the ideal beam finite element model was modified to include damping (Appendix B). The reasoning to include damping is that the experimental FRF matrix is complex valued while the FRF matrix from the finite element programs consist only of real valued elements. The results are displayed in Figure 4-14. The analysis is that the experimental system OSET eigenvalues decreased in magnitude, but the peaks associated with the experimental system natural frequencies remain. Although the appearance of the natural frequencies are not known, it remains that the OSET coordinate eigenvalues do appear as peak values. It is also interesting to note that the experimental system natural frequency peaks do not appear as clean as the OSET coordinate eigenvalues.

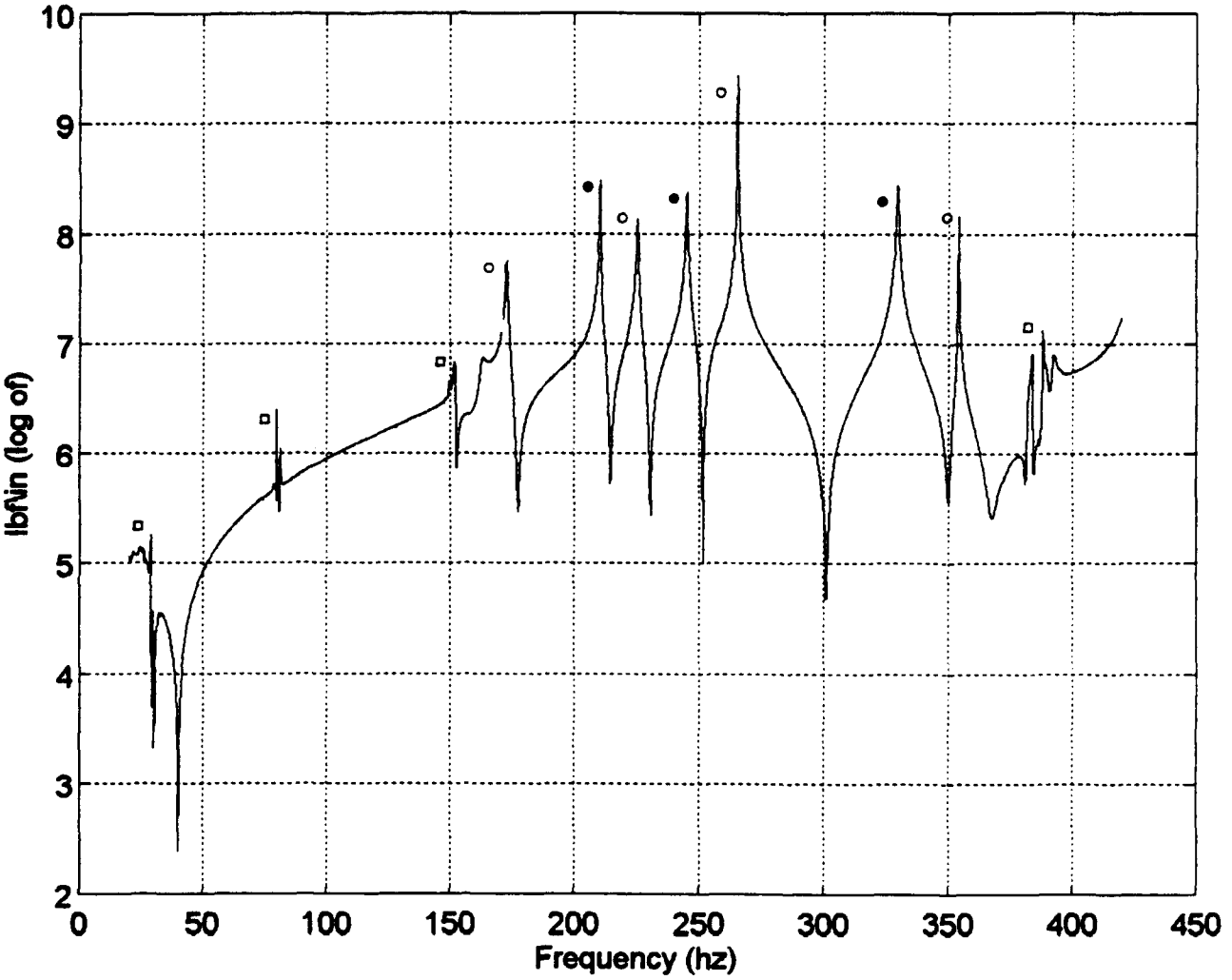

FIGURE 4-14: $\Delta Z_{11}(\Omega)$
(•) Ω^{a}_{oset} (○) Ω^{x}_{oset}
(□) Ω^{x}_{nat} - *CaseI*
Damped Model

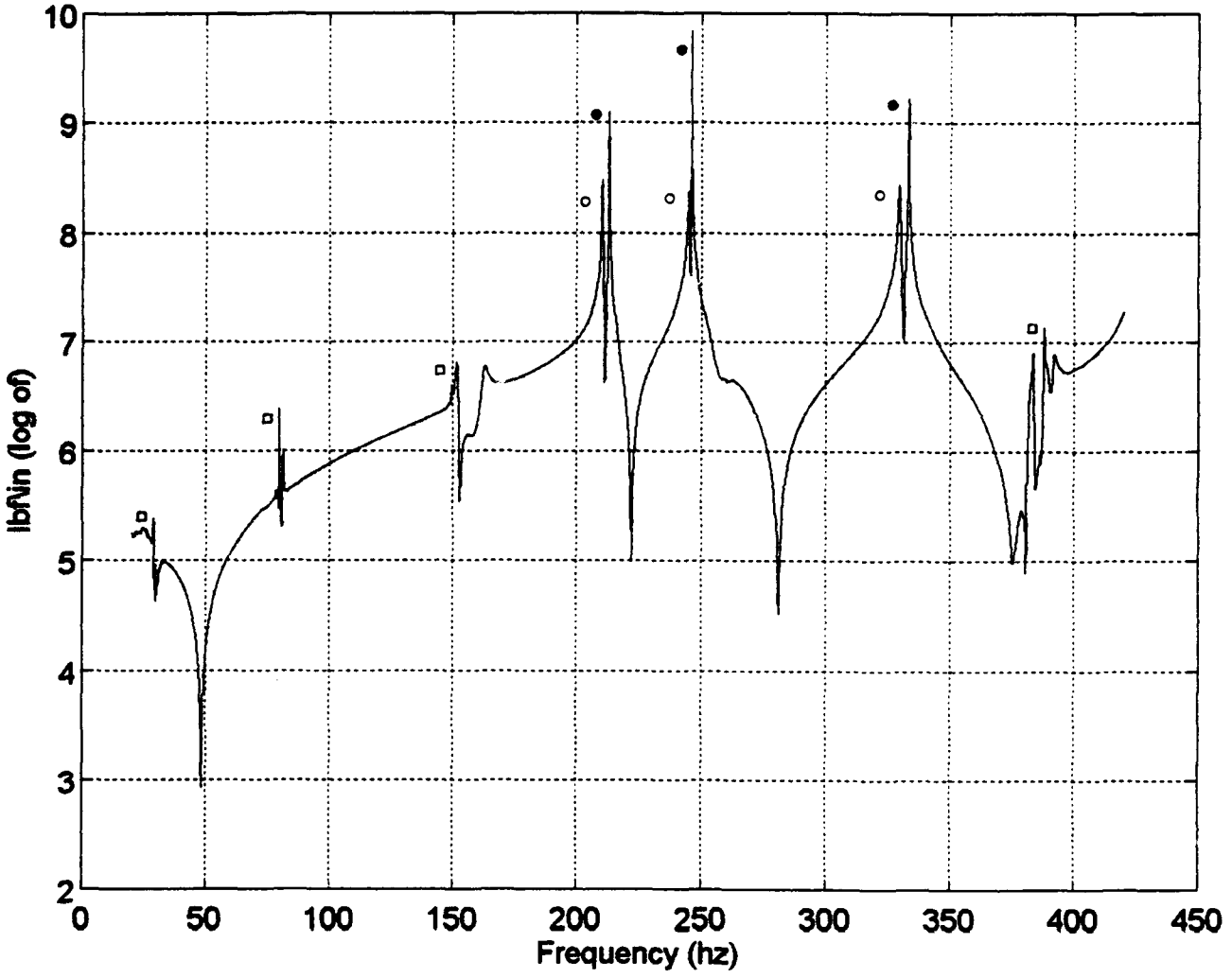

***FIGURE* 4-15:** $\Delta Z_{11}(\Omega)$
(•) Ω^{a}_{oset} (○) Ω^{x}_{oset}
(□) Ω^{x}_{nat} - *Case II*

b. Case II (Small Mass Error)

Figure 4-15 is a plot of the "1,1" element of the impedance error matrix over a frequency range from 20 to 420 hz. The peak values that appeared in Figure 4-13 also appear in Figure 4-15. The important result is the appearance of the OSET coordinate eigenvalues.

2. Improved Reduction System (IRS)

Figure 4-16 displays the plot of the impedance error over a frequency range of 20 to 420 hz utilizing IRS reduction of the analytical model FRF matrix for case I. The peak values in the plot are associated with the OSET coordinate eigenvalues of the experimental system. Two of the experimental system natural frequencies (155.90 and 387.80 hz) slightly appear. As in Section IV.C.1, the important result is the appearance of the OSET coordinate eigenvalues. These results remain consistent with the results of the computer simulation (Section III.C.2). The results for case II are identical to the results of case I.

D. IDEAL BEAM MODEL

The previous two sections have described structural identification of a flawed beam finite element model against an ideal beam finite element model and against an experimental system. The next step is to perform a structural identification of the ideal beam model versus the experimental system. This step is to determine the accuracy of the best finite element model against the experimental structure.

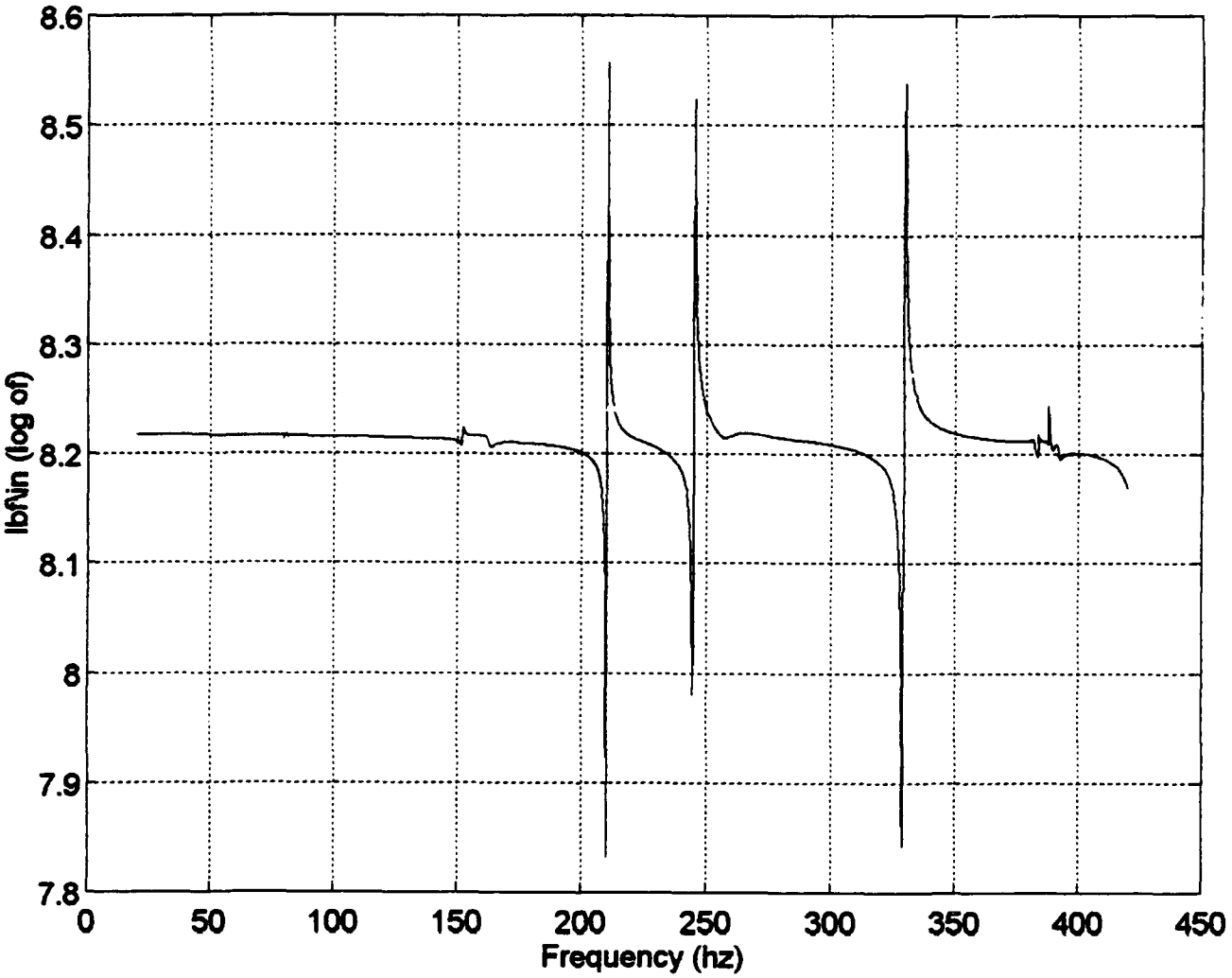

FIGURE 4-16: $\Delta Z_{11}(\Omega)$ *(IRS) - Case I*

1. Localization

The ideal beam model will provide the analytical FRF and will be reduced to match the size of the experimental system FRF matrix. The retained coordinates will correspond to the translational response and excitation coordinates.

a. Extraction Reduction

The ideal beam model was reduced using extraction reduction. Figures 4-17 thru 4-19 display elements "1,1", "3,3", and "4,4" of the localization matrix plotted over a frequency range from 20 to 420 hz. In analyzing the three figures, all the test system natural frequencies appear as expected. However, several of the analytical model OSET eigenvalues do not appear in each of the figures. Table 4-4 provides a summary of the analytical model OSET eigenvalues for the "1,1", "2,2", and "4,4" elements of the localization matrix.

TABLE 4-4: OMITTED SET COORDINATE EIGENVALUES

L_{11}	L_{33}	L_{44}
209.92 hz	Missing	Missing
244.90 hz	244.90 hz	244.90 hz
327.96 hz	Missing	327.96 hz

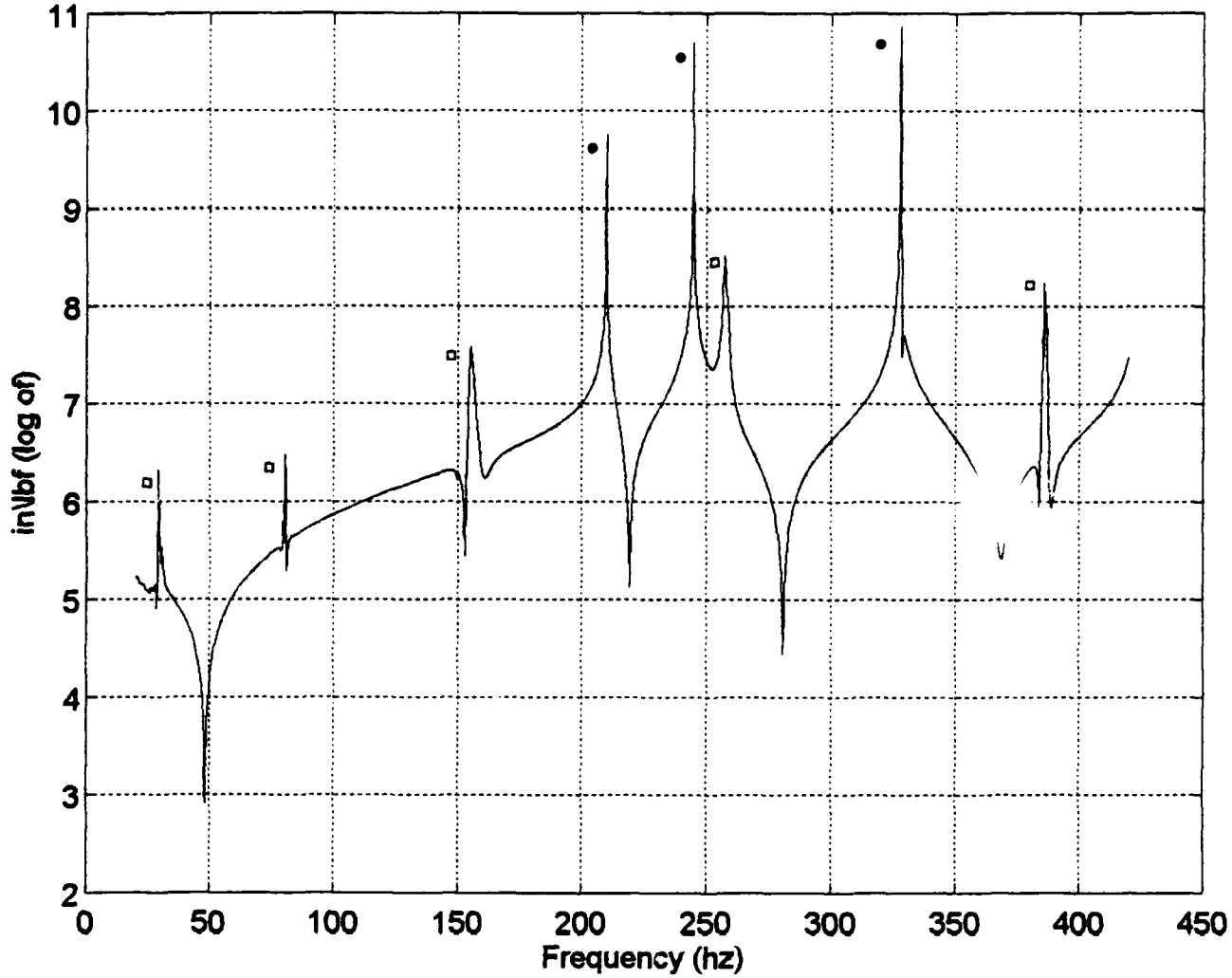

FIGURE 4-17: $L_{11}(\Omega)$
Ideal Beam Model
(•) Ω^{a}_{oset} (▫) Ω^{x}_{nat}

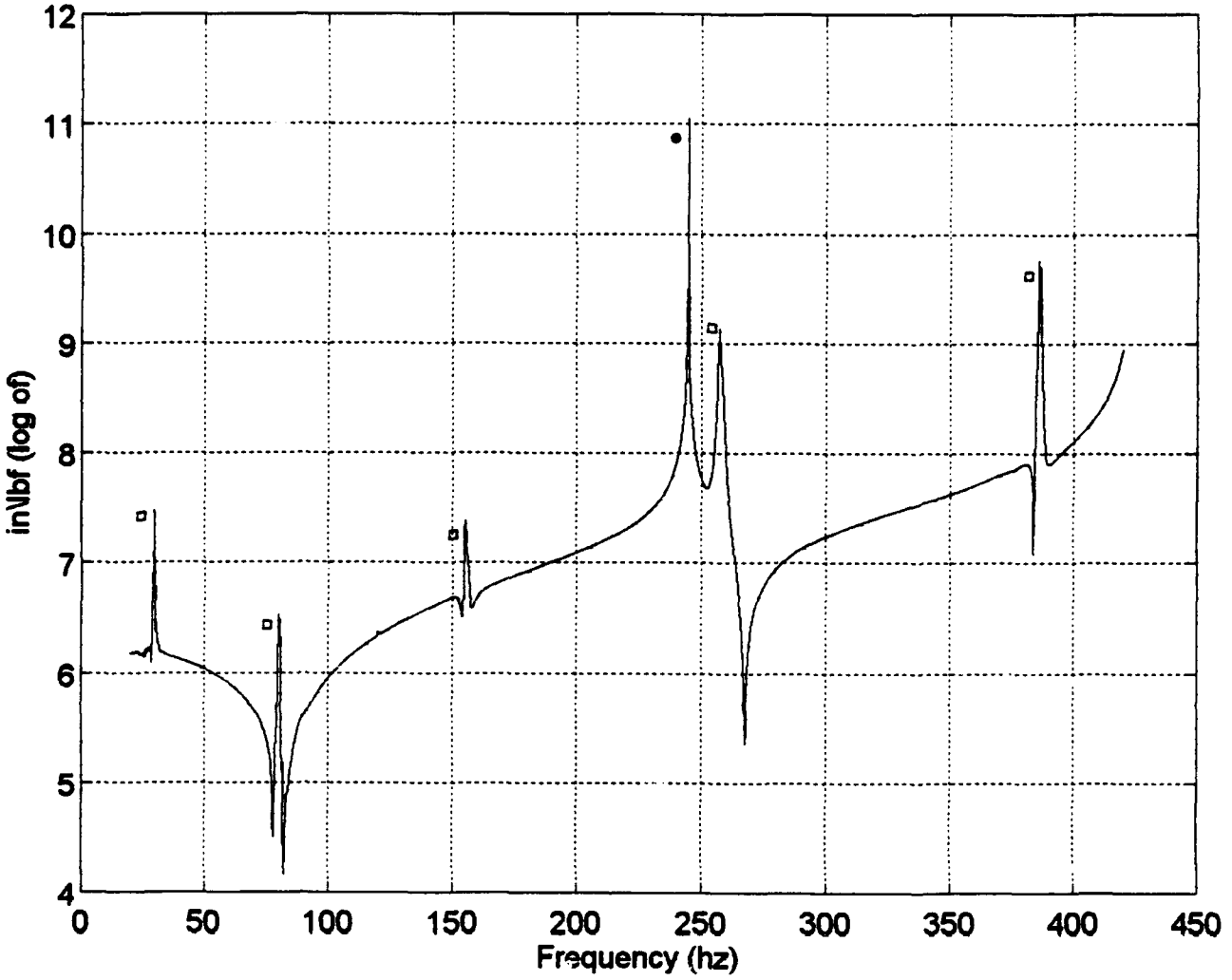

FIGURE 4-18: $L_{33}(\Omega)$
Ideal Beam Model
(•) Ω^{a}_{oset} (▫) Ω^{x}_{nat}

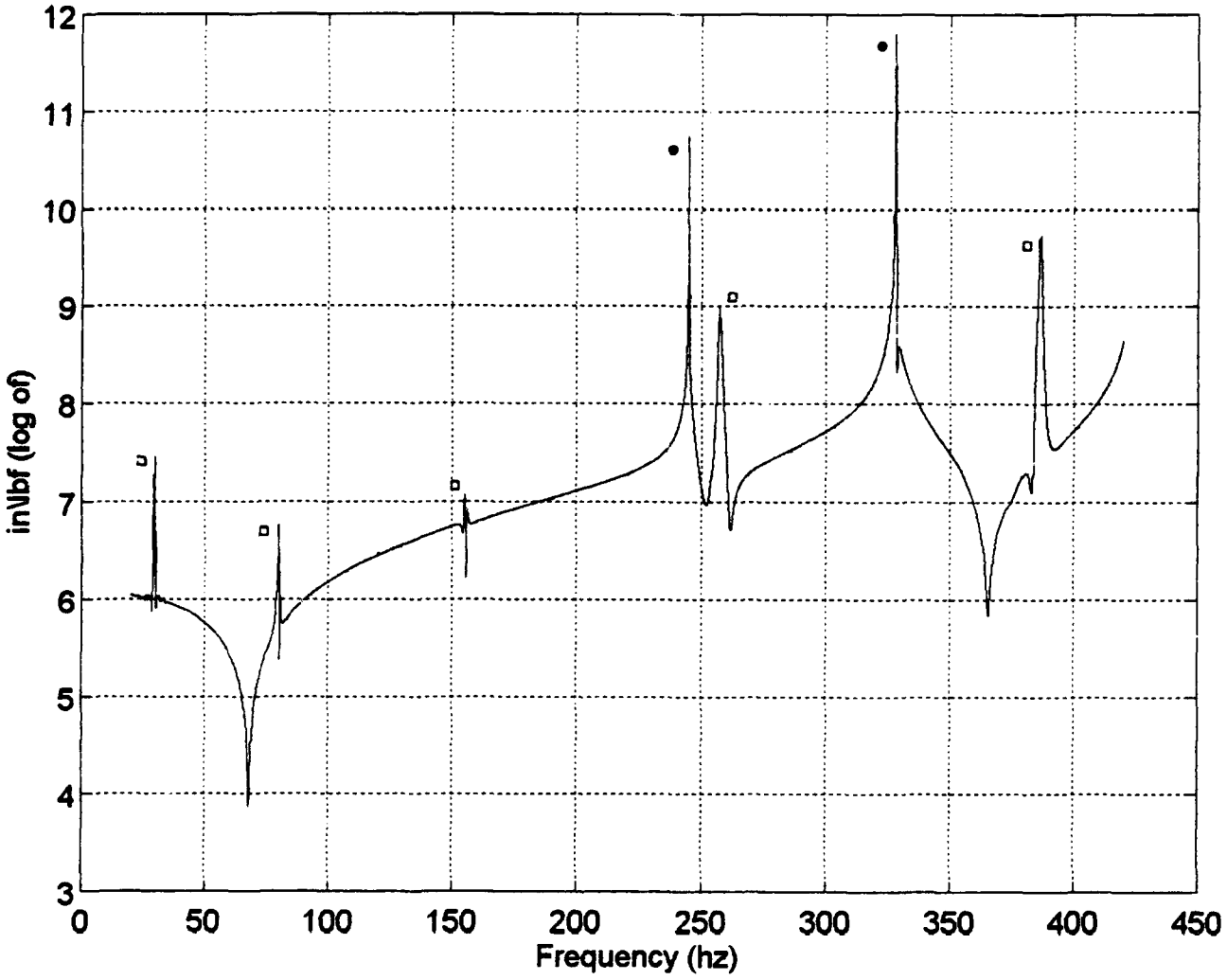

FIGURE 4-19: $L_{44}(\Omega)$
Ideal Beam Model
(•) Ω^{a}_{oset} (▫) Ω^{x}_{nat}

The missing OSET eigenvalues appear to be a result of the beam finite element model being homogeneous. Since actual structures are generally more complicated than a simple beam, the missing OSET eigenvalues are a result of the simplicity of the experimental structure and not of importance. A more detailed discussion concerning the missing OSET eigenvalues is provided in Appendix D.

b. Improved Reduction System (IRS)

Figure 4-20 displays the "1,1" element of the localization matrix over a frequency range of 20 to 420 hz. As expected, the test system natural frequencies appear as peak values.

2. Impedance Error

As was done with the localization matrix calculation, the impedance error calculation was performed using the ideal beam model as the analytical model FRF matrix. The analytical model will be reduced to match the size of the experimental system FRF matrix.

a. Extraction Reduction

Figure 4-21 thru 4-23 display the "1,1", "2,2", and "3,3" element of the impedance error over a frequency range from 20 to 420 hz. The same problem of the missing OSET eigenvalues in the localization matrix for the analytical model occur in the impedance error plots. In addition, the corresponding OSET eigenvalues for the test system are also missing from the Figures 4-22 and 4-23.

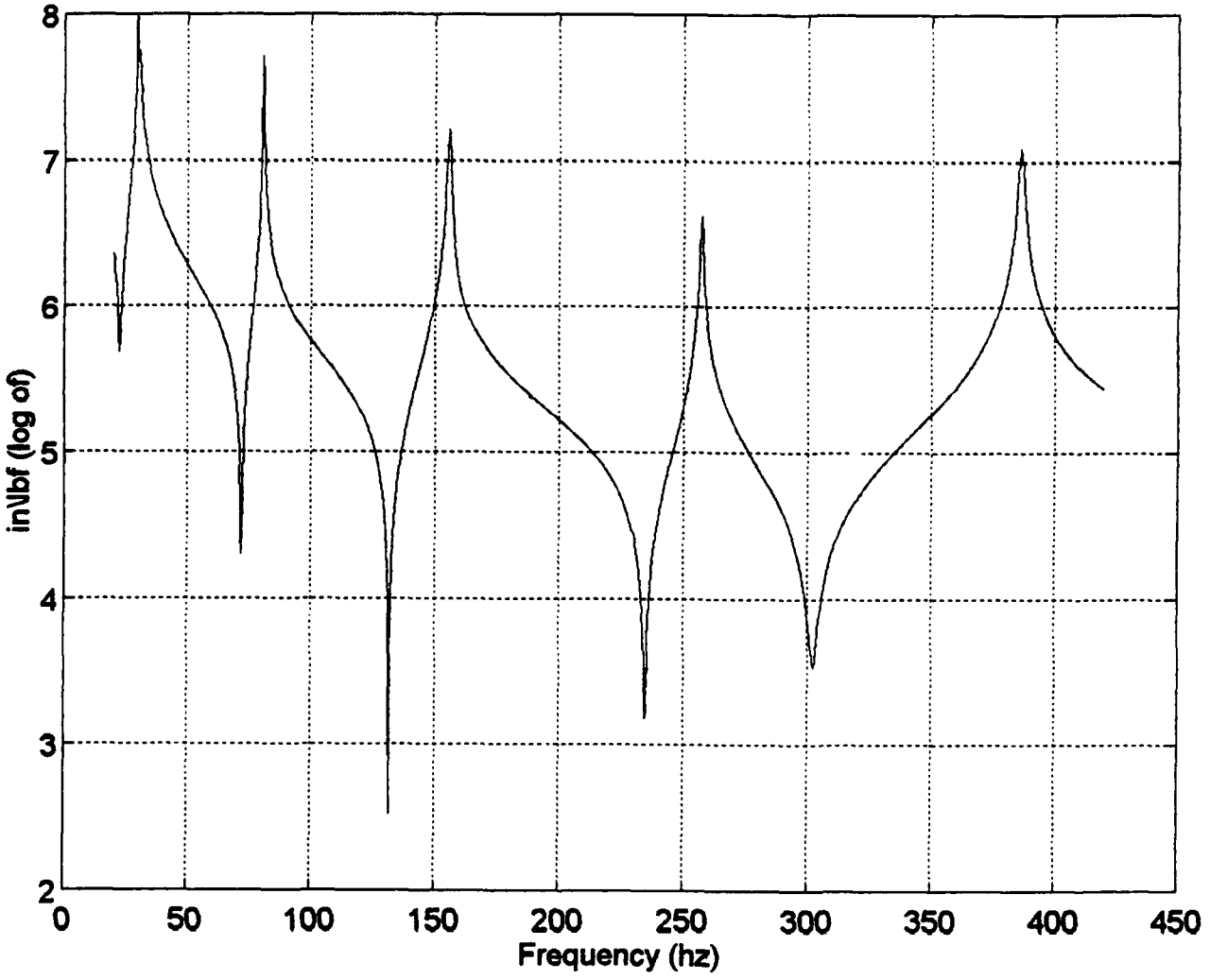

***FIGURE* 4-20:** $L_{11}(\Omega)$
Ideal Beam Model
IRS

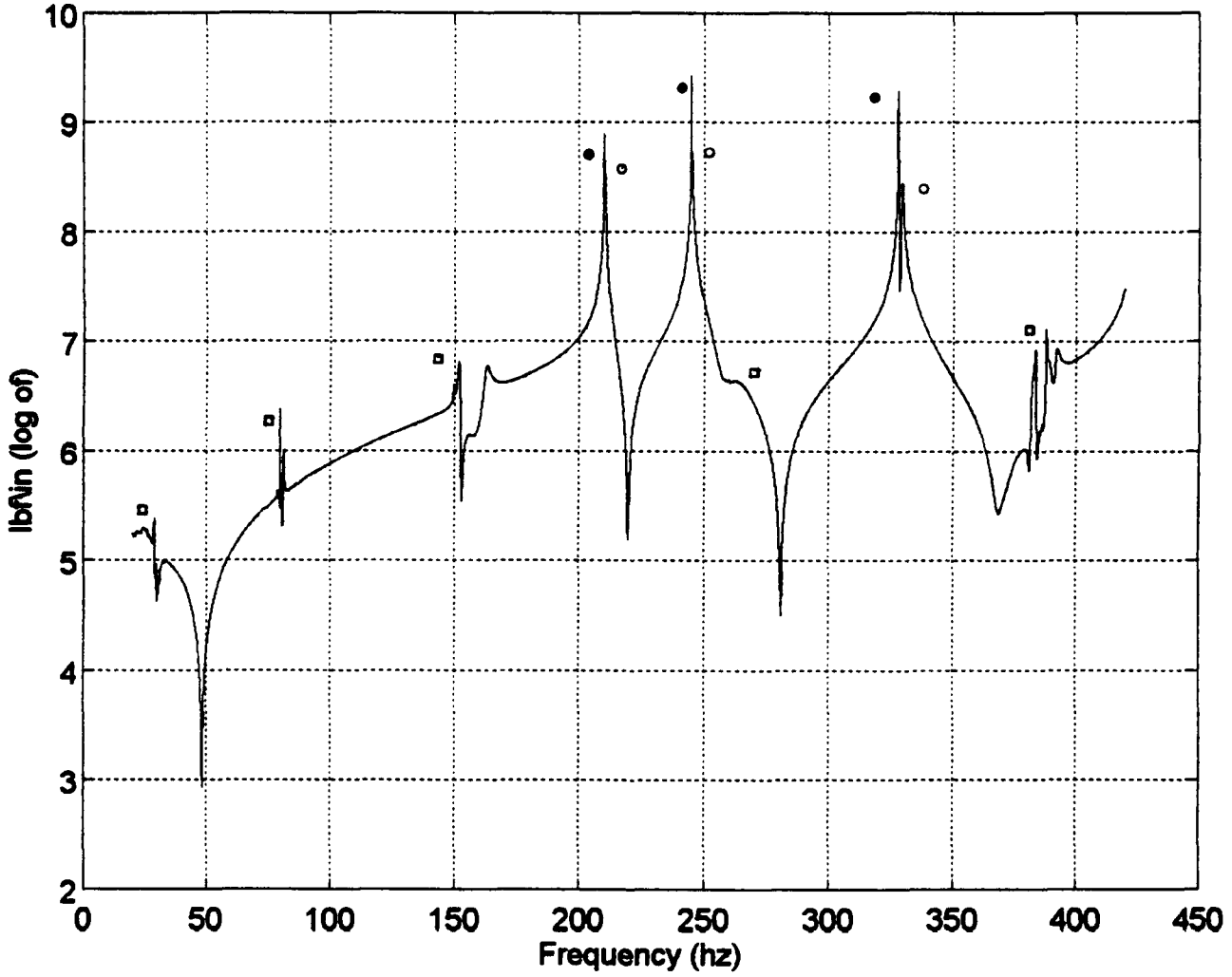

***FIGURE* 4-21:** $\Delta Z_{11}(\Omega)$
(•) Ω^{a}_{oset} (∘) Ω^{x}_{oset}
(▫) Ω^{x}_{nat} *Ideal Beam Model*

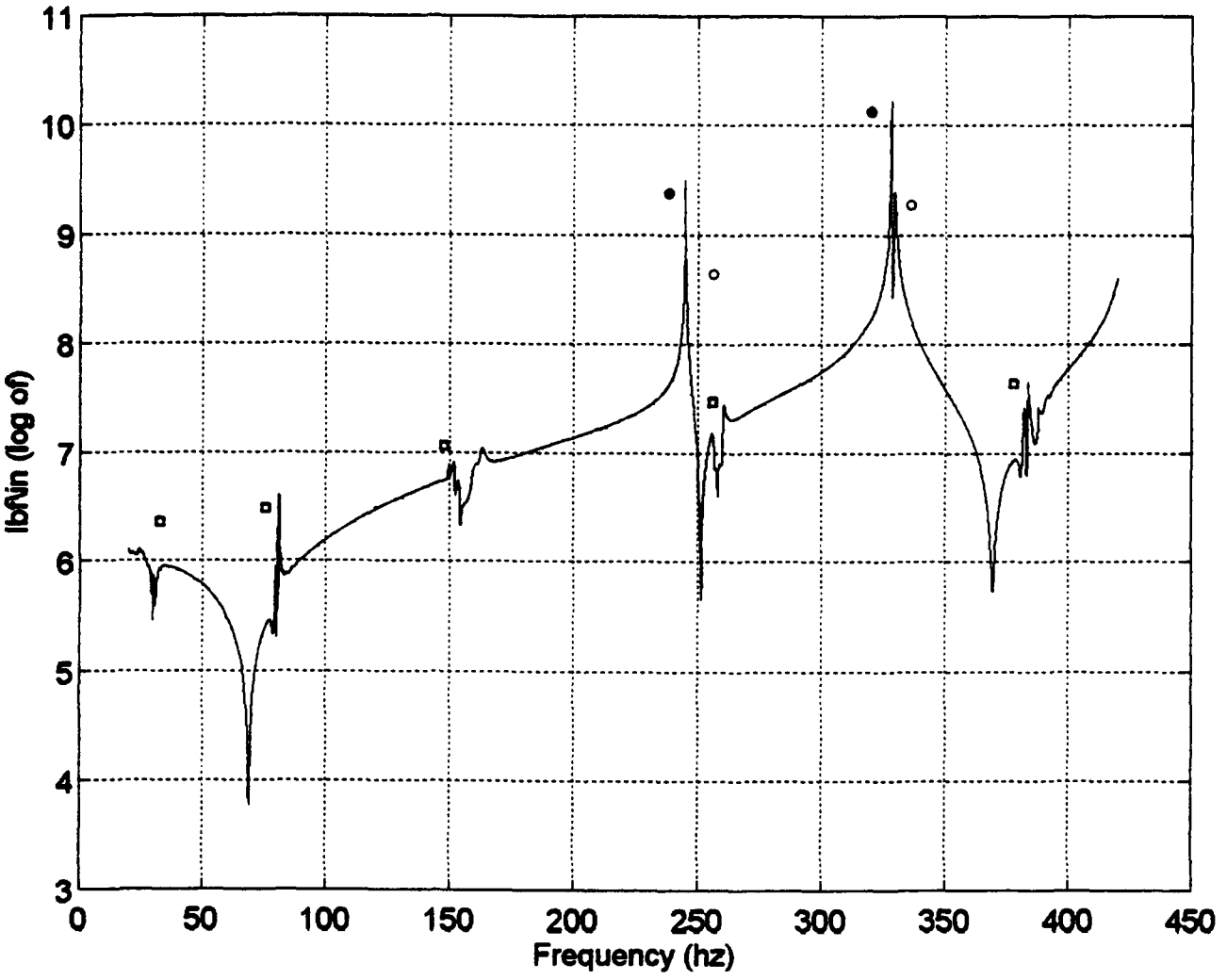

FIGURE 4-22: ΔZ_{22}

(•) Ω^{a}_{oset} (○) Ω^{x}_{oset}

(□) Ω^{x}_{nat} *Ideal Beam Model*

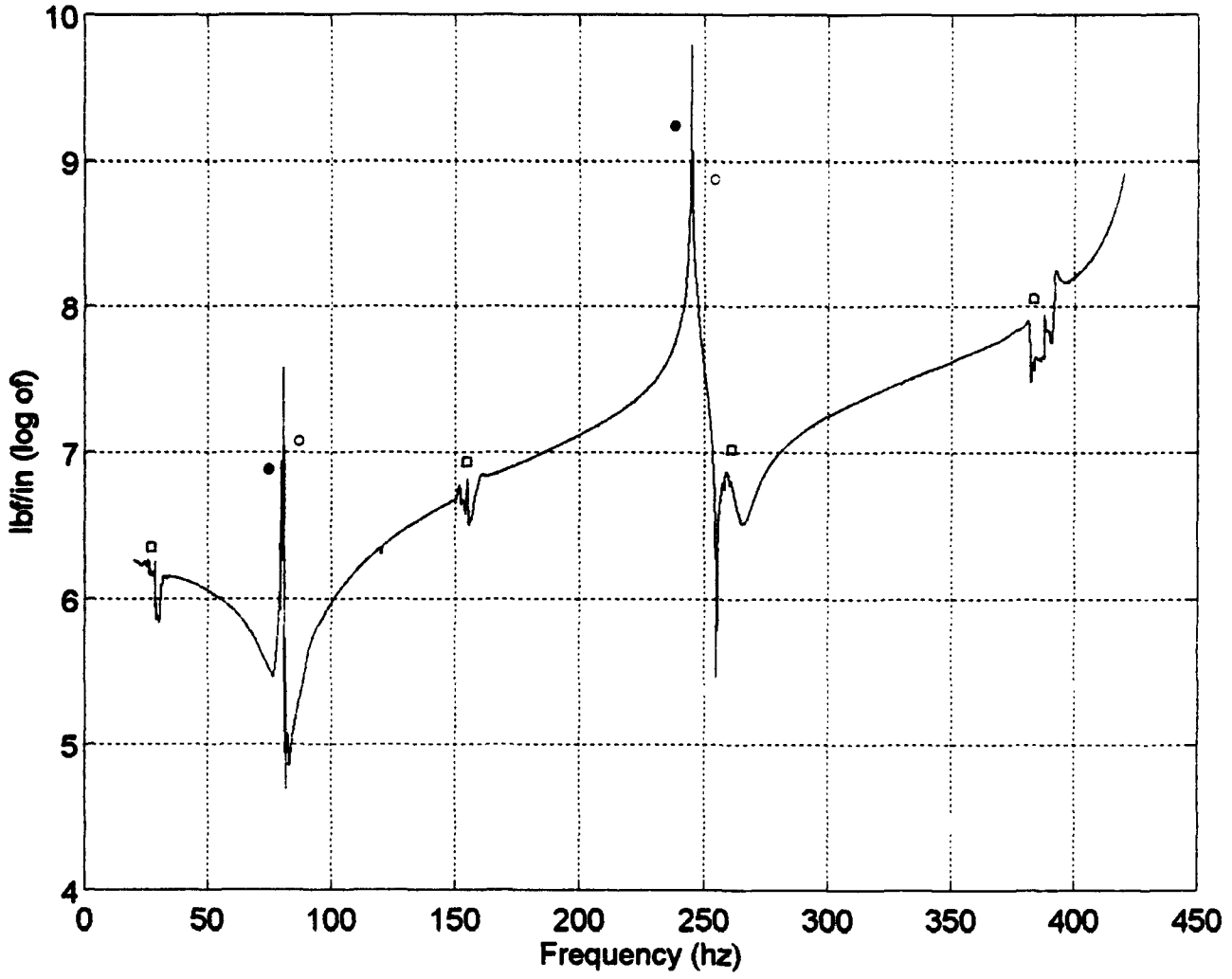

FIGURE 4-23: ΔZ_{33}

(•) Ω^{a}_{oset} (○) Ω^{x}_{oset}

(□) Ω^{x}_{nat} *Ideal Beam Model*

The missing OSET eigenvalues for the impedance error spectra is similar to those missing from the localization matrix calculations. Since the ideal beam model finite element is a very close approximation to the experimental structure, the missing OSET eigenvalues associated with the test system is consistent with those missing from the ideal beam finite element model. A detailed description is provided in Appendix D.

b. Improved Reduction System (IRS)

Figures 4-24 thru 4-26 display the plots of the same impedance error elements as Figures 4-21 thru 4-23 with the exception that the ideal beam model was reduced using the IRS method. As expected, Figure 4-24 shows all the test system OSET eigenvalues as peak values. Figures 4-25 and 4-26 are consistent with Figures 4-22 and 4-23 in that there are missing test system OSET eigenvalues. This will be addressed in Appendix D.

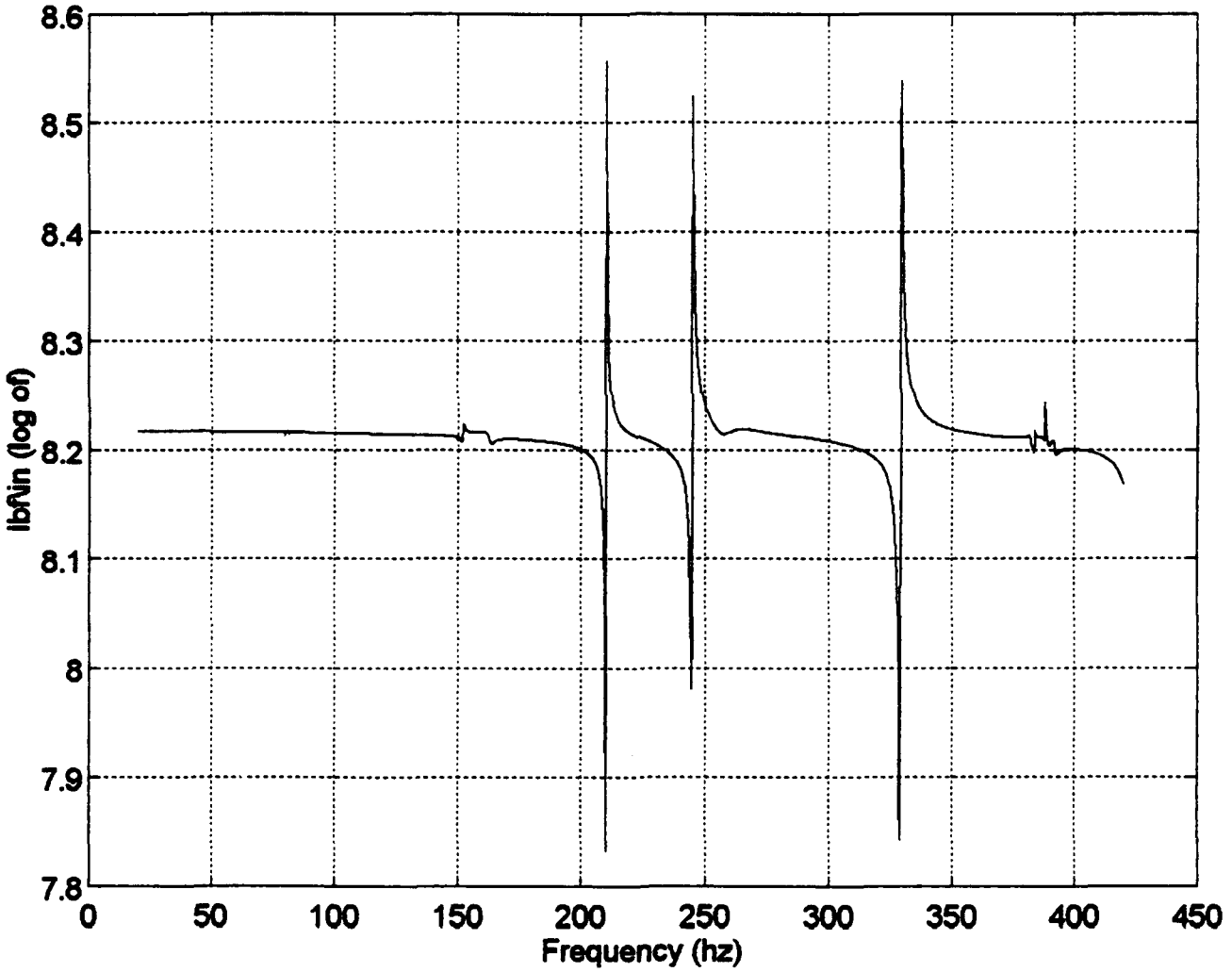

FIGURE 4-24: ΔZ_{11}
IRS - Ideal Beam Model

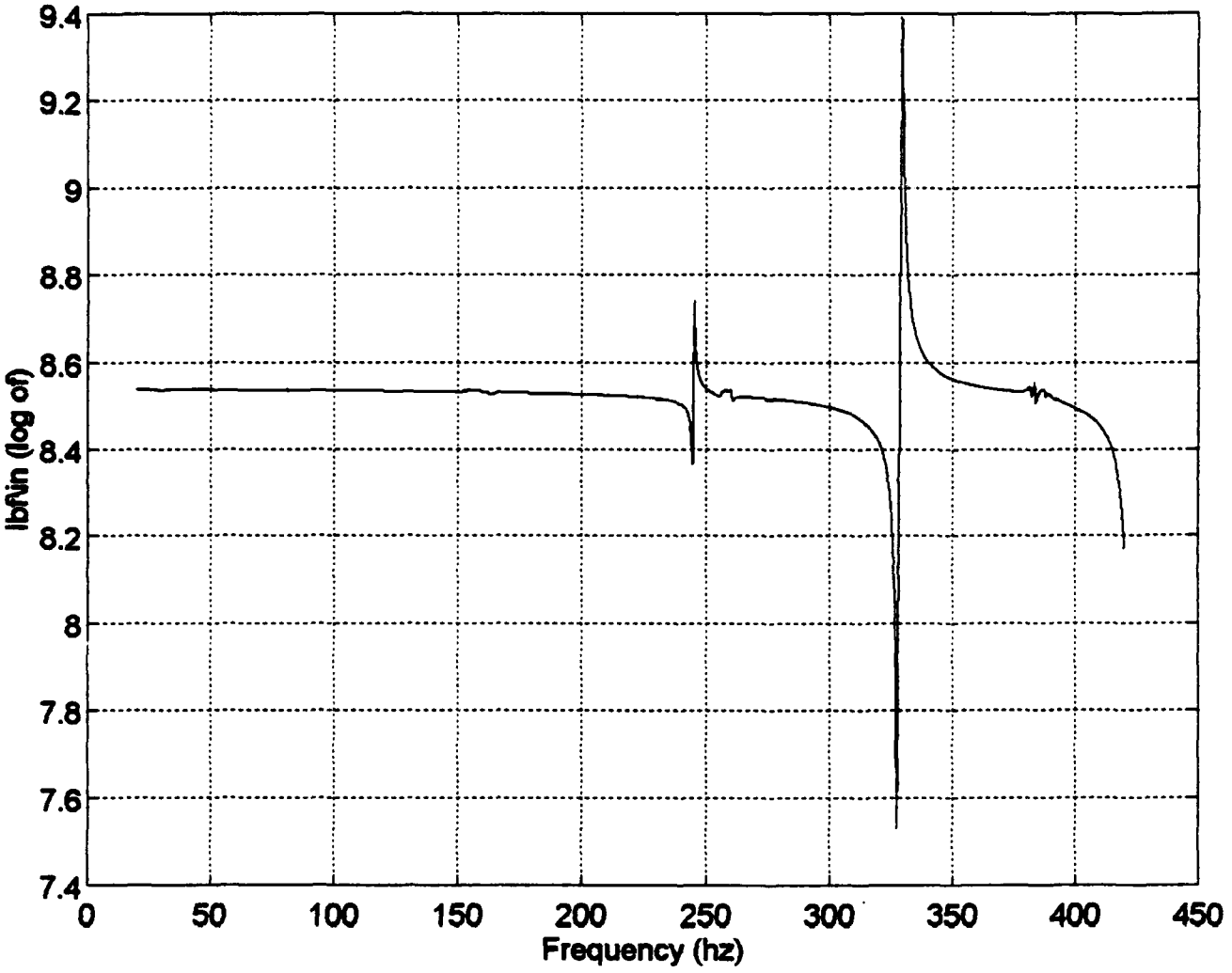

FIGURE 4-25: ΔZ_{22}
IRS Ideal Beam Model

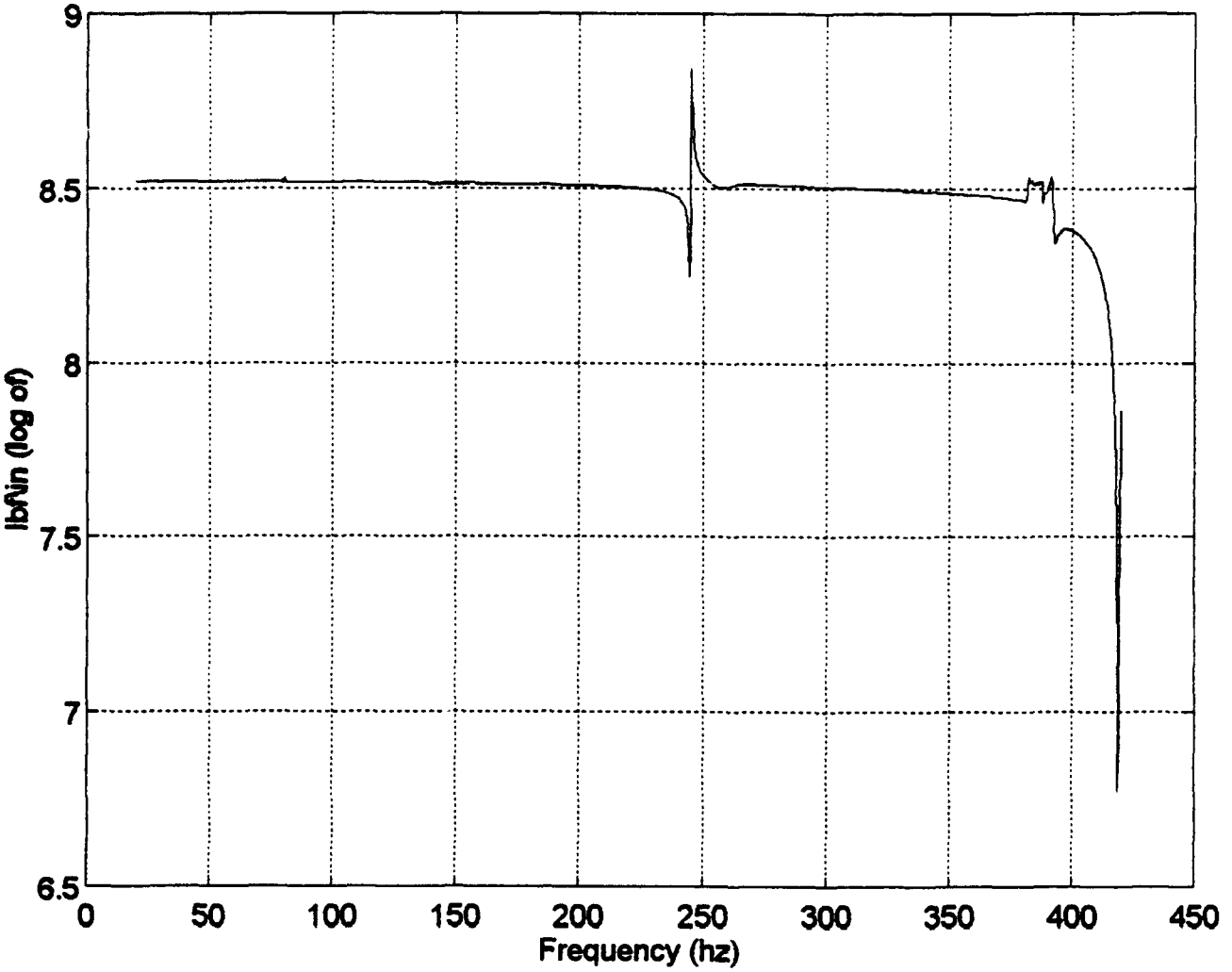

FIGURE 4-26: ΔZ_{33}
IRS - Ideal Beam Model

V. CONCLUSIONS / RECOMMENDATIONS

A. SUMMARY

1. Extraction Reduction

a. Localization

The localization matrix at a specific frequency provides an approximation to the location of the error associated with the finite element model. Spatially incomplete data will not provide a true error location.

A nonlinear dependence of the localization matrix with frequency results due to performing spatially incomplete identification. The plot of localization matrix versus frequency results in peak values corresponding to the test system natural frequencies and the analytical model OSET eigenvalues.

b. Impedance Error

The plot of the impedance error matrix versus frequency results in peak values corresponding to the OSET eigenvalues associated with the test system and analytical models. Test system natural frequencies did appear when using experimental test data.

2. Improved Reduction System (IRS)

a. Localization

Since the IRS transforms the stiffness and mass matrices, the localization matrix at a specific frequency provided no useful information about error location or identification. The plot of the localization matrix versus frequency resulted in peak values corresponding to the test system natural frequencies.

b. Impedance Error

The plot of the impedance error matrix versus frequency results in peak values corresponding to the OSET eigenvalues associated with the test system only.

B. CONCLUSIONS

This thesis has discussed a general theory for error localization and identification. When using frequency response data from a finite element model and an experimental structure, the theory extracts from the matrix difference of the FRF, a set of impedance error spectra.

Spatially complete data will provide the true frequency independent error spectra of mass, stiffness, and damping. Spatially incomplete data can provide an approximate frequency error spectra, but it is impossible to localize and identify the independent errors specifically.

The identification of a secondary dynamic system comprising the coordinates not measured in the vibration test, impacts the test results.

The eigenvalues of this secondary system provide the nonlinearity imposed on the identified parameters. The secondary system ultimately results in the inability to localize and identify the true errors associated with the spatially incomplete data.

C. RECOMMENDATIONS

The real purpose of this thesis was to test the theory provided in references [1,2] with actual frequency response data.

Although satisfactory results were achieved, investigation is still needed for the following items:

- Determine the reason for the appearance of test system natural frequencies in the impedance error spectra using experimental test data.
- The actual mechanism in the finite element model that is causing the missing OSET eigenvalues.
- Implementation of angular test data into the results.

The logical supplement to this test would be to utilize a more complex structure to localize and identify finite element model errors.

APPENDIX A

TEST EQUIPMENT \ PROCEDURE

I. GENERAL SYSTEM DESCRIPTION

A. Purpose

The overall purpose of the test system is to vibrate a given beam at a known force and frequency, and measure the beam response. A frequency response function (FRF) is obtained by repeating the test over several frequencies of interest. The FRF data is then sent to a personal computer for further calculations.

B. System Setup

Figure A-1 is the schematic of the test system. The HP 3562A Dynamic system analyzer controls, measures, and tabulates the FRF. The HP 3562A sends an electronic signal via the SS 250 amplifier that causes the shaker to vibrate at a given frequency and force. This force is measured by the load cell that is attached to the shaker and the beam. This data is sent back to the HP 3562A via the load cell power supply. The beam acceleration is measured by an accelerometer. The accelerometer data is also sent to the HP 3562A via a separate power supply. The HP 3562A performs two fast fourier transforms and develops the FRF. This data is sent to a data disc via the HP 9122 disk drive. The personal computer then obtains the data from the HP 9122 disk drive.

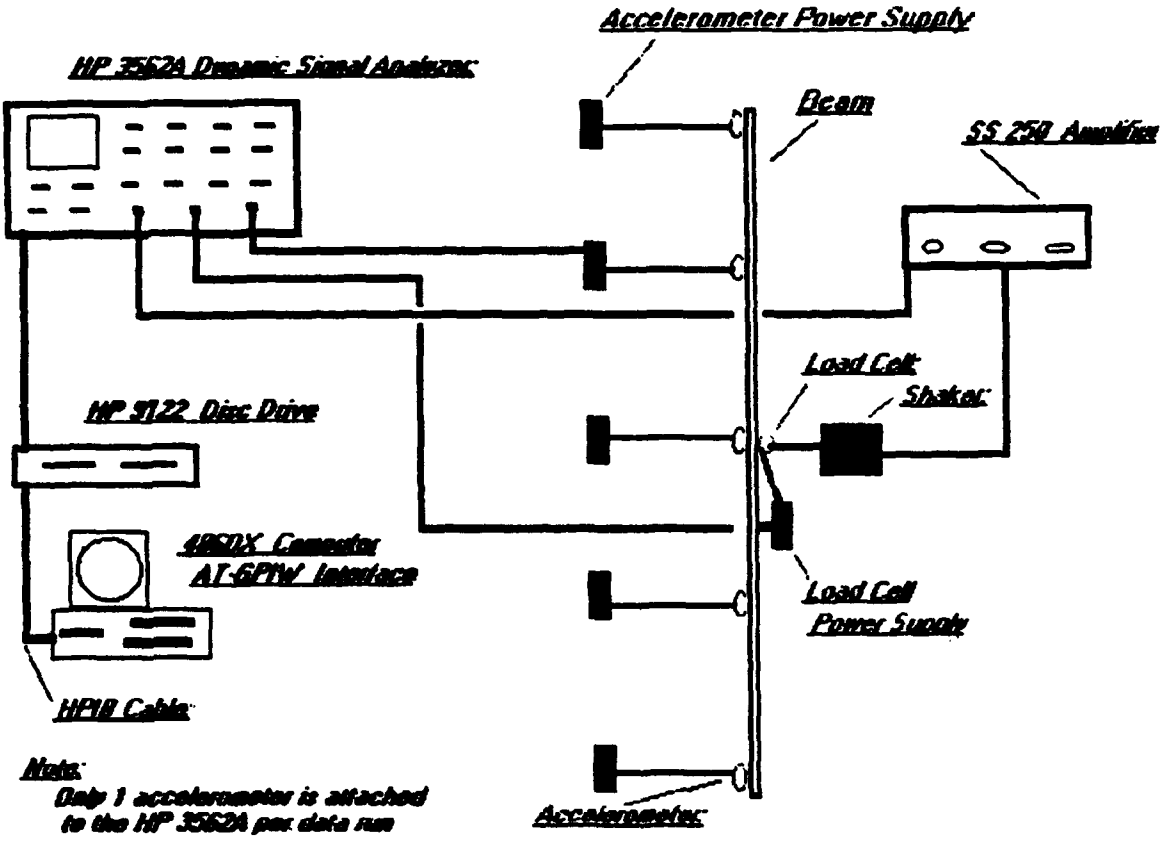

FIGURE A-1: *General System Schematic*

C. System Components

1. HP 3562A Dynamic Signal Analyzer

The HP 3562A is a two-channel analyzer. The source connection supplies the controlling information to the shaker assembly. Channel one receives data from the load cell while channel two receives data from the accelerometer. During a specific data collection operation the HP 3562A can only collect data from the load cell and one accelerometer. The resultant FRF contains 801 data points.

2. HP 9122 Disc Drive

The HP 9122 Disc Drive contains two ports for 3.5" data discs and an HPIB connection port. The HP 9122 is connected to the HP 3562A and the personal computer via the HPIB connection.

3. Personal Computer

The Personal Computer is a DataStor 486 - 66 Mhz computer. An AT-GPIW interface card is installed within the computer. This allows an HPIB interface with the HP 9122 disc drive. Software utilized is MATLAB 4.0 with windows and the HP Standard Data Format (HPSDF). The HPSDF software allows the HP 3562A LIF format data to be transformed into a MAT file for use by MATLAB.

4. Accelerometers

The accelerometers are part of the Model 8832 Translational Angular Piezobeam (TAP) system. The accelerometers measure Translational and angular acceleration (note: The HP 3562A, which is only two channels, can only accept input from the angular or translational output, not both simultaneously).

The accelerometers are mounted to the beam with a thin layer of wax. The operational theory associated with the accelerometers is provided in reference [6]. Specific accelerometer data sheets are provided in this appendix. A total of five accelerometers was used, spaced 15" apart. The accelerometer power supply used 115 volt power from a typical laboratory space outlet.

5. Load Cell

The Load Cell is an Integrated Circuit Piezoelectric (ICP) transducer. The load cell contains a 10/32" tapped connection at each end. One end is attached to the beam and the other end to the shaker assembly via two separate 10/32" screws. The operational theory is provided in reference [7]. Specific transducer data is provided in this appendix. The power supply uses a 1.5 volt battery.

6. Shaker Assembly

The Shaker Assembly is composed of the SS 250 amplifier and the PM25A Vibration Exciter. The PM25A is an electromagnetic vibrator. The SS 250 amplifier allows control of the maximum displacement produced by the vibrator. The PM25A is attached to the Load Cell via a 10/32" screw. The operational theory of the PM25A and the SS 250 is presented in reference [8].

7. Beam

Discussed in detail in Appendix B.

II. TEST PROCEDURE

A. System Designation

The beam has five accelerometers and one load cell attached at any given time. Figure A-2 shows the numbering associated with the accelerometers and load cell locations.

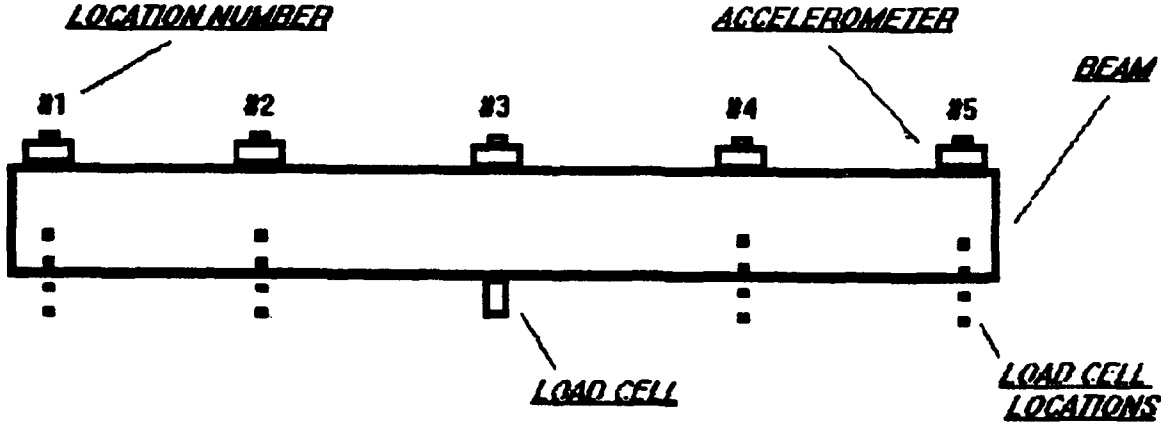

FIGURE A-2: Accelerometer/ Load Cell Designation

Each accelerometer measures translation and angular acceleration that result in ten (5x2) response coordinates. Odd numbers are associated with translational motion, and even numbers are associated with angular motion. Since the shaker only provides translation force (no moments are produced), there are only five excitation coordinates that are odd numbered. Table A.1 provides a summary of the coordinate designation.

TABLE A-1: COORDINATE SYSTEM DESIGNATION

Location Number	Response Coordinate	Excitation Coordinate
1	1,2	1
2	3,4	3
3	5,6	5
4	7,8	7
5	9,10	9

Thus, for example, consider frequency response function h2_5. The number "2" indicates that the response is the angular measurement at location #1 and the number "5" indicates the excitation at location #3.

B. System Physical Setup

1. HP 3562A

The HP 3562A is connected to the various components using a coaxial cable. The source outlet is connected to the SS 250 amplifier. Channel one is connected to the load cell power supply and channel two is connected to the accelerometer power supply. Each accelerometer power supply has two connection points; one for translational motion, the other for angular motion. Only one connection point is used per data run.

2. Shaker Assembly

The SS 250 amplifier is connected via an electrical cable to the PM25A Vibration Exciter. The PM25A is physically attached (via a 10/32" screw) to the back side of the load cell.

3. Accelerometers/Load Cells

The load cell is physically attached (via two separate 10/32" screws) to the shaker and the beam. The electrical output of the load cell is sent to the power supply. The accelerometer electrical output (one cable) is sent to the accelerometer power supply.

C. Data Acquisition

1. HP 3562A

Table A-2 provides a summary of the programmed setpoints of the HP 3562A for a single data collection operation.

TABLE A-2: HP 3562A PROGRAMMED SETPOINTS

PROGRAM SETPOINT	SETTING
Measure Mode	Swept Sine wave Linear Sweep
Select Measurement	Frequency Response
Average	Averages: 3 Auto Integral: 1%
Frequency	Start (20,120,220,320 hz) Span (100 hz)
Source	Source Level: 0.5 v
Engineering Units	Load Cell: 52.56 mv/eu Accelerometer: various
EU Label	Load Cell: mv/lbf Accelerometer: mv/g mv/(rad/s2)

2. System Operation

Placing the HP 3562A in "run" commences the data collection operation. Each data collection operation requires approximately 13 minutes. There was a total of 250 data collection operations (50 runs at each frequency span, 10 response positions and 5 excitation positions, with 5 separate starting frequencies).

If the shaker assembly was not properly aligned with the beam, response was audible at the system resonant frequencies. The FRF plot on the HP 3562A also exhibited noise vice a smooth curve.

D. Data Transformation

This portion of the procedure is the transfer of the data from the HP 3562A to the personal computer that will allow the data to be evaluated using MATLAB codes.

1. File Designation

Data files are labeled in the following format.

h#1_#2X:
- h - letter designator to indicate FRF
- #1 - number indicating response coordinate
- #2 - number indicating excitation coordinate
- X - letter indicating frequency band
  - A : 20 - 120 hz
  - B : 120 - 220 hz
  - C : 220 - 320 hz
  - D : 320 - 420 hz

Thus, for example, h2_5B indicates an FRF that is measuring the angular response at position #1, excitation occurring at position #3, and at a frequency band of 120 - 220 hz.

2. HP 3562A to Personal Computer (PC)

Once an FRF is obtained by the HP 3562A, the data is transferred from the HP 3562A to the HP 9122 Disc drive. Chapter 12 of reference [9] provide detailed procedures for saving and labeling files from the HP 3562A to the HP 9122. The files saved to the HP 9122 were labeled in the format described in Section D.1.

Using the HPSDF software, the PC accesses the file from the HP 9122 and stores the data within the HPSDF directory. The files stored in the HPSDF were also labeled in the same format as described in Section D.1. Appendix A of reference [10] provides a detailed procedure on transferring data from the HP 9122 to the PC.

Two important items that are not mentioned in the reference [10] will influence data operations. Transferred data will be located in the PC hard drive under the HPSDF directory. The second item that is more significant, involves an interface problem between the PC, HP 3562A, and the HP 9122. After accessing data from the HP 9122 with the PC, the system will not allow subsequent transfer of data from the HP 3562A to the HP 9122. The HP 3562A will display a "disc drive not online" warning. Further attempts to access data from the HP 9122 with either the HP 3562A or the PC will be unsuccessful. Complete shutdown of the PC solved the immediate problem. The overall solution is procedural in nature. All data collection operation by the HP 3562A and transfer to the HP 9122 is completed before any data transfer from the HP 9122 to the PC.

3. MAT files

After transfer from the HP 3562A to the PC is completed, the files are located and labeled as C:>HPSDF*.DAT . The * is a wild card designator that describes a specific file labeled in the format described in Section D.1.

Utilizing Appendix A of reference [10], a single *.DAT file is then transformed into a FREQRESP.MAT file. The HPSDF software will always name the transformed file FREQRESP.MAT.

If several files are being transferred, the newer files will over write the older files, thus losing the information from the older files. The FREQRESP.MAT file must be renamed before transforming any subsequent *.DAT files. The DOS command, within the HPSDF directory, RENAME FREQRESP.MAT *.MAT (* is the wild card designator previously described) will accomplish the task of preventing older files from being lost.

Each *.MAT file has two variables, o2i1x is the frequency coordinate, and o2i1 is the y-axis value. The y-axis value is a complex number.

E. Data Manipulation

After completion of data transfer and transformation, there exists 250 *.MAT files that must be further manipulated in order to achieve efficient processing with the MATLAB software.

The first step is to transfer the *.MAT files from the HPSDF directory to the MATLAB directory. The *.MAT files were sent to the directory C:>MATLAB\BEAMDATA using Microsoft Windows Version 3.1.

In order to achieve better computing efficiency, the 250 *.MAT files (each *.MAT file contains a matrix of 801 x 2 elements) is transformed into four files each containing 801 x 50 elements. The o2i1x variable is ignored since the frequency range is linear (frequency spacing between elements is 0.125 hz).

The four files were labeled into the following format.

he*.mat	he: FRF designation *: Frequency Range designator a: 20 - 120 hz b: 120 - 220 hz c: 220 - 320 hz d: 320 - 420 hz

These four files are also located in the directory C:>MATLAB\BEAMDATA. Thus, for example, to obtain the FRF matrix for a frequency of 100 hz would require accessing the hea.mat file and extracting row 640 ((100-20 hz)* 8 rows/hz), columns 1 thru 50.

These four files provide the data for the test system FRF in the MATLAB codes used to solve the localization and impedance error calculations.

KISTLER

Calibration Certificate

UUT #1

TAP™

TRANSLATIONAL ANGULAR PIEZOBEAM SYSTEM MODEL 8832

Accelerometer Model 8696.....SN C58089
Coupler Model 5130.....SN C34612

Angular Sensitivity at 250 Hz, 130 rad/s²	0.478 mV/rad/s²
Linear Sensitivity at 100 Hz, $3g_{rms}$	1019 mV/g

Linear Range	±10 g
Angular Range	±18,000 rad/s²
Mounted Resonant Frequency (nom.)	8 kHz
Transverse Sensitivity max.	2%
Bias Voltage	11 ±3 VDC
Time Constant (nom.)	1.0 s

All measurements at 21°C
g = 9.807 m/s²

NIST TRACEABILITY

This accelerometer was calibrated using a back to back comparison technique against a Kistler Working Standard. The Working Standard is periodically calibrated against a Kistler Reference Standard System which in turn is periodically recertified by the National Institute of Standards and Technology. The calibration of all Kistler acceptance test instrumentation is in conformance with MIL-STD-45662A.

	Working Standard	Reference Standard
Linear Acceleration:		
Accelerometer	Model 809K112 SN C51785	Model 8002K SN C17447
Charge Amplifier	Model 5020 SN C31904	Model 5020 SN C4870
NIST Test Report Number:		822/250337
Angular Acceleration:		
Accelerometers	Model 8602A500M1 SN C36072/SN C36073	Model 808K1 SN 1263
Charge Amplifiers	Model 504E10 SN C4797/SN C4623	Model 561T SN 251
Summing Amplifier	Model 5217 SN 186396	

By: Mark Thomas
Mark Thomas

Date: OCT 08 1993 10-04-1993

KISTLER

Calibration Certificate

WIT #2

TAP™

TRANSLATIONAL ANGULAR PIEZOBEAM SYSTEM MODEL 8832

Accelerometer Model 8696.....SN C58082
Coupler Model 5130.....SN C33393

Angular Sensitivity at 250 Hz, 130 rad/s²	0.485 mV/rad/s²
Linear Sensitivity at 100 Hz, $3g_{rms}$	1014 mV/g

Linear Range	±10 g
Angular Range	±18,000 rad/s²
Mounted Resonant Frequency (nom.)	8 kHz
Transverse Sensitivity max.	2%
Bias Voltage	11 ±3 VDC
Time Constant (nom.)	1.0 s

All measurements at 21°C
g = 9.807 m/s²

NIST TRACEABILITY

This accelerometer was calibrated using a back to back comparison technique against a Kistler Working Standard. The Working Standard is periodically calibrated against a Kistler Reference Standard System which in turn is periodically recertified by the National Institute of Standards and Technology. The calibration of all Kistler acceptance test instrumentation is in conformance with MIL-STD-45662A.

	Working Standard	Reference Standard
Linear Acceleration:		
Accelerometer	Model 809K112 SN C51785	Model 8002K SN C17447
Charge Amplifier	Model 5020 SN C31904	Model 5020 SN C4870
NIST Test Report Number:		822/250337
Angular Acceleration:		
Accelerometers	Model 8602A500M1 SN C36072/SN C36073	Model 808K1 SN 1263
Charge Amplifiers	Model 504E10 SN C4797/SN C4623	Model 561T SN 251
Summing Amplifier	Model 5217 SN 186396	

By: Mark Thomas
Mark Thomas

SEP 24 1993
Date: 09-24-1993

KISTLER

Calibration Certificate

UNIT #3.

TAP™

TRANSLATIONAL ANGULAR PIEZOBEAM SYSTEM MODEL 8832

Accelerometer Model 8696.....SN C58086
Coupler Model 5130.....SN C33406

Angular Sensitivity at 250 Hz, 130 rad/s²	0.483 mV/rad/s²
Linear Sensitivity at 100 Hz, $3g_{rms}$	1024 mV/g

Linear Range	±10 g
Angular Range	±18,000 rad/s²
Mounted Resonant Frequency (nom.)	8 kHz
Transverse Sensitivity max.	2%
Bias Voltage	11 ±3 VDC
Time Constant (nom.)	1.0 s

All measurements at 21°C
g = 9.807 m/s²

NIST TRACEABILITY

This accelerometer was calibrated using a back to back comparison technique against a Kistler Working Standard. The Working Standard is periodically calibrated against a Kistler Reference Standard System which in turn is periodically recertified by the National Institute of Standards and Technology. The calibration of all Kistler acceptance test instrumentation is in conformance with MIL-STD-45662A.

	Working Standard	Reference Standard
Linear Acceleration:		
Accelerometer	Model 809K112 SN C51785	Model 8002K SN C17447
Charge Amplifier	Model 5020 SN C31904	Model 5020 SN C4870
NIST Test Report Number:		822/250337
Angular Acceleration:		
Accelerometers	Model 8602A500M1 SN C36072/SN C36073	Model 808K1 SN 1263
Charge Amplifiers	Model 504E10 SN C4797/SN C4623	Model 561T SN 251
Summing Amplifier	Model 5217 SN 186396	

SEP 24 1993

By: Mark Thomas
Mark Thomas

Date: 09-24-1993

KISTLER

Calibration Certificate

UUT #4

TAP™

TRANSLATIONAL ANGULAR PIEZOBEAM SYSTEM MODEL 8832

Accelerometer Model 8696.....SN C58085
Coupler Model 5130.....SN C33394

Angular Sensitivity at 250 Hz, 130 rad/s²	0.493 mV/rad/s²
Linear Sensitivity at 100 Hz, $3g_{rms}$	1017 mV/g

Linear Range	±10 g
Angular Range	±18,000 rad/s²
Mounted Resonant Frequency (nom.)	8 kHz
Transverse Sensitivity max.	2%
Bias Voltage	11 ±3 VDC
Time Constant (nom.)	1.0 s

All measurements at 21°C
g = 9.807 m/s²

NIST TRACEABILITY

This accelerometer was calibrated using a back to back comparison technique against a Kistler Working Standard. The Working Standard is periodically calibrated against a Kistler Reference Standard System which in turn is periodically recertified by the National Institute of Standards and Technology. The calibration of all Kistler acceptance test instrumentation is in conformance with MIL-STD-45662A.

	Working Standard	Reference Standard
Linear Acceleration:		
Accelerometer	Model 809K112 SN C51785	Model 8002K SN C17447
Charge Amplifier	Model 5020 SN C31904	Model 5020 SN C4870
NIST Test Report Number:		822/250337
Angular Acceleration:		
Accelerometers	Model 8602A500M1 SN C36072/SN C36073	Model 808K1 SN 1263
Charge Amplifiers	Model 504E10 SN C4797/SN C4623	Model 561T SN 251
Summing Amplifier	Model 5217 SN 186396	

SEP 24 1993

By: Mark Thomas
Mark Thomas

Date: 09-24-1993

KISTLER

Calibration Certificate WIT #5.

TAP™

TRANSLATIONAL ANGULAR PIEZOBEAM SYSTEM MODEL 8832

Accelerometer Model 8696.....SN C58087
Coupler Model 5130.....SN C34610

Angular Sensitivity at 250 Hz, 130 rad/s²	0.485 mV/rad/s²
Linear Sensitivity at 100 Hz, $3g_{rms}$	1020 mV/g

Linear Range	±10 g
Angular Range	±18,000 rad/s²
Mounted Resonant Frequency (nom.)	8 kHz
Transverse Sensitivity max.	2%
Bias Voltage	11 ±3 VDC
Time Constant (nom.)	1.0 s

All measurements at 21°C
g = 9.807 m/s²

NIST TRACEABILITY

This accelerometer was calibrated using a back to back comparison technique against a Kistler Working Standard. The Working Standard is periodically calibrated against a Kistler Reference Standard System which in turn is periodically recertified by the National Institute of Standards and Technology. The calibration of all Kistler acceptance test instrumentation is in conformance with MIL-STD-45662A.

	Working Standard	Reference Standard
Linear Acceleration:		
Accelerometer	Model 809K112 SN C51785	Model 8002K SN C17447
Charge Amplifier	Model 5020 SN C31904	Model 5020 SN C4870
NIST Test Report Number:		822/250337
Angular Acceleration:		
Accelerometers	Model 8602A500M1 SN C36072/SN C36073	Model 808K1 SN 1263
Charge Amplifiers	Model 504E10 SN C4797/SN C4623	Model 561T SN 251
Summing Amplifier	Model 5217 SN 186396	

By: Mark Thomas
Mark Thomas

OCT 0 8 1993

Date: 10-04-1993

ICP CALIBRATION DATA

Model 208A02
S/N 10539

Cal Range 0 - 100 lbs.
Sens* 52.56 mV/lbs.
Linearity* < 1.0 %FS

Input TC >500 sec
Rise Time 10 usec
Nat'l Freq 70 kHz
Output Imp < 100 ohms

By Gary Redmo
Date Aug 31, 199

* By comparison with reference standard per ISA S37.10. Zero Based best straight line.

Calibration of instrumentation used to certify this sensor is traceable to NIST.

PCB Piezotronics' calibration procedure is in compliance with MIL-STD-45662A.

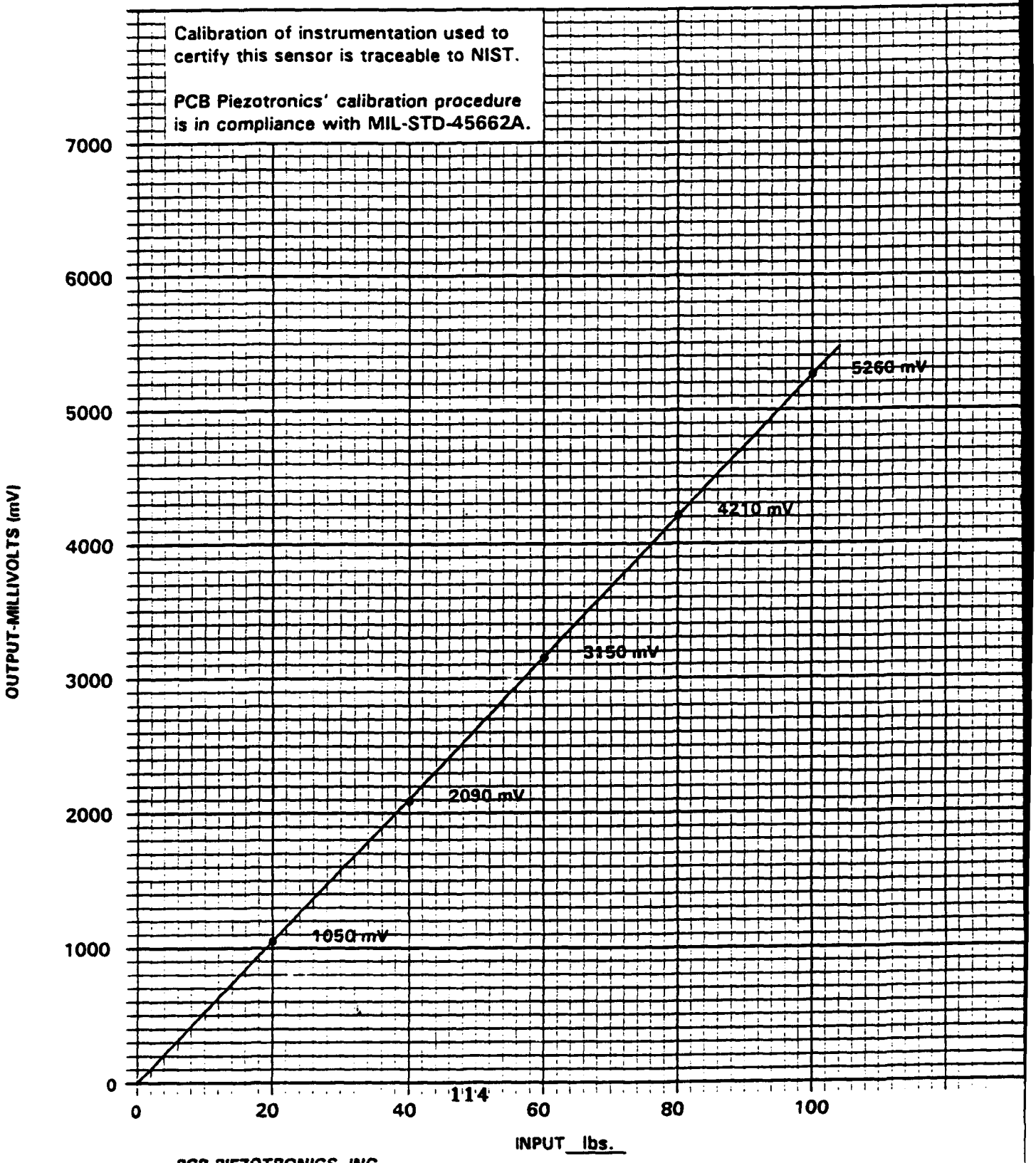

PCB PIEZOTRONICS, INC.
3425 Walden Avenue, Depew NY 14043
Tel:716-684-0001 TWX:710-263-1371

Customer

PO Number

Setting the determinant of the left hand matrix equal to zero and solving.

$$2*(\cosh(kL)\sin(kL) - \sinh(kL)\cos(kL)) = 0 \qquad (B.5)$$

Equation (B.5) defines an infinite number of solutions for the term "kl".

B. Mode Shapes

Combining equations (B.1) thru (B.4), a general expression of the wave equation for a given mode can be determined.

$$\phi_i(x) = \cosh(k_i x) + \cos(k_i x) - \alpha_i(\sinh(k_i x)+\sin(k_i x)) \qquad (B.6a)$$

$$\alpha_i = \frac{\cosh(k_i l)-\cos(k_i l)}{\sinh(k_i l)-\sin(k_i l)} \qquad (B.6b)$$

TABLE B-2: KL AND ALPHA VALUES

Mode	kl	Alpha
1	4.730041	0.982502
2	7.853205	1.000777
3	10.995607	0.999966
4	14.137165	1.000001
5	17.278760	1.000000

Numerically solving equation (B.6) and inserting values for x, the graphed solution will depict the shape of the beam for the given mode.

Figures B-1 thru B-5 display the first five mode shapes of the experimental beam. The mode shapes were normalized by using the first normalization method.

C. Natural Frequencies

Reference [12] provides the mathematical development for the equation for determining the natural frequencies. Equation (B.7) is provided without proof.

$$\omega_i = \frac{k_i^2}{2\pi}\sqrt{\frac{E\,I}{\gamma}} \qquad (B.7)$$

with $\gamma = \rho * Cross\text{-}Sectional\ Area$

TABLE B-3: CALCULATED NATURAL FREQUENCIES

MODE	FREQUENCY (HZ)
First	29.65
Second	81.72
Third	160.20
Fourth	264.38
Fifth	395.61

III. FINITE ELEMENT MODELING

The finite element model divides the beam into multiple homogenous elements. All the multiple elements of the structure are then combined to produce the overall structural model. This structural model is then utilized to calculate the system response.

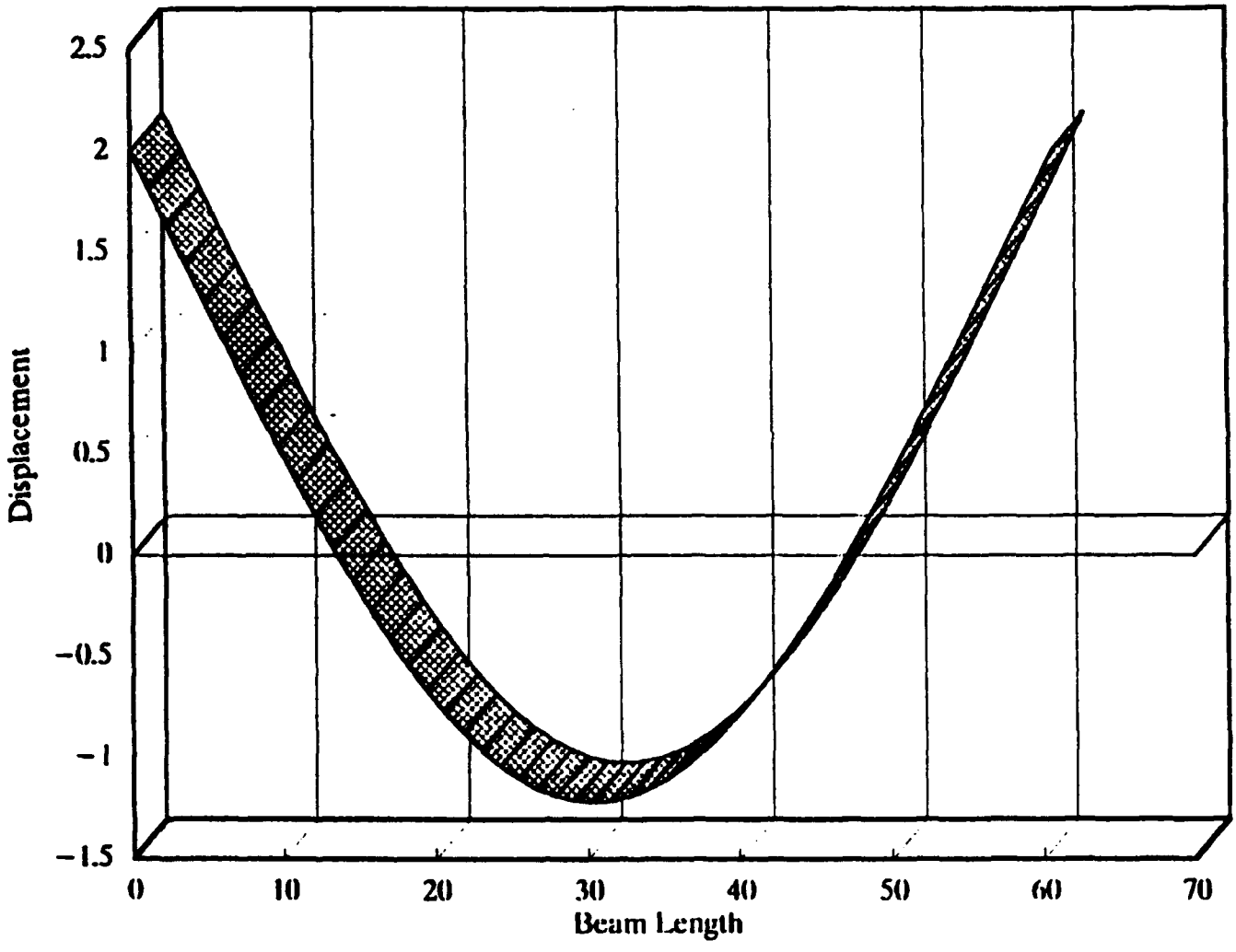

FIGURE B-1: Beam First Mode

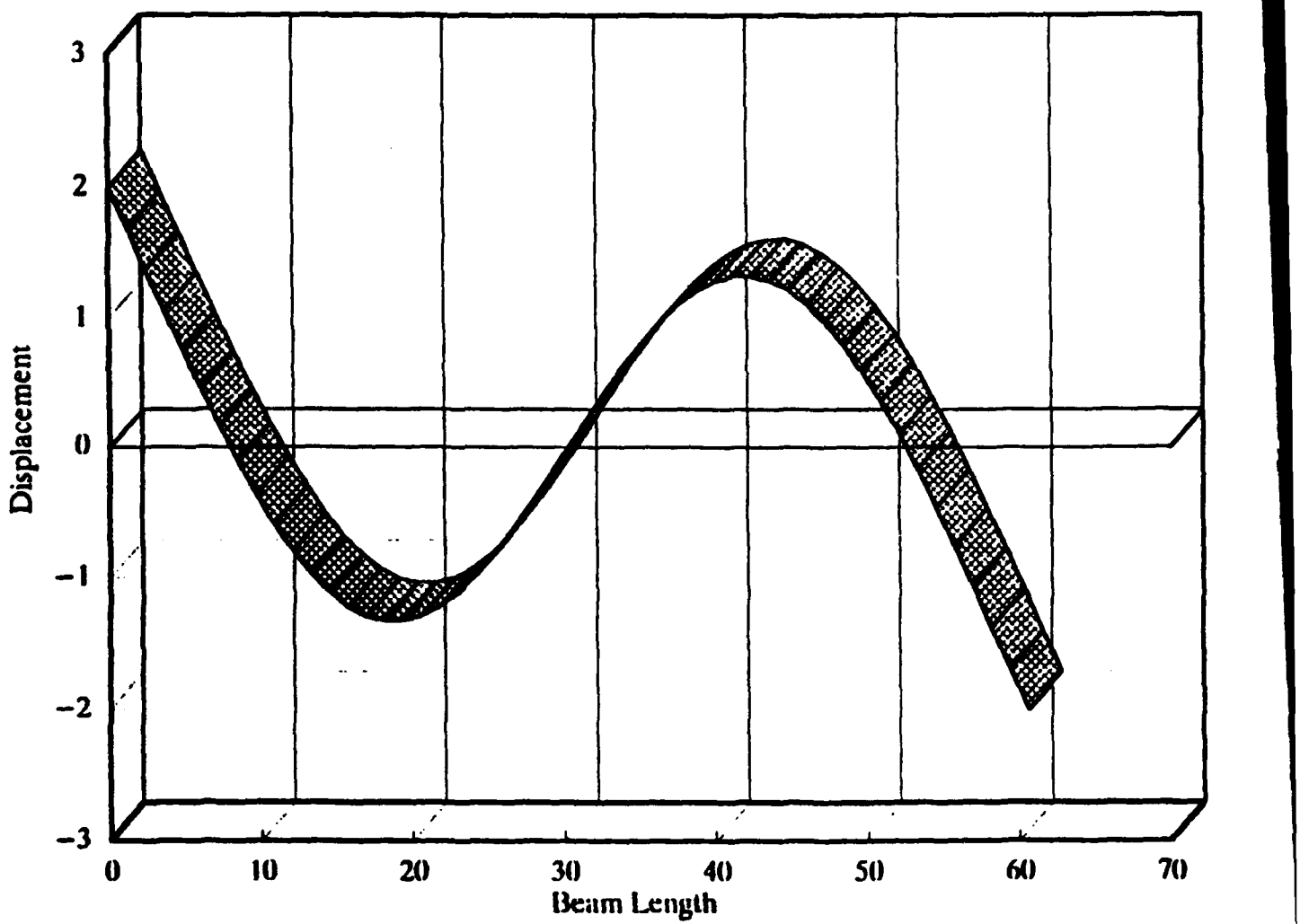

FIGURE B-2: *Beam Second Mode*

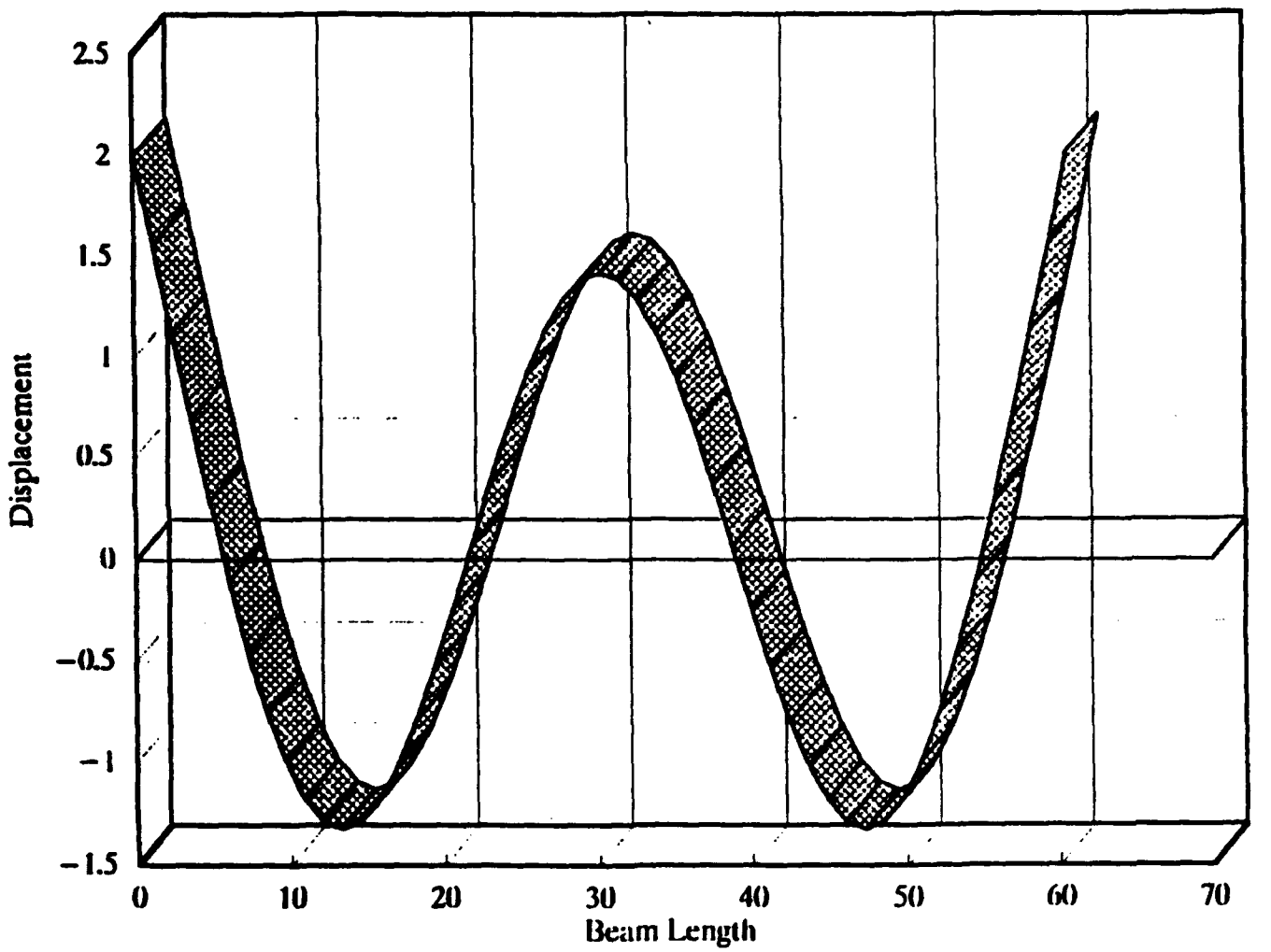

FIGURE B-3: *Beam Third Mode*

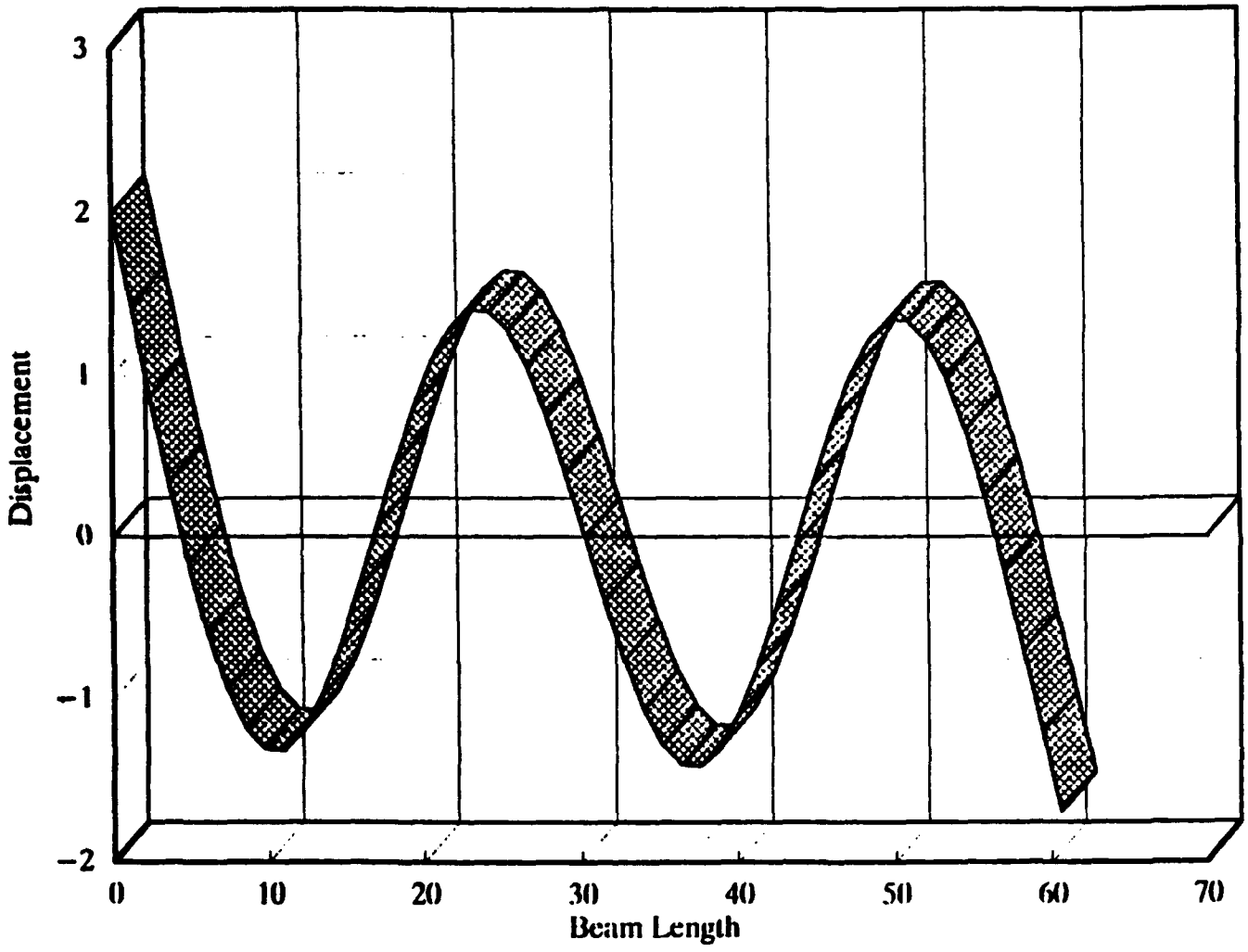

FIGURE B-4: *Beam Fourth Mode*

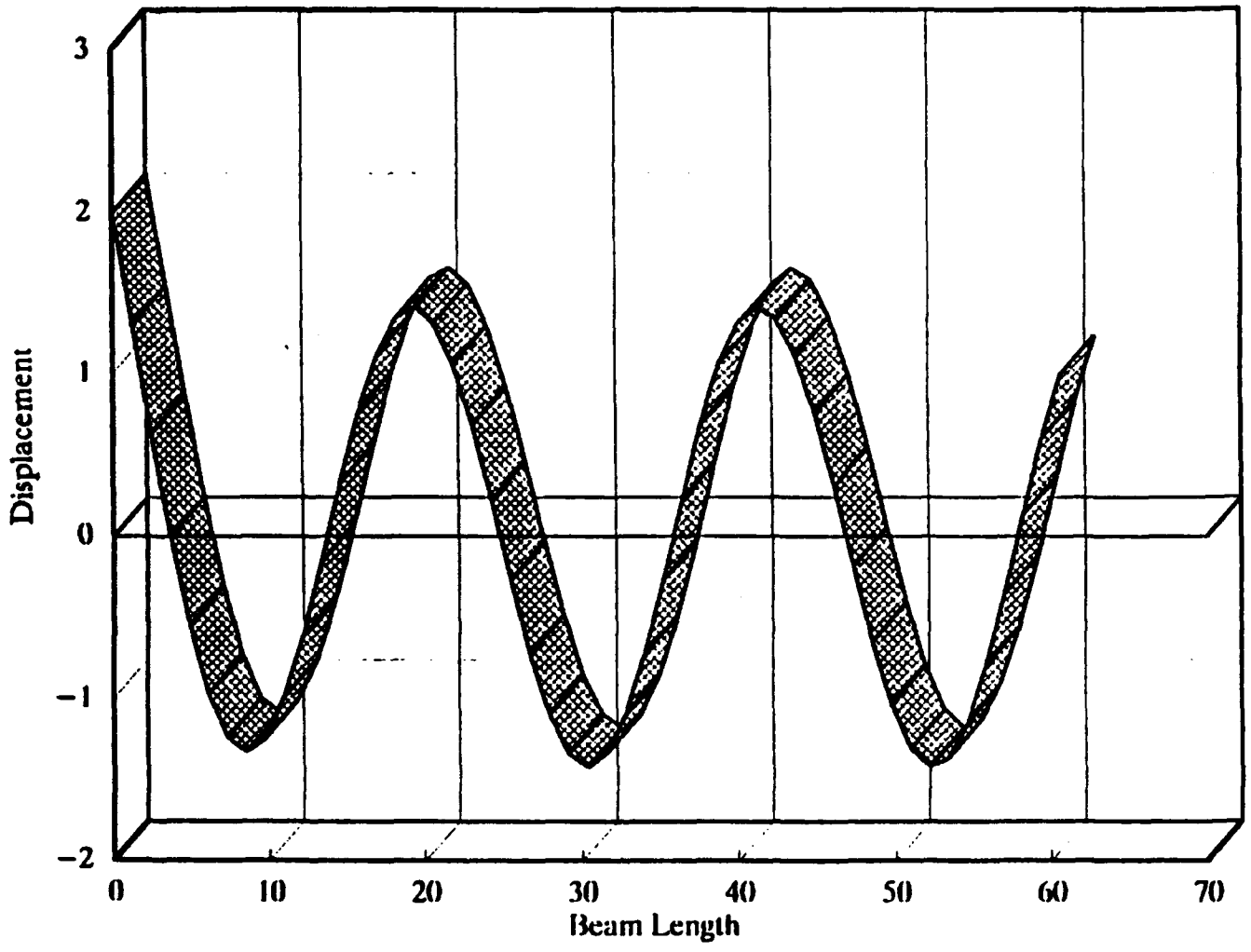

FIGURE B-5 *Beam*
Fifth Mode

Reference [13] is used as guidance for the finite element development. Bernoulli-Euler theory considers a beam element with uniform length (L), mass density (p), elastic modulus (E), cross-sectional (A), and moment of inertia (I). There are two degrees of freedom (traverse and angular motion) per node. Each element has two nodes and therefore a total of four degrees of freedom. The displacement of the beam can be described as written in equation (B.8).

$$v(x,t) = \sum_{i=1}^{4} \psi_i(x)\, \nu_i(t) \qquad (B.8)$$

$$\psi_i = \textit{shape function}$$

The subscript "i" in equation (B.8) describes the specific mode shape of the structure.

The shape function must satisfy the following boundary conditions.

$$\psi_1(0) = \psi_2'(0) = \psi_3(L) = \psi_2'(L) = 1 \qquad (B.9a)$$

$$\psi_1'(0) = \psi_1(L) = \psi_1'(L) = 0 \qquad (B.9b)$$

$$\psi_2(0) = \psi_2(L) = \psi_2'(L) = 0 \qquad (B.9c)$$

$$\psi_3(0) = \psi_3'(0) = \psi_3'(L) = 0 \qquad (B.9d)$$

$$\psi_4(0) = \psi_4'(0) = \psi_4(L) = 0 \qquad (B.9e)$$

Each element can be assumed to be loaded only at its ends. Thus the equilibrium equation is given by equation (B.10).

$$(EIv'')'' = 0 \qquad (B.10)$$

The general solution to equation (B.10) is a cubic polynomial.

$$v(x) = C_1 + C_2(\frac{x}{L}) + C_3(\frac{x}{L})^2 + C_4(\frac{x}{L})^3 \qquad (B.11)$$

Inserting the boundary conditions from equation (B.9) into equation (B.11) results in the following expressions for the shape functions.

$$\psi_1 = 1 - 3(\frac{x}{L})^2 + 2(\frac{x}{L})^3 \qquad (B.12a)$$

$$\psi_2 = x - 2L(\frac{x}{L})^2 + L(\frac{x}{L})^3 \qquad (B.12b)$$

$$\psi_3 = 3(\frac{x}{L})^2 - 2(\frac{x}{L})^3 \qquad (B.12c)$$

$$\psi_4 = -L(\frac{x}{L})^2 + L(\frac{x}{L})^3 \qquad (B.12d)$$

A. Stiffness / Mass Matrices

The Bernoulli-Euler stiffness and mass coefficients for each element can be described by equation (B.13).

$$k_{ij} = \int_0^L EI\psi_i''\psi_j'' \, dx \qquad (B.13a)$$

$$m_{ij} = \int_0^L \rho A\psi_i\psi_j \, dx \qquad (B.13b)$$

1. Basic Element

Combining equations (B.12) and (B.13) will result in the stiffness and mass matrices for the basic beam element. For example, to solve for element "1,1" (i=1 and j=1), compute the second derivative of the first shape equation (equation (B.12a)).

$$\psi_1'' = -\frac{6}{L^2} + \frac{12}{L^2}(\frac{x}{L}) \qquad (B.14)$$

Inserting equations (B.12) and (B.14) into equation (B.13) will result in a mass and stiffness expression for the "1,1" element.

$$k_{11} = 36\,\frac{EI}{L^4}\int_0^L 1 - 4\left(\frac{x}{L}\right) + 4\left(\frac{x}{L}\right)^2\,dx \qquad (B.15a)$$

$$m_{11} = \rho A\int_0^L 1 - 6\left(\frac{x}{L}\right)^2 + 4\left(\frac{x}{L}\right)^3 - 12\left(\frac{x}{L}\right)^5 + 4\left(\frac{x}{L}\right)^6\,dx \qquad (B.15b)$$

The elemental stiffness and mass matrices can be developed by solving for each coefficient. The final results, which are provided by reference [13], are as follows.

$$k = \frac{EI}{L^3}\begin{Vmatrix} 12 & 6L & -12 & 6L \\ 6L & 4L^2 & -6L & 2L^2 \\ -12 & -6L & 12 & -6L^2 \\ 6L & 2L^2 & -6L & 4L^2 \end{Vmatrix} \qquad (B.16)$$

$$m = \rho\frac{AL}{420}\begin{Vmatrix} 156 & 22L & 54 & -13L \\ 22L & 4L^2 & 13L & -3L^2 \\ 54 & 13L & 156 & -22L \\ -13L & -3L^2 & -22L & 4L^2 \end{Vmatrix} \qquad (B.17)$$

Equations (B.16) and (B.17) were used to develop the finite element model for the beam used in the experiment. The number of elements chosen are divisible by four. This will ensure that the elements are sized equally and that the load cell and accelerometers would always be located on an elemental boundary.

2. Other Model Considerations

The basic finite element model considers a beam to be 60 inches long, neglects the effects due to the weight from the accelerometers and the load cell, and the weight loss from the drilled and tapped connection points on the beam. The actual beam is 60.625 inches long. The added length allows the entire surface of the accelerometers to be mounted at both ends. The extra 0.3125 inches on each end is considered a "lumped mass" at the end coordinates.

The moment of inertia due to the lumped mass was added on to the appropriate elements of the mass matrix. Each accelerometer weighs 9.1 grams and remained at the same location throughout the experiment. The accelerometers were also considered as lumped masses at the appropriate coordinates. The load cell changed location depending on the excitation coordinate, thus to simplify the calculations the load cell mass was neglected. The weight loss due to the drilled connection points for the load cell was also considered insignificant and thus ignored in the final model.

B. Number of Elements

The decision as to the number of elements for the finite element model must be considered somewhat carefully. Table B-3 lists the natural frequencies for a given number of model elements.

The natural frequencies converge to a limiting value as the number of elements are increased. Figures B-6 and B-7 plot the frequency versus the number of elements for the fourth and fifth modes. Both plots show the convergence to a single frequency with the increase in the number of elements.

TABLE B-4: FREQUENCY (HZ) VS. BEAM ELEMENTS

# OF ELEMENT	First Mode	Second Mode	Third Mode	Fourth Mode	Fifth Mode
4	29.10	80.00	158.47	289.49	451.86
8	29.07	79.97	157.44	260.64	391.63
12	29.07	79.96	157.20	259.66	388.71
16	29.07	79.96	157.15	259.46	388.09
20	29.07	79.96	157.14	259.41	387.91
24	29.07	79.96	157.13	259.39	387.85
28	29.07	79.96	157.13	259.38	387.81

As the number of elements are increased, the finite element model accuracy increases. The disadvantage is that as the number of elements increase, so does the computing time. In the experimental calculations, the 24 beam element model was considered to provide sufficient accuracy.

IV. MODEL ACCURACY

The accuracy of the various models can be compared to the observed response from the experiment. The finite element model will always be assumed to have 24 beam elements.

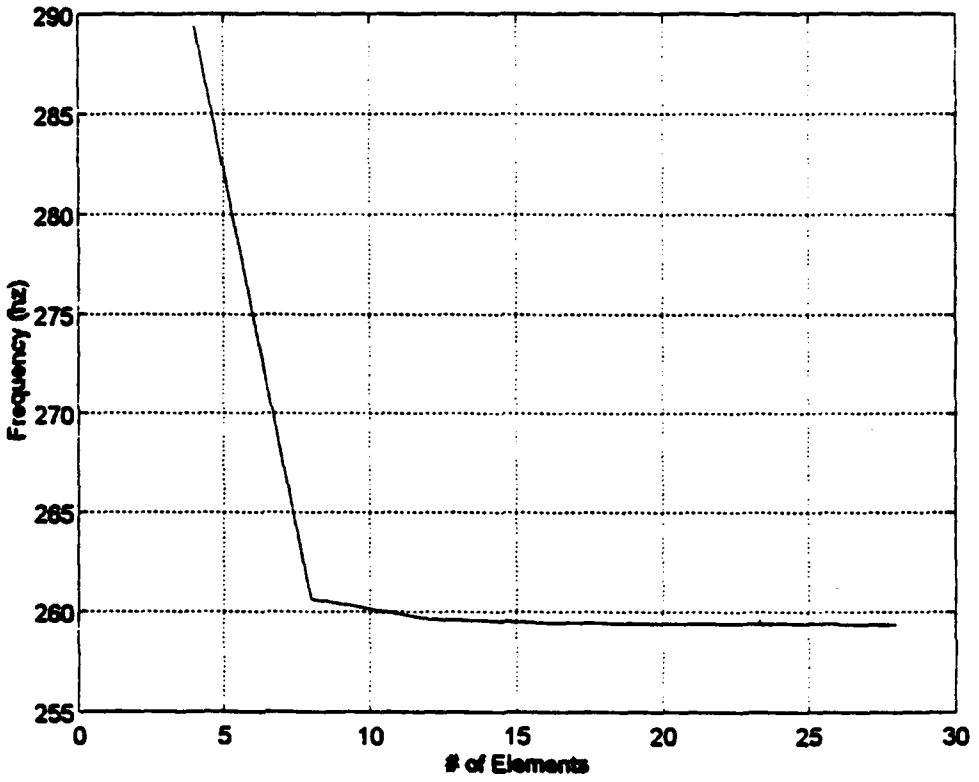

FIGURE B-6: *Fourth Mode Frequency vs # Elements*

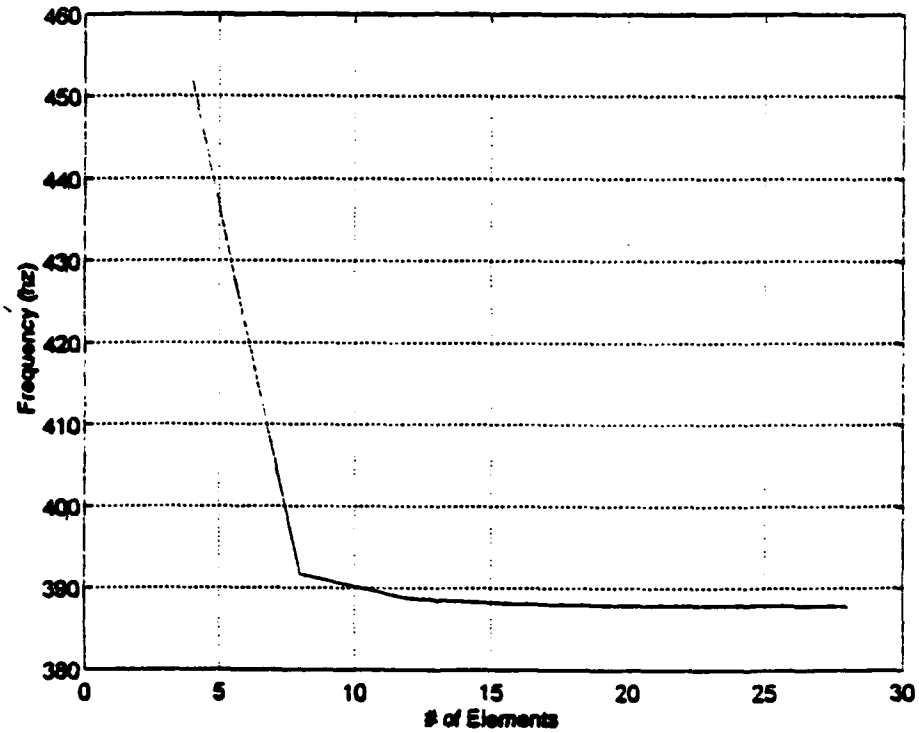

FIGURE B-7: *Fifth Mode Frequency vs # Elements*

A. Natural Frequencies

The natural frequencies obtained from the exact solution and the finite element model were compared with the observed natural frequencies from the experiment. Tables B-5 and B-6 summarize the results of the natural frequency comparison.

TABLE B-5: EXACT SOLUTION VS. OBSERVED DATA

Modes	First	Second	Third	Fourth	Fifth
Observe	29.90	81.20	155.90	258.30	387.80
Exact	29.65	81.72	160.20	264.38	395.61
% Error	0.84	0.64	2.76	2.35	2.01

TABLE B-6: FINITE ELEMENT VS. OBSERVED DATA

Modes	First	Second	Third	Fourth	Fifth
Observe	29.90	81.20	155.90	258.30	387.80
Model	29.07	79.96	157.13	259.39	387.85
% Error	2.76	1.53	0.79	0.42	0.01

As shown in Tables B-5 and B-6 both the exact solution and the finite element model results corresponded with the observed results from the experiments.

B. Frequency Response Function (FRF)

Frequency response curves from the finite element model were compared with the frequency response curves from the experiment.

Figure B-8 is a plot of the "1,1" element of the finite element model and experimental FRF curves. The close proximity of the two curves indicate that the finite element model closely approximates the experimental structure. Figure B-9 is the same plot as Figure B-8 with the exception of using a four element (vice 24 element) model. As expected, the four element model is not as good an approximation as the 24 element model. Figure B-10 is also the same as Figure B-8 with the exception that damping was added to the finite element model. The damping decreased the peak values associated with the natural frequencies of the finite element FRF curve.

V. UNIT ANALYSIS

The units of the FRF matrix from the finite element model are not equivalent to the units of the FRF matrix from the HP 3562A. Figure B-11 is a block diagram of the unit conversion associated with the translational elements of the FRF matrix. This conversion is required for comparisons and calculations involving finite element models and experimental test data. The rotational elements of the FRF matrices undergo the same conversion with the addition of dividing the experimental FRF by the gain factor associated with the accelerometer power supply.

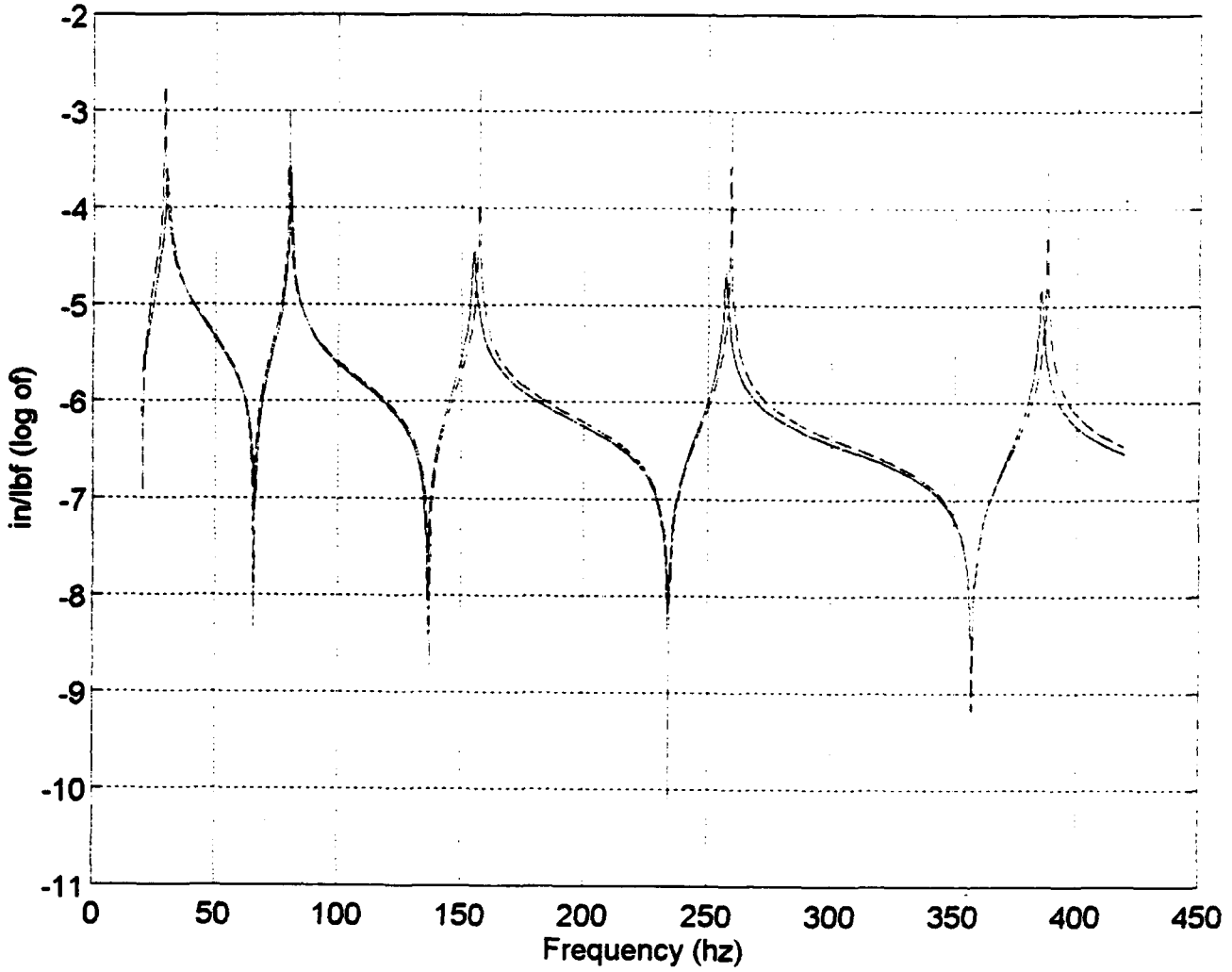

FIGURE B-8: $H_{11}(\Omega)$
24 Elements

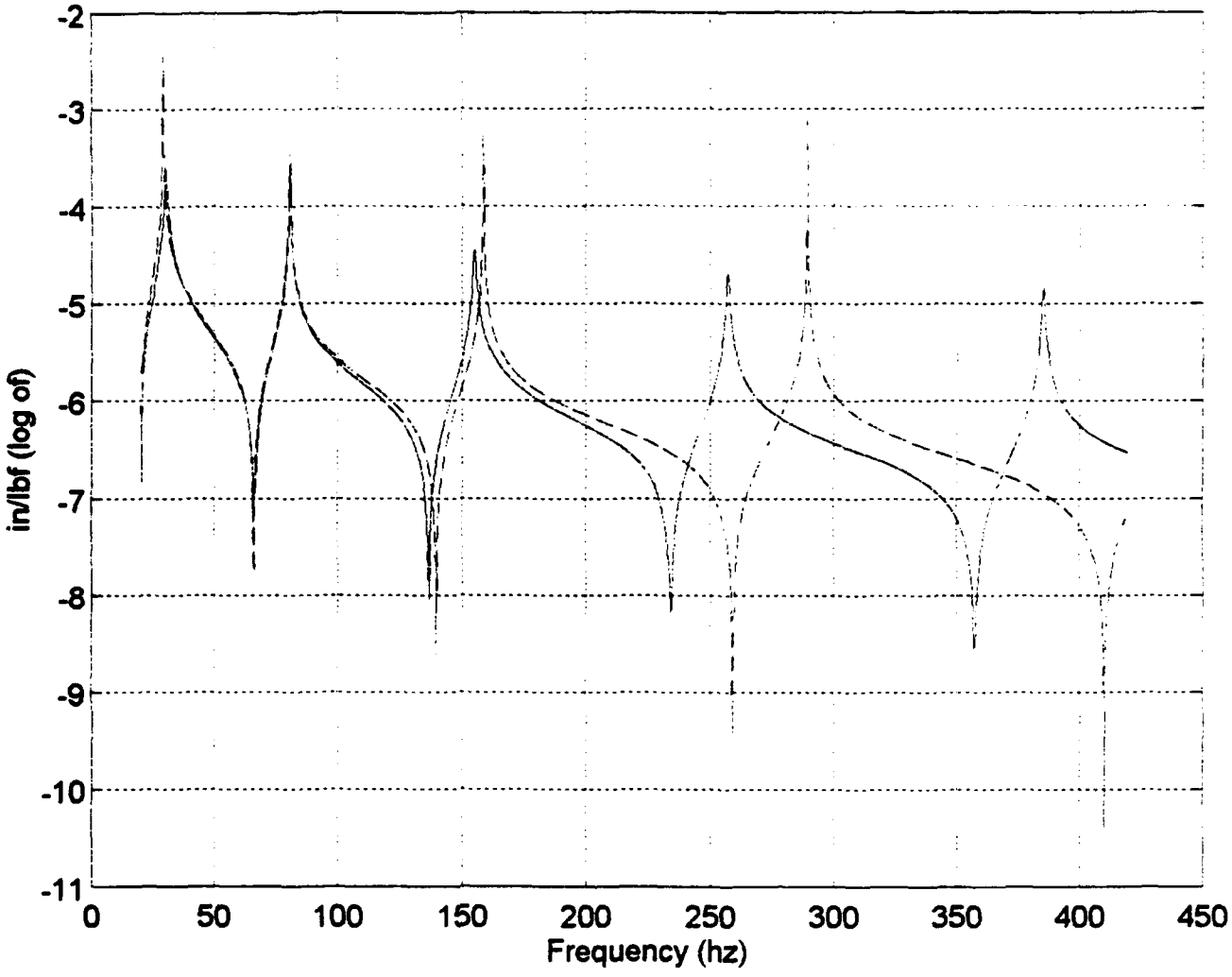

FIGURE B-9: $H_{11}(\Omega)$
4 Elements

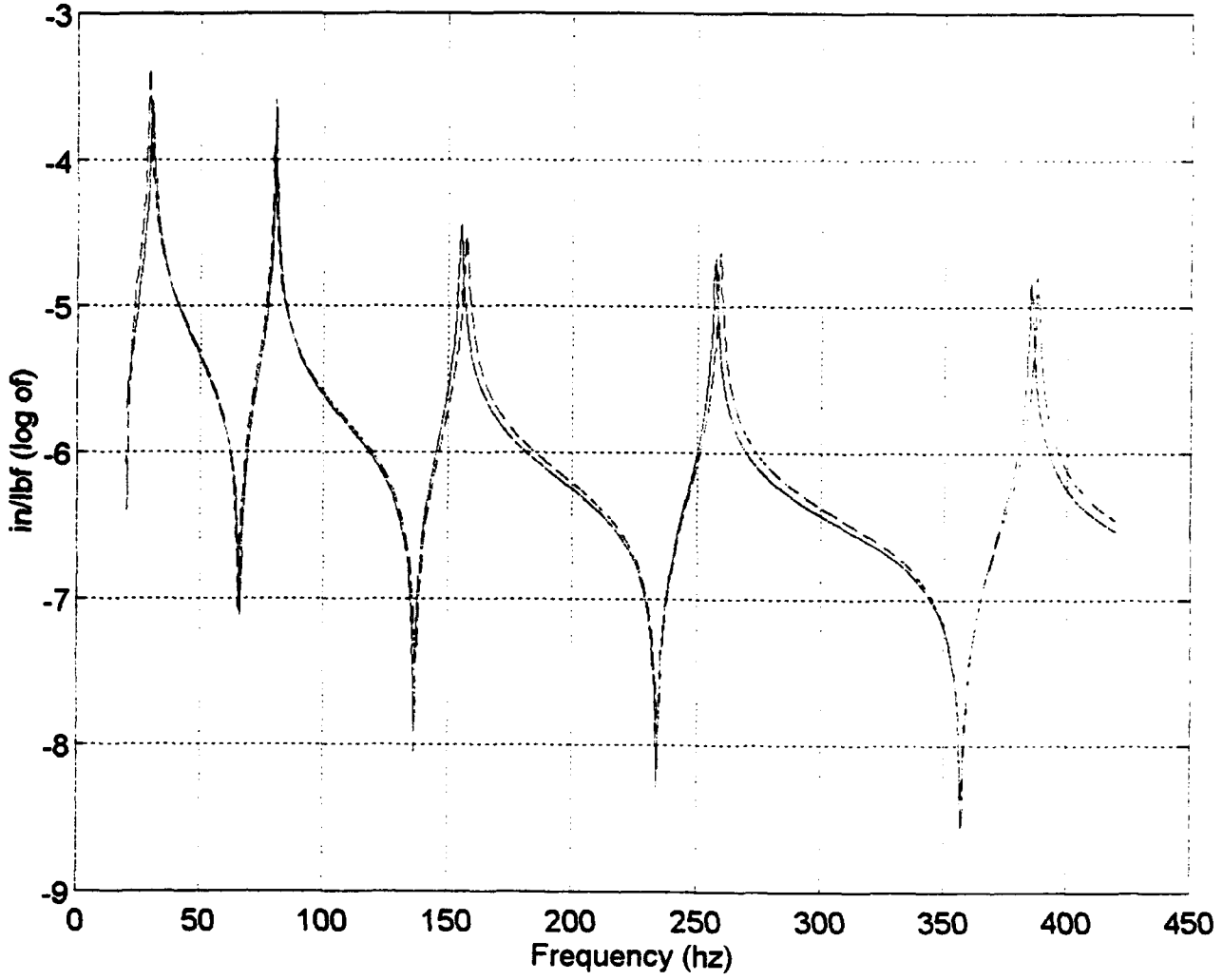

FIGURE B-10: $H_{11}(\Omega)$
24 Elements
Damped Model

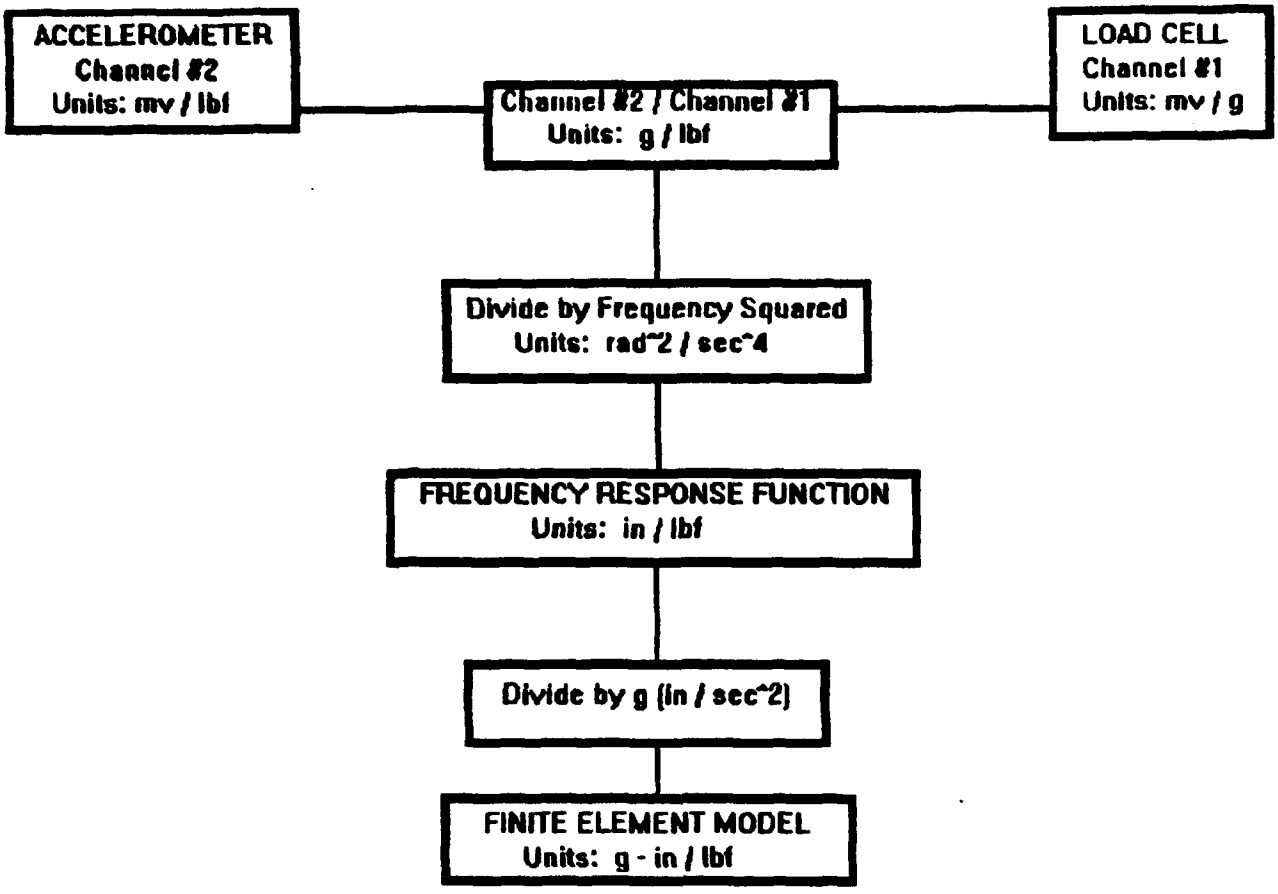

FIGURE B-11: *Unit Analysis - Translational Coordinates*

APPENDIX C

COMPUTER CODE

```
%                    BMMODEL.M
%
%              Calculates the the global mass and stiffness
%              matrices.
%
%              The beam dimensions must be adjusted in the
%              program as appropriate.  The beam is also
%              considered homogeneous throughout its entire
%              length.
%
%              This program also includes addition of an extra
%              0.3125 inches of beam as a "lumped mass" at each
%              end, and the weight due to the accelerometers.
%
%       Inputs:
%              Number of beam elements (input prior to program)
%              Ensure the number of elements is divisible by 4
%              This will ensure that the accelerometers are
%              located at a node.
%
%               Beam:  Length, Width, Depth, Modulus, Density
%
%       Outputs:
%               Mass and Stiffness Matrices
%
%
     if rem(n,4) ~= 0,
       error('# of elements must be divisible by four')
       break
     end
%
%%%%%%%%%%%%%%%%%%%%%%%%%%%%%%%%%%%%%%%%%%%%%%%%%%%%%%%%%%%%%%%%%%%%%%%%%%%
%
%                General Beam Specifications:
%
     tl = 60;                      % Beam length - total (inches)
     w  = 1.5656;                  % Beam width (inches)
     d  = 0.5339;                  % Beam depth (inches)
     E  = 28e+06;                  % Modulus of Elasticity (psi)
     D  = 0.284/386.04;            % Density (lbf/in^3)
%
%%%%%%%%%%%%%%%%%%%%%%%%%%%%%%%%%%%%%%%%%%%%%%%%%%%%%%%%%%%%%%%%%%%%%%%%%%%
%
%
```

```
      nc = (n*2)+2;                    % Number of coordinates
      el = tl/n;                       % Beam Element length (inches)
      A  = w*d;                        % Cross Sectional Area (in^2)
      I  = (w*d^3)/12;                 % Cross Sectional Inertia (in^3)
%
%
%               Develope Elemental Mass and Stiffness Matrices
%
      k   = [];                          % Zero matrix for multiple runs
      m   = [];
      kea = (I/el^3)   * [ 12   6*el;   6*el  4*el^2];
      keb = (I/el^3)   * [-12   6*el;  -6*el  2*el^2];
      kec = (I/el^3)   * [-12  -6*el;   6*el  2*el^2];
      ked = (I/el^3)   * [ 12  -6*el;  -6*el  4*el^2];
      mea = (A*el/420) * [156  22*el;  22*el  4*el^2];
      meb = (A*el/420) * [ 54 -13*el;  13*el -3*el^2];
      mec = (A*el/420) * [ 54  13*el; -13*el -3*el^2];
      med = (A*el/420) * [156 -22*el; -22*el  4*el^2];
%
%               Develope Global Mass and Stiffness Matrices
%
      k = zeros(nc);
      m = zeros(nc);
      for p = 1:n,
          a = 2*p;
          k(a-1:a,a-1:a)     = k(a-1:a,a-1:a)     + kea*E;
          k(a-1:a,a+1:a+2)   = k(a-1:a,a+1:a+2)   + keb*E;
          k(a+1:a+2,a-1:a)   = k(a+1:a+2,a-1:a)   + kec*E;
          k(a+1:a+2,a+1:a+2) = k(a+1:a+2,a+1:a+2) + ked*E;
          m(a-1:a,a-1:a)     = m(a-1:a,a-1:a)     + mea*D;
          m(a-1:a,a+1:a+2)   = m(a-1:a,a+1:a+2)   + meb*D;
          m(a+1:a+2,a-1:a)   = m(a+1:a+2,a-1:a)   + mec*D;
          m(a+1:a+2,a+1:a+2) = m(a+1:a+2,a+1:a+2) + med*D;
      end
%
%               Addition of lumped masses.
%
%               Lumped masses - accelerometers   (9.1 grms)
%
      accmass = 0.0091/(0.4536*386.04);          % 0.4536 kg/lbm
      i       = 1:1:4;
      node(i) = (i*(n/4)) + 1;
      crd(i)  = (2*node(i)) - 1;
      m(1,1)  = m(1,1) + accmass;
      m(crd(i),crd(i)) = m(crd(i),crd(i)) + accmass;
```

```
%
%                Lumped masses - End overhang
%
      ovrhng   = 2.5/8;                          % inches on each end
      ohngmass = D*w*d*ovrhng;
      m(1,1)   = m(1,1) + ohngmass;
      m(crd(4),crd(4)) = m(crd(4),crd(4)) + ohngmass;
%
                                        % inertia effect on rotation
%
      inermass = (ohngmass/12)*(d^2);
      m(2,2)   = m(2,2) + inermass;
      m(crd(4)+1,crd(4)+1) = m(crd(4)+1,crd(4)+1) + inermass;
```

```
%                       BMERR.M
%
%              Calculates the stiffness and mass matrices for
%              a finite element modeled beam that is
%              heterogeneous.
%
%              The only non-homogeneous variables compensated:
%                       Modulus :  Stiffness
%                       Density :  Mass
%
%       Inputs:
%              Number of beam elements (input prior to program)
%              Ensure number of elements is divisible by 4
%              This ensures that the accelerometers are located
%              at a node.
%              Beam: Length , Width, Depth
%              Modulus and Density including the beam elements
%              with the appropriate Modulus and density values.
%
%       Outputs:
%                Mass and Stiffness Matrices
%
%
     if rem(n,4) ~= 0,
       error('# of elements must be divisible by four')
       break
     end
%%%%%%%%%%%%%%%%%%%%%%%%%%%%%%%%%%%%%%%%%%%%%%%%%%%%%%%%%%%%%%%%%%%%%%%
%              General Beam Specifications:
%
     nc = (n*2)+2;                  % Number of coordinates
     tl = 60;                       % Beam length - total (inches)
     el = tl/n;                     % Beam Element length (inches)
     w  = 1.5656;                   % Beam width (inches)
     d  = 0.5339;                   % Beam depth (inches)
     A  = w*d;                      % Cross Sectional Area (in^2)
     I  = (w*d^3)/12;               % Cross Sectional Inertia (in^3)
%
%       Type of error mass(density) or stiffness(modulus)
%              Non - uniform Beam Modulus
%
     for x=1:n,                % Length of E vector = # of elements
        if x < 6,
          E(x) = 28e+06;
        elseif x < 13,
          E(x) = 28e+06;
        else
          E(x) = 28e+06;
        end
     end
```

```
%
%              Non - uniform Beam Density
%
     for x = 1:n,
         if x < 12,
          D(x) = 0.284/386.04;
         elseif x < 19,
          D(x) = 0.250/386.04;
         else
          D(x) = 0.284/386.04;
         end
     end
%%%%%%%%%%%%%%%%%%%%%%%%%%%%%%%%%%%%%%%%%%%%%%%%%%%%%%%%%%%%%%%%%%%%%%%%%%%%

%              Develope Elemental Mass and Stiffness Matrices

%
     k1   = [];                    % Zero matrix for multiple runs

     m1   = [];
     kea = (I/el^3)   * [ 12   6*el;   6*el  4*el^2];
     keb = (I/el^3)   * [-12   6*el;  -6*el  2*el^2];
     kec = (I/el^3)   * [-12  -6*el;   6*el  2*el^2];
     ked = (I/el^3)   * [ 12  -6*el;  -6*el  4*el^2];
     mea = (A*el/420) * [156  22*el;  22*el  4*el^2];
     meb = (A*el/420) * [ 54 -13*el;  13*el -3*el^2];
     mec = (A*el/420) * [ 54  13*el; -13*el -3*el^2];
     med = (A*el/420) * [156 -22*el; -22*el  4*el^2];
%
%              Develope Global Mass and Stiffness Matrices
%
     k1 = zeros(nc);
     m1 = zeros(nc);
     for p = 1:n,
         a = 2*p;
         k1(a-1:a,a-1:a)     = k1(a-1:a,a-1:a)     + kea*E(p);
         k1(a-1:a,a+1:a+2)   = k1(a-1:a,a+1:a+2)   + keb*E(p);
         k1(a+1:a+2,a-1:a)   = k1(a+1:a+2,a-1:a)   + kec*E(p);
         k1(a+1:a+2,a+1:a+2) = k1(a+1:a+2,a+1:a+2) + ked*E(p);
         m1(a-1:a,a-1:a)     = m1(a-1:a,a-1:a)     + mea*D(p);
         m1(a-1:a,a+1:a+2)   = m1(a-1:a,a+1:a+2)   + meb*D(p);
         m1(a+1:a+2,a-1:a)   = m1(a+1:a+2,a-1:a)   + mec*D(p);
         m1(a+1:a+2,a+1:a+2) = m1(a+1:a+2,a+1:a+2) + med*D(p);
     end
%
```

```
%               Addition of lumped masses.
%
%               Lumped masses - accelerometers   (9.1 grms)
%
      accmass = 0.0091/(0.4536*386.04);            % 0.4536 kg/lbm
      i       = 1:1:4;
      node(i) = (i*(n/4)) + 1;
      crd(i)  = (2*node(i)) - 1;
      m1(1,1)  = m1(1,1) + accmass;
      m1(crd(i),crd(i)) = m1(crd(i),crd(i)) + accmass;
%
%               Lumped masses - End overhang
%
      ovrhng   = 2.5/8;                 % inches on each end
      ohngmass = D(1)*w*d*ovrhng;
      m1(1,1)   = m1(1,1) + ohngmass;
      m1(crd(4),crd(4)) = m1(crd(4),crd(4)) + ohngmass;
%
                                        % inertia effect on rotation
      inermass = (ohngmass/12)*(d^2);
      m1(2,2)   = m1(2,2) + inermass;
      m1(crd(4)+1,crd(4)+1) = m1(crd(4)+1,crd(4)+1) + inermass;
```

```
%
%                          TSTMDL.M
%
%         Purpose of this program is to plot the FRF of a %
      baseline test model (BMMODEL.M) versus a model with a
%         known error installed (BMERR.M).
%
%         Inputs:
%              # of Beam Elements
%              Note: BMERR.M must be adjusted as appropriate for
%              changes in elements or installed errors prior to
%              running this program.
%              Start Frequency
%              Frequency Increment
%              End Frequency
%              Response and Excitation Coordinates.  These values
%              change with the change in the # of beam elements
%
%         Outputs:
%              FRF of test model versus the model with the
%              installed error.
%
%%%%%%%%%%%%%%%%%%%%%%%%%%%%%%%%%%%%%%%%%%%%%%%%%%%%%%%%%%%%%%%%%%%%%%%%%%%%%%%
%
      n   = 24;              % Number of beam elements
      f1  = 20;              % Start frequency (hz)
      inc = 0.125;           % Incremental frequency (hz)
      f2  = 420;             % End frequency (hz)
      row = 1;               % Model Response Coordinate
      col = 1;               % Model Excitation Coordinate
%%%%%%%%%%%%%%%%%%%%%%%%%%%%%%%%%%%%%%%%%%%%%%%%%%%%%%%%%%%%%%%%%%%%%%%%%%%%%%%
%
      bmmodel                      % Test Model
      bmerr                        % Model with installed error
%
%
%         Calculate the FRF
%
      i = 1;
      for w = f1:inc:f2,
           w1 = 2*pi*w;            % Converting hz to rad / sec
           z  = k - w1^2*m;
           z1 = k1- w1^2*m1;
           h  = inv (z)  / 386.04;  % Scale Corrections
           h1 = inv (z1) / 386.04;
%
           he(i)  = log10(h(row,col));  % Logarithmic Scale
           he1(i) = log10(h1(row,col));
%
           i = i+1;
      end
%
```

```
%
%          Plot the results
%
      w = f1:inc:f2;
      plot(w,he,'- -',w,he1,'g')
      xlabel('Frequency (hz)')
      ylabel('in/lbf (log of)')
```

```
%
%                          EXTSIM.M
%
%          Purpose of this program is to perform a matrix %
     extraction of the computer simulation models.
%
%          Matrix Reduction consists of extraction of the %
     translational excitation and response coordinates.
%          Localization Matrix will be a 5X5 matrix
%
%        Inputs:
%          Stiffness and Mass Matrices from BMMODEL.M and BMERR.M
%          Number of beam elements
%          Three Frequencies (low,medium,high)
%          Two error coordinates
%
%        Outputs:
%          Localization Matrix at different frequencies
%          Localization Matrix (component) vs frequency.
%
%
%%%%%%%%%%%%%%%%%%%%%%%%%%%%%%%%%%%%%%%%%%%%%%%%%%%%%%%%%%%%%%%%%%%%%%%%%%%%
%
     n     = 24;                          % Number of Elements
     f1    = 20;                          % Start Frequency (hz)
     f2    = 420;                         % End Frequency (hz)
     inc   = 0.125;                       % Incremental Frequency (hz)
     wlow  = 35;                          % Low Frequency (hz)
     wmed  = 150;                         % Medium Frequency (hz)
     whigh = 350;                         % High Frequency (hz)
     c1    = 3;                           % Left error coordinate
     c2    = 4;                           % Right error coordinate
%
%
%%%%%%%%%%%%%%%%%%%%%%%%%%%%%%%%%%%%%%%%%%%%%%%%%%%%%%%%%%%%%%%%%%%%%%%%%%%%
%
     bmerr                               % Flawed model (k,m matrices)
     bmmodel                             % Ideal model (k,m matrices)
     aset = [1:n/2:(2*n)+1];             % Retained Coordinates
%
%
%                Localization Matrix at a given frequency
%
%
     wfix  = [wlow,wmed,whigh];
     wfix1 = wfix*pi*2;                   % Convert to rads per second
%
```

```
      for i = 1:3,
           z  = (k-wfix(i)^2*m);    % Develope impedance matrices
           z1 = (k1-wfix(i)^2*m1);
           h  = inv(z);             % Frequency Response matrices
           h1 = inv(z1);
%
           h  = h(aset,aset)/386.04;  % Matrix Extraction
           h1 = h1(aset,aset)/386.04;
           z1  = inv(h1);
%
           loc = z1*(h1-h)*z1;      % Localization Matrix
%
           if i==1,
                llow = loc;
           elseif i==2,
                lmed = loc;
           else
                lhigh = loc;
           end
      end
%
%              Localization Matrix versus Frequency
%
%
      i = 1;
      for w = f1:inc:f2;
           w1 = w*pi*2;
           z  = k-w1^2*m;
           z1 = k1-w1^2*m1;
           h  = inv(z)/386.04;
           h1 = inv(z1)/386.04;
           h  = h(aset,aset);
           h1 = h1(aset,aset);
           z1  = inv(h1);
           loc = z1*(h1-h)*z1;
           lab(i) = loc(c1,c1);     %  Error component of L
           lba(i) = loc(c2,c2);     %  Error component of L
%
      i = i+1;
      end
```

```
%
%                              IRSSIM.M
%
%          Purpose of this program is to perform a matrix IRS
%          Reduction of the computer simulation models.
%          Localization Matrix will be a 5X5 matrix
%
%        Inputs:
%          Stiffness and Mass Matrices from BMMODEL.M and BMERR.M
%          Number of beam elements
%          Three Frequencies (low,medium,high)
%          Two error coordinates
%
%        Outputs:
%          Localization Matrix at different frequencies
%          Localization Matrix (component) vs frequency.
%
%%%%%%%%%%%%%%%%%%%%%%%%%%%%%%%%%%%%%%%%%%%%%%%%%%%%%%%%%%%%%%%%%%%%%%%%%%%%
%
      n     = 24;                          % Number of Elements
      f1    = 20;                          % Start Frequency (hz)
      f2    = 420;                         % End Frequency (hz)
      inc   = 0.125;                       % Incremental Frequency (hz)
      wlow  = 35;                          % Low Frequency (hz)
      wmed  = 150;                         % Medium Frequency (hz)
      whigh = 350;                         % High Frequency (hz)
      c1    = 2;                           % Left  error coordinate
      c2    = 3;                           % Right error coordinate
%
%
%%%%%%%%%%%%%%%%%%%%%%%%%%%%%%%%%%%%%%%%%%%%%%%%%%%%%%%%%%%%%%%%%%%%%%%%%%%%
%
      bmerr                                % Flawed model (k,m matrices)
      bmmodel                              % Ideal model (k,m matrices)
      aset = [1:n/2:(2*n)+1];              % Retained Coordinates
      a1   = aset(1,2);                    % Omitted Coordinates
      a2   = aset(1,3);
      a3   = aset(1,4);
      a4   = aset(1,5);
      oset = [2:a1-1,a1+1:a2-1,a2+1:a3-1,a3+1:a4-1,n*2+2];
      b    = length(aset);
%
```

```
%
%              IRS Reduction of the Error Model
%              Partition stiffness and Mass Matrices
%
      k1aa = k1(aset,aset);
      k1oa = k1(oset,aset);
      k1ao = k1(aset,oset);
      k1oo = k1(oset,oset);
      m1aa = m1(aset,aset);
      m1oa = m1(oset,aset);
      m1ao = m1(aset,oset);
      m1oo = m1(oset,oset);
%
%              Transformation Matrix
%
      k1oo1 = inv (k1oo);
      t1 = k1oo1*m1oa - k1oo1*m1oo*k1oo1*k1oa;
      T1 = [eye(b);t1];
%
%              Reduced Stiffness and Mass Matrices
%
      k1bar = T1'*k1*T1;
      m1bar = T1'*m1*T1;
%
%
%              Localization Matrix at a given frequency
%
%
      wfix  = [wlow,wmed,whigh];
      wfix1 = wfix*pi*2;                % Convert to rads per second
%
      for i = 1:3,
           z  = k  - wfix1(i)^2*m;
           z1 = k1bar - wfix1(i)^2*m1bar;
           h  = inv(z);
           h  = h(aset,aset)/386.04;
           h1 = inv(z1)/386.04;
           z1 = inv(h1);
           loc = z1*(h1-h)*z1;
           if i==1,
                llow = loc;
           elseif i==2,
                lmed = loc;
           else
                lhigh = loc;
           end
      end
%
```

```
%                Localization Matrix versus Frequency
%
%
      i = 1;
      for w = f1:inc:f2;
           w1 = w*pi*2;
           z  = k  - w1^2*m;
           z1 = k1bar - w1^2*m1bar;
           h  = inv(z);
           h  = h(aset,aset)/386.04;
           h1 = inv(z1)/386.04;
           z1 = inv(h1);
           loc = z1*(h1-h)*z1;
           lab(i) = loc(c1,c1);              % Error Component of L
           lba(i) = loc(c2,c2);              % Error Component of L
%
      i = i+1;
      end
```

```
%
%                          EXTDATA.M
%
%     Purpose:  To perform a matrix extraction of a beam finite
%               element model and determine the localization
%               matrix by comparing with experimental data.
%
%     Inputs:
%               Input finite element model (BMERR.M)
%               Number of beam elements
%               Test data (c:\matlab\beamdata directory)
%               Three frequencies (low,med,high)
%               Start / End frequencies
%
%     Outputs:
%               Localization Matrix at different frequencies
%               Localization Matrix (component) vs frequency
%
%
%%%%%%%%%%%%%%%%%%%%%%%%%%%%%%%%%%%%%%%%%%%%%%%%%%%%%%%%%%%%%%%%%%%%%%%%%%%%
%
      n     = 24;                       % Number of beam elements
      f1    = 20;                       % Start frequency (hz)
      f2    = 420;                      % End frequency (hz)
      inc   = 0.125;                    % Frequency increment (hz)
      wlow  = 35;                       % Low frequency (hz)
      wmed  = 150;                      % Medium frequency (hz)
      whigh = 350;                      % High frequency (hz)
%
%%%%%%%%%%%%%%%%%%%%%%%%%%%%%%%%%%%%%%%%%%%%%%%%%%%%%%%%%%%%%%%%%%%%%%%%%%%%
%
      bmerr                             % Flawed Model (k,m matrices)
      aset = [1:n/2:(2*n)+1];           % Retained coordinates
%
%
%          Load FRF experimental data and arrange (3201x50 matrix)
%
      load c:\matlab\beamdata\hea.mat;
      load c:\matlab\beamdata\heb.mat;
      load c:\matlab\beamdata\hec.mat;
      load c:\matlab\beamdata\hed.mat;
%
         hebar = [hea(1:800,:); heb(1:800,:)];
         hebar = [hebar; hec(1:800,:); hed(1:801,:)];
%
      clear hea heb hec hed             % Reduce Memory usage
```

```
%
%          Localization Matrix at a given frequency
%
%
      wfix  = [wlow,wmed,whigh];
      wfix1 = wfix*pi*2;                  % Convert to radians/sec
%
      n     = (8 * (wfix - 20)) +1;       % Counter to access hedata
%
      for i = 1:3,                        % Analytical FRF Matrix
          za = (k1-wfix1(i)^2*m1);
          ha = inv(za);
          ha = ha(aset,aset)/386.04;      % Extraction Reduction
          za = inv(ha);
          hx = datfreq(n(i),hebar);       % Experimental FRF Matrix
          hx = hx(1:2:9,:)/(wfix1(i)^2);
%
          loc = za*(ha-hx)*za;        % Localization Matrix
%
          if i == 1,
           llow = loc;
          elseif i == 2,
           lmed = loc;
          else
              lhigh = loc;
          end
      end
%
%
%          Localization Matrix Versus Frequency
%
      cntr =1;
      for w   = f1:inc:f2,
          w1  = w*pi*2;
          za  = k1-w1^2*m1;
          ha  = inv(za);
          ha  = ha(aset,aset)/386.04;
          za  = inv(ha);
%
          n   = (8 * (w - 20)) +1;
          hx  = datfreq(n,hebar);
          hx  = hx(1:2:9,:)/(w1^2);
          loc = za*(ha-hx)*za;
%
```

```
        l11(cntr) = loc(1,1);
        l22(cntr) = loc(2,2);
        l33(cntr) = loc(3,3);
%
%         Impedance Error Calculation
%
        haext = inv(ha);
        hxext = inv(haext*(ha-hx)*haext);
        dzext = inv(hxext - ha);
        dz1(cntr) = dzext(1,1);
        dz2(cntr) = dzext(2,2);
        dz3(cntr) = dzext(3,3);
    %
        cntr = cntr+1;
    end
    w = f1:inc:f2;
```

```
%
%                          IRSDATA.M
%
%     Purpose:
%          To perform a IRS reduction of a beam finite
%          element model and determine the localization
%          matrix by comparing with experimental data.
%
%     Inputs:
%          Input finite element model (BMERR.M)
%          Number of beam elements
%          Test data (c:\matlab\beamdata directory)
%          Three frequencies (low,med,high)
%          Start / End frequencies
%
%     Outputs:
%          Localization Matrix at different frequencies
%          Localization Matrix (component) vs frequency
%
%
%%%%%%%%%%%%%%%%%%%%%%%%%%%%%%%%%%%%%%%%%%%%%%%%%%%%%%%%%%%%%%%%%%%%%%%%%%%%
%
      n     = 24;                 % Number of beam elements
      f1    = 20;                 % Start frequency (hz)
      f2    = 420;                % End frequency (hz)
      inc   = 0.125;              % Frequency increment (hz)
      wlow  = 35;                 % Low frequency (hz)
      wmed  = 150;                % Medium frequency (hz)
      whigh = 350;                % High frequency (hz)
%
%%%%%%%%%%%%%%%%%%%%%%%%%%%%%%%%%%%%%%%%%%%%%%%%%%%%%%%%%%%%%%%%%%%%%%%%%%%%
%
      bmerr                       % Flawed Model (k,m matrices)
      aset = [1:n/2:(2*n)+1];     % Retained coordinates
%
      c1  = aset(1,2);
      c2  = aset(1,3);            % omitted coordinates
      c3  = aset(1,4);
      c4  = aset(1,5);
      oset=[2:c1-1,c1+1:c2-1,c2+1:c3-1,c3+1:c4-1,n*2+2];
      b   = length(aset);
%
%
%          Partition model k & m matrices
%
      kaa = k1(aset,aset);        maa = m1(aset,aset);
      koa = k1(oset,aset);        moa = m1(oset,aset);
      kao = k1(aset,oset);        mao = m1(aset,oset);
      koo = k1(oset,oset);        moo = m1(oset,oset);
```

```
%
%
%          Transformation Matrix
%
      koo1 = inv(koo);
      t = koo1*moa-koo1*moo*koo1*koa;
      T = [eye(b);t];
%
      kbar = T'* k1 * T;          % Reduced k matrix
      mbar = T'* m1 * T;          % Reduced m matrix
%

%
%     Load FRF experimental data and arrange (3201x50 matrix)
%
      load c:\matlab\beamdata\hea.mat;
      load c:\matlab\beamdata\heb.mat;
      load c:\matlab\beamdata\hec.mat;
      load c:\matlab\beamdata\hed.mat;
%
      hebar = [hea(1:800,:); heb(1:800,:)];
      hebar = [hebar; hec(1:800,:); hed(1:801,:)];
%
      clear hea heb hec hed          % Reduce Memory usage
%
%          Localization Matrix at a given frequency
%
%
      wfix  = [wlow,wmed,whigh];
      wfix1 = wfix*pi*2;             % Convert to radians/sec
%
%               Counter to access he data
%
      n     = (8 * (wfix - 20)) + 1;
%
      for i = 1:3,                   % Analytical FRF Matrix
          za = (kbar-wfix1(i)^2*mbar);
          ha = inv(za)/386.04;
          hx = datfreq(n(i),hebar); % Experimental FRF Matrix
%
          hx = hx(1:2:9,:)/(wfix1(i)^2);
%
          loc = za*(ha-hx)*za;       % Localization Matrix
%
          if i == 1,
           llow = loc;
          elseif i == 2,
           lmed = loc;
          else
              lhigh = loc;
          end
      end
```

```
%
%
%          Localization Matrix Versus Frequency
%
      cntr =1;
      for w   = f1:inc:f2,
          w1  = w*pi*2;
          za  = kbar-w1^2*mbar;
          ha  = inv(za)/386.04;
%
          n   = (8 * (w - 20)) + 1;
          hx  = datfreq(n,hebar);
          hx  = hx(1:2:9,:)/(w1^2);
          loc = za*(ha-hx)*za;
%
          l11(cntr) = loc(1,1);
          l22(cntr) = loc(2,2);
          l33(cntr) = loc(3,3);
%
%
%          Impedance Error Calculation
%
          haext = inv(ha);
          hxext = inv(haext*(ha-hx)*haext);
          dzext = inv(hxext - ha);
          dz1(cntr) = dzext(1,1);
          dz2(cntr) = dzext(2,2);
          dz3(cntr) = dzext(3,3);
%
          cntr = cntr+1;
      end
      w = f1:inc:f2;
```

```
%                          DATFREQ.M
%
function hx = datfreq (n,hebar)
%
%     Input:
%           Frequency (20-420 hz)
%           FRF experimental data base (3201x50 matrix)
%
%     Output:
%           Experimental FRF matrix for the desired frequency
%

      hx = [hebar(n,1:5);hebar(n,6:10);hebar(n,11:15)];
      hx = [hx;hebar(n,16:20);hebar(n,21:25)];
      hx = [hx;hebar(n,26:30);hebar(n,31:35)];
      hx = [hx;hebar(n,36:40);hebar(n,41:45)];
      hx = [hx;hebar(n,46:50)];
```

```
%                          HEBUILD.M
%
%
%          Purpose:
%               Build a matrix from experimental data
%
%          Input:
%               Start frequency (20+n*100) hz n=[1,2,3]
%                 Note: Letter code in this program must be
%                 adjusted in accordance with the file coding
%               End frequency (120+n*100) hz n=[1,2,3]
%               Data Files: - files must be in *.mat format
%                 file location c:\matlab\beamdata directory
%
%          Output:
%               *.mat file:  - size 801x50 matrix
%               file name = he#.mat  #:letter code
%
%
      clear
      i = 20;                       % Start frequency
      j = 120;                      % End frequency
%
      a = 1;                        % Align frequency with vector
      b = 801;
%
%               Establish root code based on frequency range
%
      if i == 20,
           root = 'a';              % a:  20 - 120 hz
      elseif i == 120,
           root = 'b';              % b: 120 - 220 hz
      elseif i == 220,
           root = 'c';              % c: 120 - 220 hz
      else,
           root = 'd';              % d: 320 - 420 hz
      end
%
      for d2 = 1:10,
        for d1 = 1:2:9,
          flname = ['h',num2str(d2),'_',num2str(d1),root];
          eval(['load c:\matlab\beamdata\',flname,'.mat']);
          eval(['he',root,'=[he',root,',o2i1];']);
        end
      end
%
      eval(['save c:\matlab\beamdata\he',root,'.mat']);
```

```
%                          FRFMTCH.M
%
%          Purpose:
%               Compare modeled FRF response with tabulated
%               FRF response from the beam experiment.
%
%          Modeled FRF:
%               Calculated using k,m from BMMODEL.M
%               Must insert a value for n (# elements)
%                  If n is other than 4, then the location of
%                  the h matrix must be considered carefully
%                  to ensure proper comparison.
%
%          Tabulated FRF:
%               Data is received from the .mat files
%               File location c:\matlab\beamdata
%               Tabulated frequency range is 20-420 hz
%               Beam has 5 accelerometers and 4 beam elements
%
%          Program will progress thru each file <cntrl c >
%          terminates the program
%%%%%%%%%%%%%%%%%%%%%%%%%%%%%%%%%%%%%%%%%%%%%%%%%%%%%%%%%%%%%%%%%%%%%%%%
%
      n   = 24;              % # of beam elements
      row = 1;               % Model response coordinate
      col = 1;               % Model Excitation coordinate
      flnm = 'h1_1';         % measured FRF file of interest
      f1  = 20;              % Start frequency (hz) (min=20hz)
      f2  = 420;             % End frequency (hz) (max=420hz)
      inc = 0.125;           % mat file 801 elements-100 hz span
%%%%%%%%%%%%%%%%%%%%%%%%%%%%%%%%%%%%%%%%%%%%%%%%%%%%%%%%%%%%%%%%%%%%%%%%
%
%          Tabulated FRF
%
%               Loading initial *.mat file based on f1
%
      y=[]; ya=[]; yb=[]; yd=[];
      if f1 < 120,
        a = 8*(fix(f1)-20)+((f1-fix(f1))/0.125)+1;
        eval(['load c:\matlab\beamdata\',flnm,'a.mat']);
        ya = o2i1(1:801);
        eval(['load c:\matlab\beamdata\',flnm,'b.mat']);
        yb = o2i1(1:801);
        eval(['load c:\matlab\beamdata\',flnm,'c.mat']);
        yc = o2i1(1:801);
        eval(['load c:\matlab\beamdata\',flnm,'d.mat']);
        yd = o2i1(1:801);
```

```
elseif f1 < 220,
  a = 8*(fix(f1)-120)+((f1-fix(f1))/0.125)+1;
  eval(['load c:\matlab\beamdata\',flnm,'b.mat']);
  yb = o2i1(1:801);
  eval(['load c:\matlab\beamdata\',flnm,'c.mat']);
  yc = o2i1(1:801);
  eval(['load c:\matlab\beamdata\',flnm,'d.mat']);
  yd = o2i1(1:801);
elseif f1 < 320,
  a = 8*(fix(f1)-220)+((f1-fix(f1))/0.125)+1;
  eval(['load c:\matlab\beamdata\',flnm,'c.mat']);
  yc = o2i1(1:801);
  eval(['load c:\matlab\beamdata\',flnm,'d.mat']);
  yd = o2i1(1:801);
else
  a = 8*(fix(f1)-320)+((f1-fix(f1))/0.125)+1;
  eval(['load c:\matlab\beamdata\',flnm,'d.mat']);
  yd = o2i1(1:801);
end
%                 Data length based on frequencies
%
if f2 <= 120,
  b = 8*(fix(f2)-20)+((f2-fix(f2))/0.125)+1;
  y = ya(a:b);
elseif f2 <= 220,
  b = 8*(fix(f2)-120)+((f2-fix(f2))/0.125)+1;
  if f1 < 120,
        y = [ya(a:801);yb(2:b)];
  else
     y = yb(a:b);
  end
elseif f2 <= 320,
  b = 8*(fix(f2)-220)+((f2-fix(f2))/0.125)+1;
  if f1 < 120,
        y = [ya(a:801);yb(2:801);yc(2:b)];
  elseif f1 < 220,
        y = [yb(a:801);yc(2:b)];
   else
     y = yc(a:b);
  end
else
  b = 8*(fix(f2)-320)+((f2-fix(f2))/0.125)+1;
  if f1 < 120,
        y = [ya(a:801);yb(2:801);yc(2:801);yd(2:b)];
  elseif f1 < 220,
        y = [yb(a:801);yc(2:801);xd(2:b)];
  elseif f1 < 320
     y = [yc(a:801);yd(2:b)];
  else
        y = yd(a:b);
  end
end
```

```
%
%          Calculate the model FRF
%
          bmmodel                % calculate k and m matrices
      i = 1;
      if rem(row,2) ~= 0,
%
%               Translation accelerometer adjust
%
          for w = f1:inc:f2,
           w1      = 2*pi*w;       % convert hz to rad/sec
            z      = k - w1^2*m;
            h      = inv(z);
            he(i) = h(row,col)/386.04;  % unit correction
            y (i) = y(i)/(w1^2);        % unit correction
            i      = i+1;
        end
      else                         % Angular accelerometer adjust
        for w = f1:inc:f2,
            w1      = 2*pi*w;
             z      = k-w1^2*m;
             h      = inv(z);
                he(i) = h(row,col);  % 10* : due to TAP gain
          y(i)  = y(i)/(10*(w1^2)),
          i      = i+1;
        end
      end

%          Plot results
%
%          Plot coordinate scale
      w=f1:inc:f2;
      hedb = log(he)/log(10);
      ydb  = log(y)/log(10);
      plot(w,hedb,'- -',w,ydb,'g')
      xlabel('Frequency (hz)')
      ylabel('in/lbf (log of)')
```

```
%
%                              DAMP.M
%
%     Damping data of beam experiment.
%     Results were obtained by the half power point method
%
%     Format:      zeta1 (first mode)
%              zeta2 thru zeta5 (2nd thru 5th modes)
%
%     zeta is a 10x5 matrix
%           zeta =  z11  z13  z15  z17  z19
%                   z21  z23  z25  z27  z29
%             :::: :::: :::: :::: ::::
%            z101 z103 z105 z107 z109
%
%
      z1 = [.0146 .0127 .0042 .0051 .0035];
      z2 = [.0185 .0102 .0042 .0127 .0043];
      z3 = [.0167 .0063 .0034 .0169 .0048];
      z4 = [.0184 .0081 .0038 .0153 .0043];
      z5 = [.0184 .0106 .0038 .0047 .0045];
      z6 = [.0167 .0144 .0042 .0059 .0045];
      z7 = [.0166 .0147 .0042 .0102 .0060];
      z8 = [.0146 .0129 .0055 .0127 .0048];
      z9 = [.0146 .0120 .0055 .0047 .0046];
      z0 = [.0167 .0064 .0042 .0047 .0052];
      zeta1 = [z1;z2;z3;z4;z5;z6;z7;z8;z9;z0];
%
      z1 = [.0016 .0023 .0000 .0018 .0102];
      z2 = [.0019 .0023 .0000 .0018 .0102];
      z3 = [.0016 .0031 .0000 .0018 .0104];
      z4 = [.0016 .0023 .0088 .0016 .0066];
      z5 = [.0033 .0000 .0000 .0090 .0063];
      z6 = [.0016 .0023 .0018 .0019 .0111];
      z7 = [.0016 .0023 .0148 .0016 .0105];
      z8 = [.0016 .0018 .0000 .0017 .0113];
      z9 = [.0016 .0023 .0047 .0014 .0107];
      z0 = [.0016 .0020 .0127 .0018 .0092];
      zeta2 = [z1;z2;z3;z4;z5;z6;z7;z8;z9;z0];
%
      z1 = [.0032 .0054 .0041 .0039 .0029];
      z2 = [.0038 .0054 .0046 .0048 .0030];
      z3 = [.0060 .0034 .0044 .0033 .0015];
      z4 = [.0035 .0050 .0050 .0047 .0015];
      z5 = [.0075 .0048 .0048 .0032 .0021];
      z6 = [.0027 .0034 .0039 .0068 .0020];
      z7 = [.0076 .0050 .0046 .0023 .0022];
      z8 = [.0068 .0050 .0031 .0048 .0028];
      z9 = [.0072 .0051 .0046 .0022 .0033];
      z0 = [.0071 .0050 .0031 .0023 .0028];
      zeta3 = [z1;z2;z3;z4;z5;z6;z7;z8;z9;z0];
%
```

```
z1 = [.0017 .0017 .0053 .0018 .0023];
z2 = [.0019 .0019 .0044 .0022 .0023];
z3 = [.0021 .0014 .0051 .0011 .0018];
z4 = [.0019 .0021 .0061 .0019 .0017];
z5 = [.0000 .0000 .0000 .0000 .0000];
z6 = [.0017 .0021 .0025 .0018 .0016];
z7 = [.0022 .0017 .0000 .0015 .0019];
z8 = [.0023 .0022 .0000 .0019 .0023];
z9 = [.0023 .0018 .0000 .0015 .0021];
z0 = [.0023 .0018 .0000 .0015 .0021];
zeta4 = [z1;z2;z3;z4;z5;z6;z7;z8;z9;z0];
%
z1 = [.0013 .0009 .0010 .0014 .0012];
z2 = [.0013 .0010 .0012 .0007 .0013];
z3 = [.0016 .0010 .0008 .0012 .0017];
z4 = [.0014 .0011 .0009 .0009 .0017];
z5 = [.0016 .0005 .0007 .0011 .0014];
z6 = [.0015 .0009 .0008 .0010 .0016];
z7 = [.0014 .0006 .0008 .0011 .0013];
z8 = [.0014 .0009 .0015 .0009 .0011];
z9 = [.0014 .0005 .0009 .0011 .0010];
z0 = [.0014 .0007 .0012 .0013 .0011];
zeta5 = [z1;z2;z3;z4;z5;z6;z7;z8;z9;z0];
```

```
%
%                          CMATRIX.M
%
%          Purpose:
%               Produce a damping matrix from damping data
%
%          Inputs:
%               Zeta: DAMP.M
%               K,M Matrices: BMERR.M and BMMODEL.M
%
%          Outputs:
%               Damping Matrix
%
%
%          Input zeta and determine an average value
%
     damp
%
% Input data from half power calculations
%
     z(1) = sum(sum(zeta1)')/50;    % 1st Mode average value
     z(2) = sum(sum(zeta2)')/50;    % 2nd Mode average value
     z(3) = sum(sum(zeta3)')/50;    % 3rd Mode average value
     z(4) = sum(sum(zeta4)')/50;    % 4th Mode average value
     z(5) = sum(sum(zeta5)')/50;    % 5th Mode average value
%
%          Determine eigenvalues and eigenvectors
%
%      Stiffness and Mass matrices are assumed to have been
%       previously initialized from a previous statement
%
     [phi,lam]  = eig(k1,m1);       % Sort in ascending order
     [lambda,cntr] = sort(diag(lam));
     phi        = phi(:,cntr);
%
%          Mass normalized the eigenvector
%
     phi        = phi/sqrt(phi'*m1*phi);
%
     lambda     = lambda(3:7,:);    % Keep first five modes
     phi     = phi(:,3:7);
%
     lamzeta    = zeros(5);    % develope 2*zeta*omega matrix
%
     for i = 1:5,
         lamzeta(i,i) = 2*z(i)*sqrt(lambda(i));
     end
%
%          Calculate final damping matrix
%
     c = m1 * phi * lamzeta * phi' * m1;
```

APPENDIX D

MISSING OSET ANALYSIS

As discovered in Section IV, expected peak values of the localization matrix and the impedance error associated with the OSET frequencies, were missing for the inner elements of the localization and impedance error matrices.

Evaluation of the various models to determine which OSET frequencies are missing is a good starting point for this analysis. Tables D-1 thru D-4 will summarize the peak values of the "1,1", "2,2", and "3,3" elements of the localization and impedance error matrices using various combinations of analytical and test models. The summary will also include the effects of extraction and IRS reduction.

The tables will list the actual peak frequencies. A dashed line indicates the specific frequency peak is not expected (and did not occur).

TABLE D-1: IDEAL VS. EXPERIMENTAL

Analytical System: Ideal Beam Model
Test System: Experimental Data

Extraction Reduction			IRS Reduction		
L_{11}	L_{22}	L_{33}	L_{11}	L_{22}	L_{33}
29.90	29.90	29.90	29.90	29.90	29.90
81.20	81.20	81.20	81.20	81.20	81.20
155.90	155.90	155.90	155.90	155.90	155.90
209.92	Missing	Missing	------	------	------
244.90	244.90	244.90	------	------	------
258.30	258.30	258.30	258.30	258.30	258.30
327.96	327.96	Missing	------	------	------
387.85	387.85	387.85	387.85	387.85	387.85

Impedance Error Matrix (hz)

Extraction Reduction			IRS Reduction		
dz_{11}	dz_{22}	dz_{33}	dz_{11}	dz_{22}	dz_{33}
29.90	29.90	29.90	------	------	------
81.20	81.20	81.20	------	------	------
155.90	155.90	155.90	------	------	------
209.92	Missing	Missing	------	------	------
210.25	Missing	Missing	210.25	Missing	Missing
244.90	244.90	244.90	------	------	------
245.05	245.05	245.05	245.05	245.05	245.05
258.30	258.30	258.30	------	------	------
327.96	327.96	Missing	------	------	------
329.50	329.50	Missing	329.50	329.50	Missing
387.80	387.80	387.80	------	------	------

TABLE D-2: CASE I VS. IDEAL

Analytical System: Flawed Model (Case I)
Test System: Ideal Beam Model

Extraction Reduction			IRS Reduction		
L_{11}	L_{22}	L_{33}	L_{11}	L_{22}	L_{33}
29.07	29.07	29.07	29.07	29.07	29.07
79.96	79.96	79.96	79.96	79.96	79.96
157.14	157.14	157.14	157.14	157.14	157.14
172.60	172.60	172.60	------	------	------
225.34	225.34	225.34	------	------	------
259.39	259.39	259.39	259.39	259.39	259.39
265.46	265.46	265.46	------	------	------
354.07	354.07	354.07	------	------	------
387.85	387.85	387.85	387.85	387.85	387.85

Impedance Error Matrix (hz)

Extraction Reduction			IRS Reduction		
dz_{11}	dz_{22}	dz_{33}	dz_{11}	dz_{22}	dz_{33}
172.60	172.60	172.60	------	------	------
209.92	Missing	Missing	209.92	Missing	Missing
225.34	225.34	225.34	------	------	------
244.90	244.90	244.90	244.90	244.90	244.90
265.46	265.46	265.46	------	------	------
327.96	327.96	Missing	327.96	327.96	Missing
354.07	354.07	354.07	------	------	------

TABLE D-3: CASE I VS. EXPERIMENTAL

Analytical Model: Flawed Model (Case I)
Test System: Experimental Data

Extraction Reduction			IRS Reduction		
L_{11}	L_{22}	L_{33}	L_{11}	L_{22}	L_{33}
29.90	29.90	29.90	29.90	29.90	29.90
81.20	81.20	81.20	81.20	81.20	81.20
155.90	155.90	155.90	155.90	155.90	155.90
172.60	172.60	172.60	------	------	------
225.34	225.34	225.34	------	------	------
258.30	258.30	258.30	258.30	258.30	258.30
265.46	265.46	265.46	------	------	------
354.07	354.07	354.07	------	------	------
387.80	387.80	387.80	387.80	387.80	387.80

Impedance Error (hz)

Extraction Reduction			IRS Reduction		
dz_{11}	dz_{22}	dz_{33}	dz_{11}	dz_{22}	dz_{33}
29.90	29.90	29.90	------	------	------
81.20	81.20	81.20	------	------	------
155.90	155.90	155.90	------	------	------
172.60	172.60	172.60	------	------	------
209.92	Missing	Missing	209.92	Missing	Missing
225.34	225.34	225.34	------	------	------
244.90	244.90	244.90	244.90	244.90	244.90
265.46	265.46	265.46	------	------	------
327.96	327.96	Missing	327.96	327.96	Missing
354.07	354.07	354.07	------	------	------
387.85	387.85	387.85	------	------	------

TABLE D-4: CASE I VS. CASE II

Analytical Model: Flawed Model (Case I)
Test System: Flawed Model (Case II)

Extraction Reduction			IRS Reduction		
L_{11}	L_{22}	L_{33}	L_{11}	L_{22}	L_{33}
29.56	29.56	29.56	29.56	29.56	29.56
81.32	81.32	81.32	81.32	81.32	81.32
159.94	159.94	159.94	159.94	159.94	159.94
172.60	172.60	172.60	------	------	------
225.34	225.34	225.34	------	------	------
263.26	263.26	263.26	263.26	263.26	263.26
265.46	265.46	265.46	------	------	------
354.07	354.07	354.07	------	------	------
396.23	396.23	396.23	396.23	396.23	396.23

Impedance Error (hz)

Extraction Reduction			IRS Reduction		
dz_{11}	dz_{22}	dz_{33}	dz_{11}	dz_{22}	dz_{33}
172.60	172.60	172.60	------	------	------
213.03	213.03	213.03	213.03	213.03	213.03
225.34	225.34	225.34	------	------	------
246.12	246.12	246.12	246.12	246.12	246.12
265.46	265.46	265.46	------	------	------
333.20	333.20	333.20	333.20	333.20	333.20
354.07	354.07	354.07	------	------	------

Table D-1 reveals missing OSET frequency peaks associated with the ideal beam model and the experimental test data. Table D-2 shows missing OSET frequency peaks associated with the ideal beam model. Case I flawed beam finite element model displayed all the expected OSET frequency peaks. The results of Table D-3 are the same as Table D-2 with the exception that the experimental test data is used vice the ideal beam model. Table D-4 involves a structural identification between the case I and case II flawed beam finite element models. All expected eigenvalues appeared in the localization and impedance error spectra plots.

Further information which is not detailed in this appendix, is that the "4,4" element plots displayed the same missing OSET frequency peaks as the "2,2" element, and the "5,5" element contained all the expected OSET frequency peaks. The "5,5" element plot corresponded to the "1,1" element plot.

The overall pattern indicates that some mechanism in the ideal beam finite element model and the experimental data is causing the missing OSET frequency peaks.

The next step is to try to identify the mechanism using the reduction process. Equation (2.34b) indicates that the FRF is dependent on the inverse of the OSET partitioned impedance matrix. Figures D-1 and D-2 plot the inverse of the OSET partitioned impedance matrix over a frequency range from 20 to 420 hz for the ideal beam and Case II flawed beam finite element models.

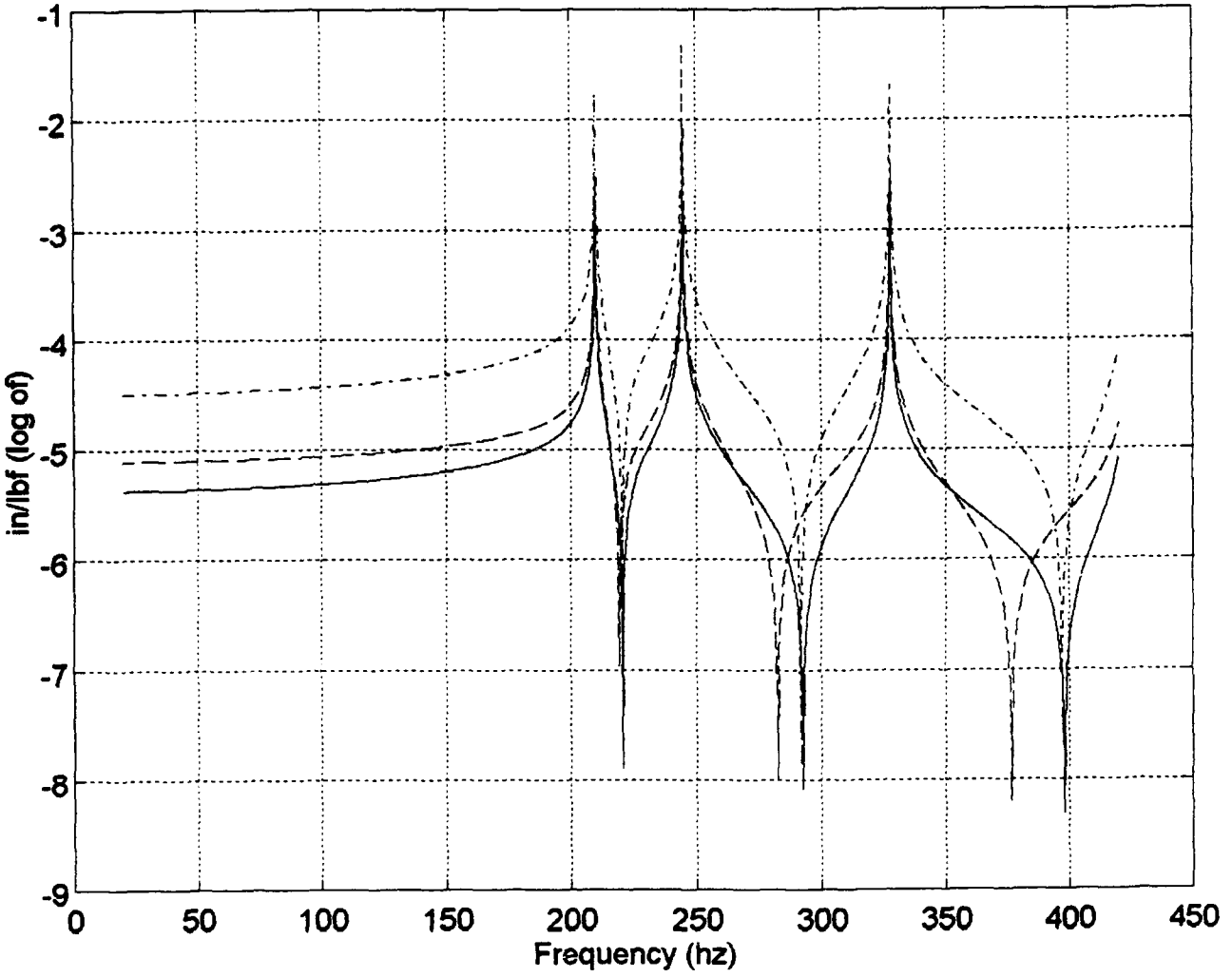

FIGURE D-1: Z_{oo}^{-1}
(--) "1,1" (-.-) "2,2" (—) "3,3"
Ideal Beam Model

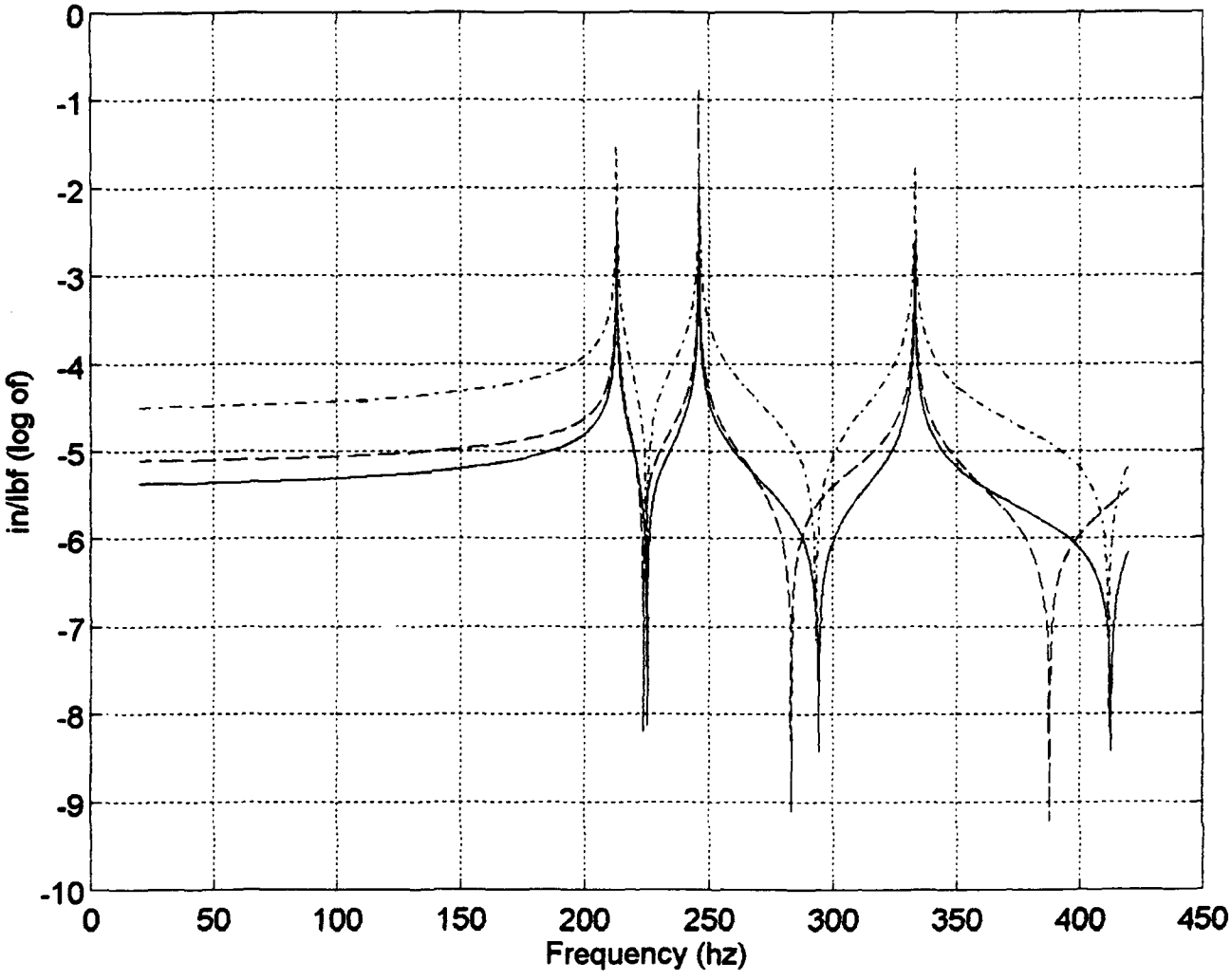

FIGURE D-2: Z_{∞}^{-1}

(--) "1,1" (-.-) "2,2" (—) "3,3"

Case II

All the expected OSET frequency peak values appear in both figures. The next calculation is a plot of the product of Zoa, Zao, and the inverse of the OSET impedance matrix. Figures D-3 and D-4 display this product over the same frequency range of 20 to 420 hz for the ideal beam and case II flawed beam finite element models.

Figure D-3 displays missing OSET frequency peaks that correspond to the missing peak values described in Tables D-1 and D-2. Figure D-4 contains all expected OSET frequency peaks. The "1,1" element does have a frequency peak at 213.03 hz, it is not visible in this particular plot.

The missing OSET frequency peaks correspond to a mechanism in the ideal beam model. Since the experimental data closely resembles the ideal beam model, the same mechanism is impacting both these results. The flawed beam models do not exhibit the missing OSET frequency peak values.

The final conclusion is that since the product of the partitioned impedance matrix described above is providing missing OSET peak frequencies, the effects of a symmetrical matrix is causing the missing OSET peak values. This symmetrical matrix would result from a homogeneous beam finite element model or structure. This conclusion is supported by the lack of missing OSET peak values displayed in the flawed finite element models which are heterogeneous.

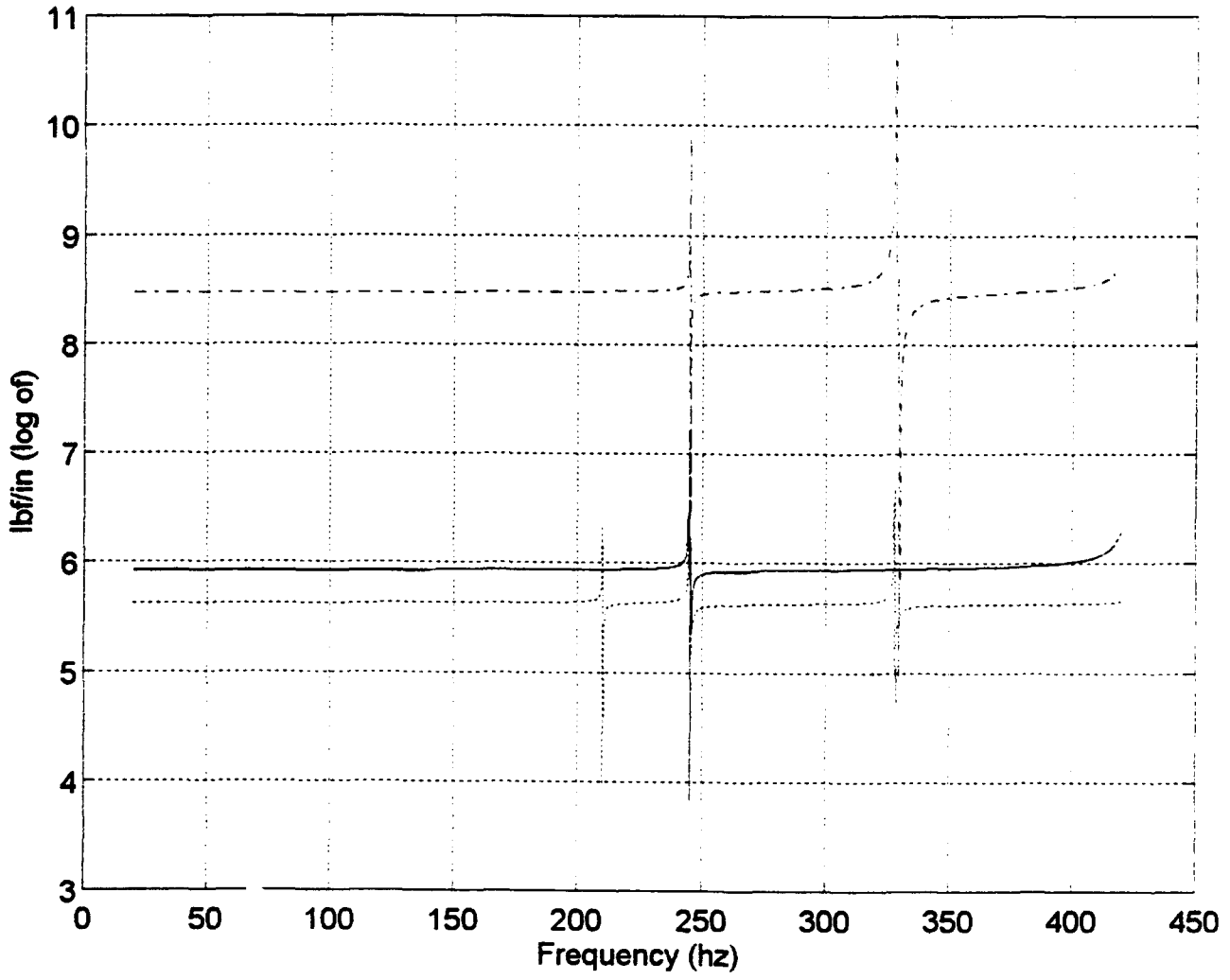

FIGURE D-3: $Z_{ao} * Z_{oo}^{-1} * Z_{oa}$
(--) "1,1" (-.-) "2,2" (—)"3,3"

Ideal Beam Model

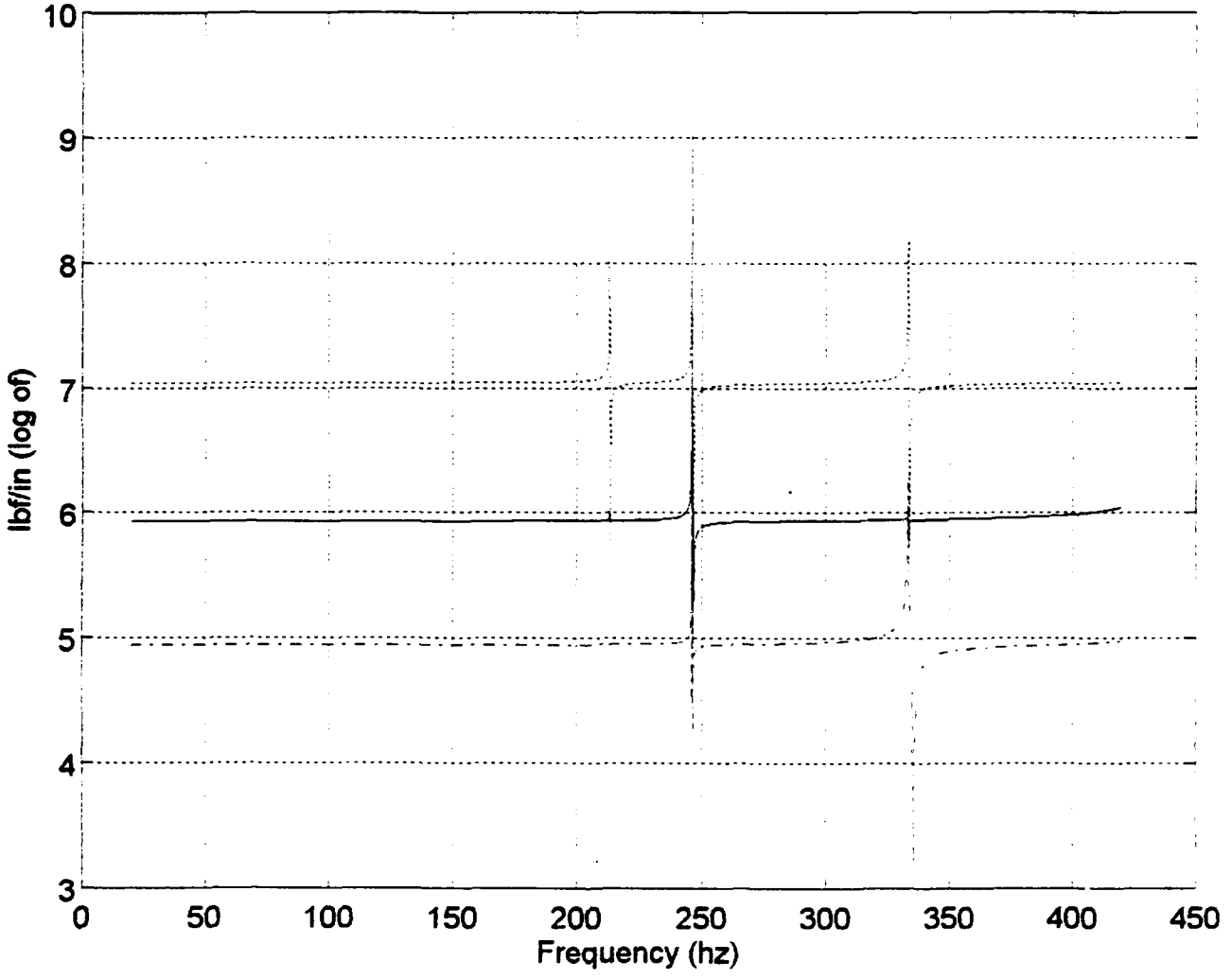

FIGURE D-4: $Z_{ao} * Z_{oo}^{-1} * Z_{oa}$
(--) "1,1" (-.-) "2,2" (—) "3,3"

Case II

LIST OF REFERENCES

1. Gordis, J.H., "Spatial, Frequency Domain Updating of Linear, Structural Dynamic Models", AIAA-93-1652-CP, 1993, pp. 3050-3058.

2. Gordis, J.H., Bielwa, R.L., and Flannery, W. G., "A General Theory for Frequency Domain Structure Synthesis", Journal of Sound and Vibration, 150(1), Sep 1989, pp. 139-158.

3. Guyan, R.J., "Reduction of Stiffness and Mass Matrices", Journal of the American Institute of Aeronautics and Astronautics, Vol. 3, Feb 1965, p 380.

4. Irons, B., "Structural Eigenvalue Problems: Elimination of Unwanted Variables", Journal of the American Institute of Aeronautics and Astronautics, Vol. 3, May 1965.

5. O'Callahan, J., "A Procedure for an Improved Reduction System (IRS) Model.", 7th International Modal Analysis Conference, Las Vegas, NV 1989.

6. Kistler Instrument Corporation, Operating Instructions Model 8832 TAP System, March 1990.

7. PCB Piezotronics, Inc., General Guide to ICP Instrumentation.

8. MB Dynamics, Instruction Manual Model PM25A Vibration Exciter, 16 November 1988.

9. Hewlett-Packard Company, HP 3562A Operator Introduction to the HP 3562A Dynamic Signal Analyzer, Product Note 3562A-1.

10. Hewlett-Packard Company, Standard Data Format Utilities User's Guide, September 1993.

11. Logan, D.L., Mechanics of Materials, Back Table, Harper Collins, 1991.

12. James, M.L., and others, Vibrations of Mechanical and Structural Systems with Microcomputer Applications, pp. 600-609, Harper and Row, 1989.

13. Craig, R.R., Structural Dynamics, An Introduction to Computer Methods, pp. 383-387, John Wiley and Sons, Inc., 1981.

INITIAL DISTRIBUTION LIST

		Number of Copies
1.	Defense Technical Information Center Cameron Station Alexandria, Virginia 22304-6145	2
2.	Library, Code 52 Naval Postgraduate School Monterey, California 93943-5002	2
3.	Professor J.H. Gordis, Code ME/GO Department of Mechanical Engineering Naval Postgraduate School Monterey, California 93943	3
4.	Naval Engineering Curricular Office Code 34 Naval Postgraduate School Monterey, California 93943-5000	1
5.	LCDR Vincent C. Gomes Route 4, Box 1252 Gloucester, Virginia 23061	1